Geotechnical Resistance Factors for Ultimate Limit State Design of Deep Foundations Under Axial Compression Loading

by

Mehrangiz Naghibi

Submitted in partial fulfillment of the requirements
for the degree of Doctor of Philosophy

at

Dalhousie University
Halifax, Nova Scotia
March 2010

Dalhousie University
Department of Engineering Mathematics and Internetworking

The undersigned hereby certify that they have examined, and recommend to the Faculty of Graduate Studies for acceptance, the thesis entitled “Geotechnical Resistance Factors for Ultimate Limit State Design of Deep Foundations Under Axial Compression Loading” by Mehrangiz Naghibi in partial fulfillment of the requirements for the degree of Doctor of Philosophy.

Dated: March 26, 2010

Supervisor: Dr. Gordon A. Fenton _____

Readers: Dr. Dennis E. Becker _____

Dr. Craig B. Lake _____

Dr. Serguei Iakovlev _____

Department Representative: Dr. Nuaman Aslam _____

Dalhousie University

DATE: March 26, 2010

AUTHOR: Mehrangiz Naghibi

TITLE: Geotechnical Resistance Factors for Ultimate Limit State Design of Deep Foundations Under Axial Compression Loading

DEPARTMENT OR SCHOOL: Department of Engineering Mathematics and Internetworking

DEGREE: PhD **CONVOCATION:** May **YEAR:** 2010

Table of Contents

List of Tables

List of Figures

Abstract

For many years, engineers have designed foundations, walls and culverts for highway and other geotechnical applications using allowable stress design (ASD) methods. In ASD, all uncertainties in the load and resistance are combined into a global factor of safety which, unfortunately, leads to uncertain safety margins in the design. The determination of system failure probability requires a coherent method of design for the geotechnical system. The Load and Resistance Factor Design (LRFD) approach allows designs to be targeted to acceptable failure probability levels, which depend on the limit state being avoided.

This research proposes Load and Resistance Factor Design provisions for the ultimate limit state punching shear failure of deep foundations. The load factors currently used are as specified by the National Building Code of Canada. The geotechnical resistance factors required to achieve a certain acceptable failure probability are estimated as a function of the spatial variability of the soil and of the degree of site understanding. A mathematical theory is developed to analytically estimate the failure probability of deep foundations in which the spatially random soil field is modeled using random field theory. The analytical results are validated by simulation and then used to estimate failure probabilities and geotechnical resistance factors required for design.

List of Abbreviations and Symbols Used

ASD	Allowable Stress Design
CPT	cone penetration test for in-situ soil testing
FHWA	Federal Highway Administration
LAS	Local Average Subdivision
LRFD	Load and Resistance Factor Design
LSD	Limit States Design
RBD	Reliability-Based Design
SLS	Serviceability Limit State
SPT	standard penetration test for in-situ soil testing
ULS	Ultimate Limit State
WSD	Working Stress Design
a	earth pressure coefficient
b	pile interface friction angle coefficient
$\mathrm{Cov}\left[\cdot,\cdot\right]$	covariance operator
c	cohesion
$\overline{c}$	arithmetic average of cohesion field along pile surface
$\hat{c}$	arithmetic average of observed (sampled) cohesion values
$\hat{c}_i$	observed (sampled) cohesion value
$\overline{c}_i$	local average of cohesion over i'th element along pile surface
D	depth of soil sample
$\mathrm{E}\left[\cdot\right]$	expectation operator
F_s	factor of safety
$G_{\ln c}$	standard normal random field (log-cohesion)
G_ϕ	standard normal random field of friction angle
H	designed pile length

I_i	importance factor corresponding to i'th characteristic load effect
l	critical depth of changing vertical stress
F	total true (random) load
$\hat{F}_i$	i'th characteristic load effect
$F_{_D}$	true (random) dead load
$F_{_L}$	true (random) live load
$\hat{F}_{_D}$	characteristic dead load = $k_{_D}\mu_{_D}$
$\hat{F}_{_L}$	characteristic live load = $k_{_L}\mu_{_L}$
m	number of soil observations
p	pile perimeter length
p_f	probability of failure
p_m	maximum acceptable probability of failure
q	factored design load = $\alpha_{_L}\hat{F}_{_L}$ + $\alpha_{_D}\hat{F}_{_D}$
r	distance between soil sample and pile centerline
$\hat{R}_u$	ultimate characteristic resistance (based on characterstic soil properties)
R_u	true ultimate resistance (random)
v_c	coefficient of variation of cohesion
v_ϕ	coefficient of variation of friction angle
z	spatial coordinate, (z_1, z_2) in 2-D
z_i^o	spatial coordinate of the center of the i'th soil sample
W	true load times ratio of characteristic to equivalent total stress resistance in soils under total stress condition
Y	true load times ratio of characteristic to equivalent effective stress resistance in soils under effective stress condition
α	adhesion coefficient
α_i	load factor corresponding to the i'th load effect
$\alpha_{_L}$	live load factor
$\alpha_{_D}$	dead load factor
Δz	vertical dimension of soil samples
φ_{gu}	geotechnical resistance factor

Φ	standard normal cumulative distribution function
$\gamma(H)$	variance function giving variance reduction due to averaging over length H
$\gamma(D)$	variance function giving variance reduction due to averaging over sample depth D
γ_{HD}	average correlation coefficient between the friction angle samples over length D and the friction angle along the pile of length H
M	safety margin
μ_c	cohesion mean
$\mu_{\ln c}$	log-cohesion of mean
$\mu_{\ln \hat{c}}$	mean of the characteristic log-cohesion (based on an arithmetic average of cohesion observations)
$\mu_{\ln \bar{c}}$	mean of the equivalent log-cohesion (based on a arithmetic average of cohesion over pile length H)
$\hat{\phi}$	arithmetic average of friction angle field along the pile surface
$\bar{\phi}$	arithmetic average of observed (sampled) friction angle values
$\hat{\phi}_i$	observed (sampled) friction angle values
$\bar{\phi}_i$	local average of friction angle over *i*'th element along pile surface
μ_ϕ	friction angle mean
$\mu_{\hat{\phi}}$	mean of the characteristic friction angle (based on an arithmetic average of friction angle observations)
$\mu_{\bar{\phi}}$	mean of the equivalent friction angle (based on a arithmetic average of friction angle over pile length H)
μ_D	mean dead load
μ_F	mean total load on pile
μ_L	mean live load
$\mu_{\ln F}$	mean total log-load on pile
$\mu_{\ln W}$	mean of $\ln W$
$\mu_{\ln Y}$	mean of $\ln Y$
θ	correlation length of the random field
$\rho(t)$	common correlation function
σ_c	cohesion standard deviation

σ_{ϕ}	friction angle standard deviation
σ_{D}	dead load standard deviation
σ_{F}	live load standard deviation
$\sigma_{\ln F}$	standard deviation of total log-load
$\sigma_{\ln c}$	log-cohesion standard deviation
$\sigma_{\ln \overline{c}}$	standard deviation of $\ln \overline{c}$
$\sigma_{\ln \hat{c}}$	standard deviation of $\ln \hat{c}$
$\sigma_{\ln W}$	standard deviation of $\ln W$
σ_{ϕ}	friction angle standard deviation
$\sigma_{\overline{\phi}}$	standard deviation of $\overline{\phi}$
$\sigma_{\hat{\phi}}$	standard deviation of $\hat{\phi}$
$\sigma_{\ln Y}$	standard deviation of $\ln Y$

Acknowledgements

I would like to express my deep and sincere gratitude to my advisor Dr. Gordon A. Fenton for his patience, kindness, guidance and support during the various stages of this research. His wide knowledge and his logical way of thinking have been of great value for me. His understanding, encouraging and personal guidance have provided a good basis for the present thesis. Any success attained in this research is largely due to his patient directions.

Much appreciation goes to Dr. Craig B. Lake and Dr. Serguei Iakovlev for reading this thesis. Their valuable suggestions have improved the quality of this research.

In addition, I wish to extend my gratitude to Karen Conrod for her kindness and all the help she has given me over the past three years.

And last but not least, I greatly owe what I am now to my parents and my sister and brother in-law for believing in me, constant support, love and encouragement.

Chapter 1: Introduction

1.1 General

Deep foundations will be hereafter collectively referred to as *piles* for simplicity in this thesis. Piles are designed to transfer load to the surrounding soil and/or to a firmer stratum, thereby providing vertical and lateral load bearing capacity to a supported structure. In this thesis, the random behavior of a pile subjected to a vertical load and supported by a spatially variable soil is investigated.

The geotechnical resistance, or bearing capacity, of a pile arises as a combination of side friction, where load is transmitted to the soil through friction along the sides of the pile, and end bearing, where load is transmitted to the soil (or rock) through the tip of the pile. If soil-boring records establish the presence of bedrock or rocklike material at a site within a reasonable depth, piles can be extended to the rock surface. In this case, the ultimate capacity of the piles depends primarily on the load bearing capacity of the underlying material; these piles are called *end bearing piles*. When piles become very long, they are referred to as friction piles because most of the resistance is drived from skin friction (Fenton and Griffiths, 2008).

The required length of a friction pile depends on the soil characteristics, the applied load, and the pile size. To determine the necessary length of these piles, an engineer needs a good understanding of soil-pile interaction, good judgment, and experience. Theoretical procedures for calculating the load-bearing capacity of piles for soils under effective and total stress conditions are presented in Chapters 2 and 3.

Pile foundations are needed in a variety of circumstances. The following are some situations in which piles may be considered for the construction of a foundation.

1) When the upper soil layers are highly compressible and too weak to support the load transmitted by the superstructure, piles are used to transmit the load to underlying bedrock or a stronger soil layer. When bedrock is not encountered at a reasonable depth below the ground surface, piles are used to transmit the structural load to the soil. The resistance to the applied structural load is derived mainly from the effective and/or total stress resistance developed at the soil-pile interface.

2) When subjected to horizontal forces, pile foundations resist by bending while still supporting the vertical load transmitted by the superstructure. This situation is generally encountered in the design and construction of earth retaining structures and foundations of tall structures that are subjected to strong wind and/or earthquake forces.

3) In many cases, the soils at the site of a proposed structure maybe expansive and collapsible. These soils may extend to a great depth below the ground surface. Expansive soils swell and shrink as the moisture content increases and decreases, respectively, and the swelling pressure of such soils can be considerable. In the extreme case, soils such as loess are collapsible. When the moisture content of these soils increases, their structures may break down. In such cases, pile foundations may be used, in which piles are extended into stable soil layers beyond the zone of possible moisture change.

4) The foundations of some structures, such as transmission towers, offshore platforms, and basement mats below the water table, may be subjected to uplifting forces. Piles are sometimes used for these foundations to resist uplifting forces.

5) Bridge abutments and piers are usually constructed over pile foundations to avoid the possible loss of bearing capacity that a shallow foundation might suffer because of soil erosion at the ground surface (Fenton and Griffiths, 2008).

1.2 Reliability-Based Design

Before talking about reliability-based design in geotechnical engineering, it is worth investigating the levels of risk that a reliability-based design is aiming to achieve. In many areas of design, particularly in Civil Engineering, the design is evaluated strictly in terms of the probability of failure, rather than by assessing both the probability of failure and the cost or consequences of failure. This is probably mostly due to the fact that the value of human life is largely undefined and a subject of considerable political and social controversy.

Most civil engineering structures are currently designed so that individual elements making up the structure have a "nominal" probability of failure of about one in one thousand and the same might be said about an individual geotechnical element such as a footing or pile. More specifically, we say that for a random load, F, on an element with resistance, R, we design such that

$$\mathrm{P}\left[F > R\right] \simeq \frac{1}{1000}$$

In fact, building codes are a bit vague on the issue of acceptable risk, partly because of

the difficulty in assessing overall failure probabilities for systems as complex as entire buildings. The above failure probability is based on the loss of load carrying capacity of a single building element, such as a beam or pile, but the codes also strive to achieve a much lower probability of collapse by

1) ensuring that the system has many redundancies (if one element fails, its load is picked up by other elements),
2) erring on the safe side in parameter estimates entering the probability estimate,

So, in general, the number of failures resulting in loss of life is a good deal less than one in a thousand (perhaps ignoring those failures caused by deliberate sabotage or acts of war which buildings are not generally designed against).

1.2.1 Background to Design Methodologies

For over 100 years, *working stress design* (WSD), also referred to as *allowable stress design* (ASD), has been the traditional basis for geotechnical design relating to settlements or failure conditions. Essentially, WSD ensures that the *characteristic load* acting on a foundation or structure does not exceed some allowable limit. Characteristic values of either loads or soil properties are also commonly referred to as *nominal*, *working*, or *design* values. The word "characteristic" will be used to avoid confusion.

In WSD, the allowable limit is often based on serviceability limit state. Uncertainty in loads, soil strength, construction quality, and model accuracy is taken into account through a *nominal global factor of safety*, F_s, defined as the ratio of the characteristic resistance to the characteristic load,

$$F_s = \frac{\text{characteristic resistance}}{\text{characteristic load}} = \frac{\hat{R}}{\hat{F}} = \frac{\hat{R}}{\sum_{i=1}^{n} \hat{F}_i} \tag{1.1}$$

In general, the *characteristic resistance*, $\hat{R}$, is computed by geotechnical relationships using conservative estimates of the soil properties while the *characteristic load*, $\hat{F}$, is the sum of conservative unfactored estimates of characteristic load actions, $\hat{F}_i$, acting on the system. $\hat{F}$ is sometimes taken as an upper percentile (i.e. a load only exceeded by a certain small percentage of loads in any one year), as illustrated in Figure 1.1, while $\hat{R}$ is sometimes taken as a cautious estimate of the mean resistance.

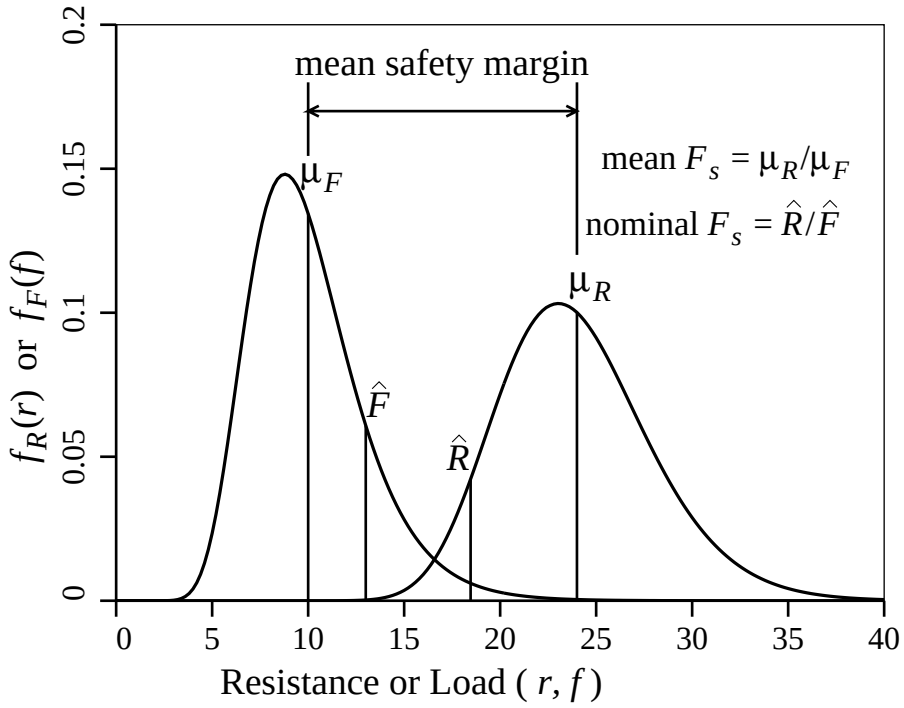

Figure 1.1 Load and resistance distributions.

A geotechnical design proceeds by solving Eq. (1.1) for the characteristic resistance, leading to the following design requirement,

$$\hat{R} = F_s \sum_i \hat{F}_i \tag{1.2}$$

where $\hat{F}_i$ is the i^{th} characteristic load effect. For example, $\hat{F}_1$ might be the characteristic dead load, $\hat{F}_2$ might be the characteristic live load, $\hat{F}_3$ might be the characteristic earthquake load, and so on. Although Eq. (1.1) is the formal definition of F_s, F_s is typically selected using engineering judgment and experience and then used in Eq. (1.2) to determine the required characteristic resistance.

Although WSD is simple and useful, it is also accompanied by difficulties and ambiguities.

First, the traditional argument made against the use of a single factor of safety is that two soils with the same characteristic strength and characteristic load will have the same F_s value regardless of the actual variabilities in load and strength. This is true when the characteristic values are equal to the means, i.e. when the factor of safety is defined in terms of the means, e.g.

$$F_s = \frac{\text{mean resistance}}{\text{mean load}} \tag{1.3}$$

as it commonly is. The mean F_s was illustrated in Figure 1.1. Figure 1.2 shows how different geotechnical systems, having the same mean factor of safety, can have vastly different probabilities of failure. In other words, the mean factor of safety does not adequately reflect the actual design safety. The probability of failure, p_f, is computed as the probability that load exceeds resistance,

$$p_f = \mathrm{P}\left[F > R\right] = \mathrm{P}\left[R/F < 1\right] = \mathrm{P}\left[\ln R - \ln F < 0\right] \tag{1.4}$$

where, if it is assumed that R and F are lognormally distributed, then $(\ln R - \ln F)$ is normally distributed. If we let $M = R/F$, where M is called the *safety margin* (M is less than one if the load exceeds the resistance so that failure occurs), then

$$\ln M = \ln R - \ln F \tag{1.5}$$

which is normally distributed with parameters

$$\mu_{\ln M} = \mu_{\ln R} - \mu_{\ln F} \tag{1.6a}$$

$$\sigma^2_{\ln M} = \sigma^2_{\ln R} + \sigma^2_{\ln F} \tag{1.6b}$$

where it is assumed R and F are independent. Now we find that

$$\begin{aligned}
\mathrm{P}\left[F > R\right] = \mathrm{P}\left[\ln M < 0\right] &= \mathrm{P}\left[Z < \frac{0 - \mu_{\ln M}}{\sigma_{\ln M}}\right] \\
&= \mathrm{P}\left[Z < \frac{0 - (\mu_{\ln R} - \mu_{\ln F})}{\sqrt{\sigma^2_{\ln R} + \sigma^2_{\ln F}}}\right] \\
&= \Phi\left(-\frac{\mu_{\ln R} - \mu_{\ln F}}{\sqrt{\sigma^2_{\ln R} + \sigma^2_{\ln F}}}\right)
\end{aligned} \tag{1.7}$$

where $Z = (\ln M - \mu_{\ln M})/\sigma_{\ln M}$ has a standard normal distribution, and Φ is the standard normal cumulative distribution function. We can now define the *reliability index*, β, to be

$$\beta = \frac{\mu_{\ln R} - \mu_{\ln F}}{\sqrt{\sigma^2_{\ln R} + \sigma^2_{\ln F}}} \tag{1.8}$$

which represents the number of standard deviations that $(\ln R - \ln F)$ is away from the "failure" region (i.e. 0). As β becomes smaller, the probability of failure increases. Typically, a β value of 3.0 to 3.5 is aimed for in structural engineering.

Another key problem with WSD is that it does not explicitly differentiate between the behavior of the structure under ultimate and serviceability limit states. However, as will

be discussed follows, when we combine Limit States Design (LSD) with Load and Resistance Factor Design (LRFD), we can both consider different modes of failure and achieve appropriate levels of safety for each failure mode.

It should be noted that the evolution from WSD to more advanced reliability-based design methodologies is entirely natural. For at least the first half of the 20th century little was understood about geotechnical loads and resistances beyond their most important characteristics; their means. So it was appropriate to define a design code largely in terms of means and some single global factor of safety. In more recent years, as our understanding of the load and resistance distributions improve, it makes sense to turn our attention to somewhat more sophisticated design methodologies which incorporate these distributions.

The working stress approach to geotechnical design has nevertheless been quite successful and has led to many years of empirical experience. The primary impetus to moving away from working stress design towards reliability-based design is to allow a better feel for the actual reliability of a system and to harmonize with structural codes which have been reliability-based for some time now.

Most current reliability-based design codes start with an approach called *Limit States Design*. The 'Limit States' are those conditions in which the system ceases to fulfill the function for which it was designed. Those states concerning safety are called *ultimate limit states*, which include exceeding the load carrying capacity (e.g., bearing failure),

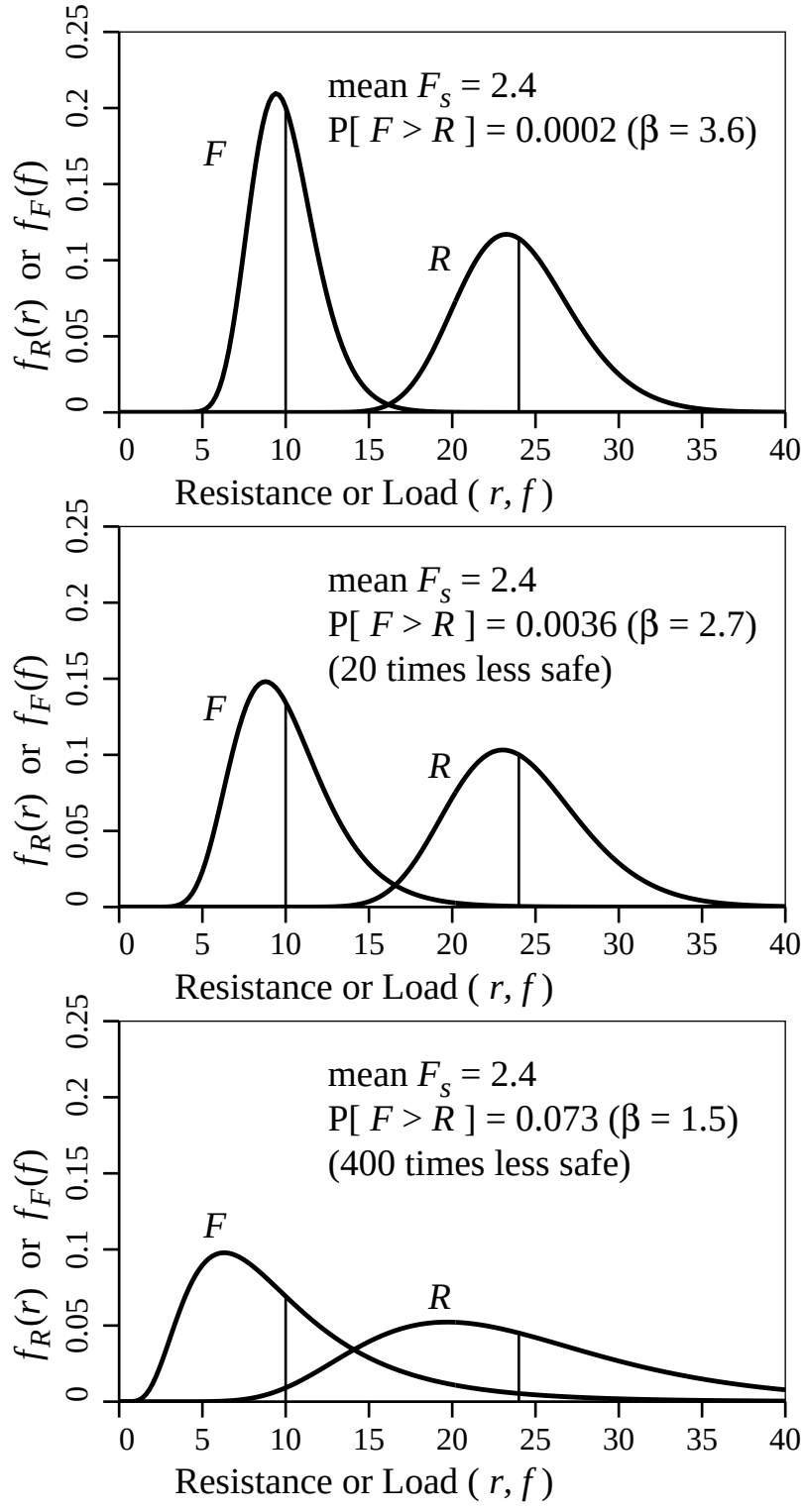

Figure 1.2 Three geotechnical problems can have precisely the same mean factor of safety and yet different probabilities of failure, P [$F > R$].

overturning, sliding, and loss of stability. Those states which restrict the intended use of the system are called *serviceability limit states*, which include deflection, permanent deformation, and cracking.

1.2.2 Load and Resistance Factor Design

Once the limit states have been defined for a particular problem, the next step is to develop design relationships for each of the limit states. The selected relationships should yield a constructed system having a target reliability or, conversely, an acceptably low probability of failure. A methodology which at least approximately accomplishes this goal and which has gained acceptance amongst the engineering community is the *Load and Resistance Factor Design* (LRFD) approach. In its simplest form, the load and resistance factor design for any limit state can be expressed as follows: design the system such that its characteristic resistance, $\hat{R}$, satisfies the following inequality

$$\varphi_{gu}\hat{R} \geq \alpha\hat{F} \tag{1.9}$$

where φ_{gu} is a geotechnical resistance factor acting on the (geotechnical) characteristic resistance, $\hat{R}$, and α is a load factor acting on the characteristic load, $\hat{F}$. Typically the resistance factor, φ_{gu}, is less than 1.0 – it acts to reduce the characteristic resistance to a less likely *factored resistance*, having a suitably small probability of occurrence. Since, due to uncertainty, this smaller resistance may nevertheless occur in some small fraction of all similar design situations, it is the resistance assumed to exist in the design process. Similarly, the load factor, α, is typically greater than 1.0 (unless the load acts in favor of the resistance). It increases the characteristic load to a *factored load* which may occur in some (very) small fraction of similar design situations. It is this higher, albeit unlikely, load which must be designed against.

A somewhat more general form for the LRFD relationship appears as follows;

$$\varphi_{gu}\hat{R} \geq \sum_{i=1}^{m} I_i\alpha_i\hat{F}_i \tag{1.10}$$

where we apply separate load factors, α_i, to each of m types of characteristic loads, $\hat{F}_i$. For example, $\hat{F}_1$ might be the sustained or *dead* load, $\hat{F}_2$ might be the maximum lifetime dynamic or *live* load, $\hat{F}_3$ might be a load due to thermal expansion, and so on. Each of these load types will have their own distribution, and so their corresponding load factors can be adjusted to match their variability. The parameter I_i is an importance factor corresponding to each load which is greater than 1.0 for important structures (e.g. structures which provide

essential services after a disaster, such as hospitals) and less than 1.0 for structures whose failure is unlikely to threaten safety (eg. storage sheds). Most typical structures have an importance factor of 1.0. Some building codes, such as the National Building Code of Canada (National Research Council, 2005) adjust the load factors individually to reflect building importance, rather than use a single global importance factor.

LRFD is currently being used in many structural design codes and reports, such as the National Building Code of Canada (NBCC, 2005), American Association of State Highway and Transportation Officials (AASHTO, 2007), Canadian Highway Bridge Design Code (CHBDC, 2006), the National Cooperative Highway Research Program (NCHRP) Report 343 (Barker et al., 1991) and the Federal Highway Administration (FHWA) Load and Resistance Factor Design (LRFD) for Highway Bridge Substructures (FHWA, 2001).

In general, LRFD replaces single factor of safety on the ratio of total resistance to total load with a set of partial safety factors on individual components of resistance and load, and uses limit states as the checking points for design. The design loads are typically increased and design resistances are reduced through multiplication by partial safety factors that are greater than one and less than one, respectively, as discussed above. There are advantages and disadvantages associated with use of LRFD for geotechnical aspects of foundation design, the advantages are as follow;

1) The use of separate load and resistance factors is logical and realistic because loads and resistance have separate and unrelated sources of uncertainty. Using separate factors is a convenient and rational way of accounting for the sources of uncertainty in design. In addition, soil can act either as a load or as a resistance or both. For example, the soil behind a retaining wall acts as a load while soil in front of the retaining wall may act as a resistance. It would be better to factor these actions separately.
2) The application of LRFD to geotechnical design helps harmonize with the structural community and minimize any incompatibility between structural and foundation engineers. This leads to a consistent design approach/philosophy orchestrated by the structural and geotechnical engineers.
3) Finally, the fact that all components of the structural system, including the foundation, are designed to a consistent and appropriate level of safety or reliability leads to a more economical design.

The disadvantage of using LRFD can be stated as follow;

1) The random characteristics of loads and strength (resistance) in structural engineering are fairly well known and reasonably well established (Allen, 1975, MacGregor, 1976).

This is because, for structural material such as concrete, steel, and wood, representative testing can easily be performed so that distributions are relatively easily estimated. Because structural materials are typically quality controlled, their distributions remain relatively constant at any building site. Thus, it is typically only necessary to take a few samples of the building material at the site to ensure that design criteria are met. The difficulty with geotechnical engineering in terms of LRFD is that geotechnical materials, e.g. soil or rocks, are not manufactured to specified criteria, as is the case for most structural materials. In order to have a reasonably accurate estimation of soil variability we must conduct intensive site investigations. It is also hard to deliver undisturbed soil samples to test facilities to accurately determine their properties. In other words, to capture the variability of soil accurately many carefully taken samples would be required to estimate both mean and variance values, which adds expense and difficulties to foundation design.

2) Another difficulty with geotechnical engineering is the determination of spatial randomness of soil and its effect on the design reliability. Soil properties often vary dramatically from point to point within the same site and a thorough awareness of this inherent variability can be vital to the success of the design. Because soil properties vary from point to point soils should be modeled using random field theory (Vanmarcke, 1984).

Even though the evolution from WSD to Load and Resistance Factor Design (LRFD) in the geotechnical engineering community is entirely natural with the development of the public awareness of the benefits, there is some concerns about the position of engineering judgment and experience. It should be pointed out that engineering judgment and experience are, and always will be, an essential part of geotechnical engineering, especially for the design aspects that are beyond the scope of mathematical analysis. For example, the selection of characteristic values for any given limit state will involve engineering judgment and experience.

1.3 Research Objectives

Early use of LSD for geotechnical applications was examined by the Danish Geotechnical Institute (Hansen 1953, 1956) and later formulated into code (Hansen, 1966). Independent load and resistance factors were used, with the resistance factors applied directly to the soil properties rather than to the characteristic resistance.

Considerable effort has been directed over the past decade to the application of LRFD in

geotechnical engineering. LRFD approaches have been developed in offshore engineering (e.g., Tang, 1993; Hamilton and Murff, 1992), general foundation design (e.g., Kulhawy and Phoon, 1996), and pile design for transportation structures (Barker et al., 1991; ONeill, 1995).

In geotechnical practice, uncertainties concerning resistance principally manifest themselves in design methodology, site characterization, soil behavior, and construction quality. The uncertainties have to do with the formulation of the physical problem, interpreting site conditions, understanding soil behavior (e.g., its representation in property values), and accounting for construction effects. Uncertainties in external loads are small compared with uncertainties in soil and the strength-deformation behaviors of soils. The applied loads, however, are traditionally based on superstructure analysis, whereas actual load transfer to substructures is poorly researched.

This research considers an individual pile placed in a spatially varying random soil. In general, the soil will vary in three dimensions, but there is little advantage in considering the 3rd dimension since piles are essentially one-dimensional and only the 2nd dimension is needed to provide distance from the pile location. Hence, this study considers a two-dimensional random field in which the pile is place vertically at a certain position and soil samples are take vertically at some possibly different position (as in a CPT or STP sounding).

A random field $X(\underset{\sim}{t})$ is a collection of random variables, $X_1 = X(\underset{\sim}{t}_1)$, $X_2 = X(\underset{\sim}{t}_2)$, ..., whose values are mapped onto a space (of n dimensions), one for each point in the field. Values in a random field are usually spatially correlated in one way or another.

In the present study three parameters are considered to describe the random soil model, the mean, μ, the standard deviation, σ, and the correlation length, θ. Frequently, it is more convenient to express standard deviation (or variance) as a coefficient of variation, v, defined as the ratio of standard deviation, σ, to the mean, μ, $v = \sigma/\mu$.

A convenient measure of the variability of a random field is the *correlation length*, θ, also sometimes referred to as the *scale of fluctuation*. Loosely speaking, θ is the distance within which points are significantly correlated. Conversely, two points separated by a distance more than θ will be largely uncorrelated. Mathematically, θ is defined here as the area under the correlation function (Vanmarcke, 1984),

$$\theta = \int_{-\infty}^{\infty} \rho(t)\, dt \tag{1.11}$$

Fields with small θ tend to be 'rough', while fields with larger θ are usually smoother.

Figure 1.3 shows two random field realizations. The field on the left has a small correlation length (θ = 0.04) and can be seen to be quite rough. The field on the right has a large correlation length (θ = 2) and can be seen to be more slowly varying. (Fenton et al., 2008)

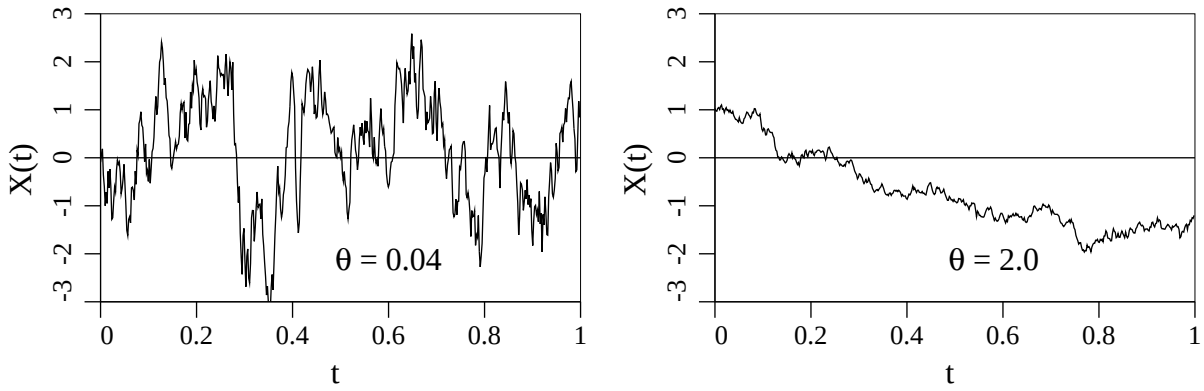

Figure 1.3 Sample realizations of $X(t)$ for two different correlation lengths.

In random fields a correlation coefficient can be used to characterize the spatial dependence of the fields. The correlation coefficient will be given by correlation function parameterized by the correlation length, θ. There are several commonly used correlation functions, in this research the Markov correlation function, $\rho(t)$, is used. It is because of its simplicity and because, in one-dimension, it is a memoryless process. This means for a stochastic process the future of the random process only directly depends on the present and not on the past. The Markov correlation function has the form

$$\rho(t) = \exp\left(-\frac{2|t|}{\theta}\right) \tag{1.12}$$

where $t = z_1 - z_2$ is the distance between two points and θ is the correlation length (Fenton and Griffiths, 2008).

This study proposes a reliability-based design methodology for piles, with the aim of reducing cost without compromising safety. For deep foundation design, this will be accomplished by assessing the probability of failure of piles under effective stress and total stress conditions.

The final goal is to investigate the effect of a soil's spatial variability and site investigation intensity on the resistance factors via theory and via simulation, the latter using Monte Carlo simulation.

It seems reasonable to assume that if the spatial correlation structure of a soil is caused by changes in the constitutive nature of the soil over space, then both cohesion and friction

angle would have similar correlation lengths. Thus, friction angle, ϕ is assumed to have the same correlation structure as cohesion, c, i.e., $\rho(t)$. Both correlation lengths will be referred to generically from now on simply as θ, and both correlation functions as $\rho(t)$.

The two random fields, c and ϕ, are assumed to be independent. Non-zero correlations between c and ϕ were found by Fenton and Griffiths (2003) to have only a minor influence on the estimated probabilities of bearing capacity failure. Since the general consensus is that c and ϕ are negatively correlated (Cherubini, 2000) and the mean bearing capacity for independent c and ϕ was slightly lower than for the negatively correlated case (Fenton and Griffiths, 2003), the assumption of independence between c and ϕ is slightly conservative.

1.4 Scope of Work

This study concentrates on the determination of geotechnical resistance factors for use in the design of a pile in soils under effective stress and total stress conditions, using reliability-based design methodology. An introduction of deep foundations and the history of geotechnical designs are outlined in Chapter 1.

Chapter 2 presents an analytical solution to estimating the failure probability of deep foundation in soils under total stress condition. Chapter 2 also describes the Monte Carlo simulations used in this thesis to validate the analytical solution.

The results of the simulation are then compared to the analytical results. Recommended resistance factors for four different maximum acceptable failure probabilities are shown in Chapter 2 and a comparison is made between these recommended values and the values recommended in existing LRFD codes.

Chapter 3 is similar to Chapter 2, except to determine the required resistance factors for piles founded in effective stress soils.

Finally, the limitations of overall results and recommendations are discussed, and conclusions are drawn in Chapter 4. Suggestions for future research are also provided.

Chapter 2: Geotechnical Resistance Factors for Total Stress Limit State Design of Deep Foundations

2.1 General

Deep foundations, or piles, may fail through a punching shear failure, an ultimate limit state (ULS), where the load applied to the pile exceeds the shear strength of the surrounding soil (Fenton and Griffiths, 2007). The soil supports the pile through a combination of end-bearing and friction and/or cohesion between the soil and the pile sides. In this chapter, only total stress resistance is considered, as would typically be found in a soil under total stress condition, and end-bearing is ignored.

As the load on the pile is increased, the bond between the soil and the pile surface will break down and the pile will slip through the surrounding soil. At this point, the ultimate geotechnical resistance of the pile has been reached. The ultimate geotechnical resistance of a pile due to cohesion, c, between the pile surface and its surrounding soil is given by ,

$$R_u = \int_0^H p\tau(z)\,dz \tag{2.1}$$

where p is the effective perimeter length of the pile section and $\tau(z)$ is the ultimate shear stress acting on the surface of the pile at depth z.

The ultimate shear stress acting between the soil and the pile under total stress condition can be obtained by several methods. One commonly accepted procedure, the α method, is described briefly by Das (2000). According to the α method, the unit surface shear resistance in soils under total stress condition can be represented by the equation,

$$\tau(z) = \alpha c(z) \tag{2.2}$$

where $c(z)$ is the average soil cohesion around the pile perimeter at depth z, and α is an empirical adhesion factor, typically in the range of 0.3 to 1, as specified by the Canadian Foundation Engineering Manual (CFEM, 2006). For a normally consolidated clay with cohesion, c, less than about 33 kPa, the adhesion factor suggested by Das (2000) is 1.0. The

adhesion coefficient can be also written as a function of the cohesion over the pile length as (CFEM, 2006),

$$\alpha = \begin{cases} 0.21 + \frac{0.26 P_a}{\mu_c} & \text{if } \mu_c \geq 33 \text{ kPa} \\ 1 & \text{if } \mu_c < 33 \text{ kPa} \end{cases} \tag{2.3}$$

where P_a is the standard atmosphere (101.325 kPa).

In this research the average cohesion, μ_c, is assumed to be 50 kPa and so its corresponding adhesion coefficient, α, by using Eq. (2.3) can be estimated to be α = 0.74. The simulations and analytical results presented in this research are based on average values of cohesion, μ_c = 50kPa, and adhesion factor μ_α = 0.74. With this information, the true ultimate total stress resistance of a pile with length H and perimeter p, can be estimated to be,

$$R_u = \int_0^H p\alpha c(z)\, dz \tag{2.4}$$

In the design of a pile, geotechnical engineers must find the effective perimeter, p, and length, H, required to avoid a total stress resistance failure. In this research, it is assumed that the pile type is already known, so that p is known and the design involves determining H. To find H, ultimate limit state (ULS) conditions are checked using separate factors on loads and on ultimate geotechnical resistance. This leads to the load and resistance factor design (LRFD) methodology, collectively referred to as Limit States Design (LSD) in Canada, which requires that the factored geotechnical resistance exceed the factored load at each limit state. At the ultimate limit state, the design requirement is

$$\varphi_{gu}\hat{R}_u \geq \sum_i I_i \alpha_i \hat{F}_i \tag{2.5}$$

where φ_{gu} is the ultimate geotechnical resistance factor, $\hat{R}_u$ is the characteristic (design) ultimate geotechnical resistance, I_i is an importance factor corresponding to the i'th characteristic load effect, $\hat{F}_i$, and α_i is the i'th load factor.

The importance factor, I_i, reflects the severity of the failure consequences and may be larger than 1.0 for important structures, such as hospitals, whose failure consequences are severe and whose target probabilities of failure are less than those for typical structures. Typical structures are usually designed using I_i = 1, which will be assumed in this research. Structures with low failure consequences (minimal risk of loss of life, injury, and/or economic impact) may have $I_i < 1$.

Only one load combination will be considered in this research,

$$\hat{\alpha}_T \hat{F} = \alpha_L \hat{F}_L + \alpha_D \hat{F}_D \tag{2.6}$$

where $\hat{\alpha}_T$ is the total load factor, $\hat{F}$ is combination of characteristic live and dead loads, $\hat{F}_L$ is the characteristic live load, $\hat{F}_D$ is the characteristic dead load, and α_L and α_D are the live and dead load factors, respectively. The load factors used in this study will be as specified by the National Building Code of Canada (NBCC; NRC, 2005); α_L = 1.5 and α_D = 1.25. The theory presented here, however, is easily extended to other load combinations and factors, as long as their (possibly time-dependent) distributions are known.

In any reliability-based design, uncertain quantities such as load and resistance are represented by random variables having some distribution. Distributions are usually characterized by their mean, standard deviation, and some shape (e.g. normal or lognormal). In some cases, the characteristic load values used in design are defined to be the means, but they can be more generally defined in terms of the means as

$$\hat{F}_L = k_L \mu_L \tag{2.7a}$$

$$\hat{F}_D = k_D \mu_D \tag{2.7b}$$

where μ_L and μ_D are the means of the live and dead loads, and k_L and k_D are live and dead load bias factors, respectively (Fenton and Griffiths, 2008). For typical multi-storey office buildings, Allen (1975) estimates k_L = 1.41, based on a 30 year lifetime. Becker (1996) estimates k_D to be 1.18. The characteristic loads, $\hat{F}_L$ and $\hat{F}_D$, are thus obtained as: $\hat{F}_L = 1.41\mu_L$ and $\hat{F}_D = 1.18\mu_D$ (Fenton et al., 2008).

The characteristic ultimate geotechnical resistance, $\hat{R}_u$, is determined using characteristic soil properties, in this case characteristic values of the soil's cohesion, c. To obtain the characteristic soil properties, the soil is assumed to be sampled over a single column somewhere in the vicinity of the pile, for example by a single CPT sounding near or field vane test taken the pile. The sample is assumed to yield a sequence of m observed cohesion values, $\hat{c}_1, \hat{c}_2, \ldots, \hat{c}_m$. The characteristic value of the cohesion, $\hat{c}$, is defined in this chapter as an arithmetic average of the sampled observations, $\hat{c}_i$, which, can be computed as,

$$\hat{c} = \frac{1}{m} \sum_{i=1}^{m} \hat{c}_i \tag{2.8}$$

The characteristic ultimate geotechnical resistance, $\hat{R}_u$, can now be obtained from Eq. (2.4) to be

$$\hat{R}_u = pH\alpha\hat{c} \tag{2.9}$$

In order to determine the geotechnical resistance factor, φ_{gu}, required to achieve a certain acceptable reliability, the failure probability of the pile must be estimated. This probability

will depend on the load distribution, the load factors selected, and the resistance distribution. The resistance distribution is discussed in Sections 2.2 and the load distribution is discussed in Section 2.3. Sections 2.4 and 2.5 develop the analytical framework and simulation algorithm for the failure probability estimate, and illustrate how the theoretical estimates agree with simulation.

The Load and Resistance Factor Design (LRFD) approach involves selecting a maximum acceptable failure probability level, p_m. The choice of p_m derives from a consideration of acceptable risk and directly influences the value of φ_{gu}. Different levels of p_m may be considered to reflect the "importance" of the supported structure – p_m may be much smaller for a hospital than for an uninhabited storage warehouse.

The choice of a maximum acceptable failure probability, p_m, should consider the margin of safety implicit in current foundation designs and the levels of reliability for geotechnical design as reported in the literature. The values of p_m for foundation designs should be nearly the same or somewhat less than that of the supported structure because of the difficulties and high expense of foundation repairs. A literature review of the suggested maximum acceptable failure probability for foundations is listed in Table 2.1.

Table 2.1 Literature review of lifetime probabilities of failure of foundations.

Source	p_m
Meyerhof (1970, 1993, 1995)	$10^{-2} - 10^{-4}$
Simpson et al. (1981)	10^{-3}
NCHRP (1991)	$10^{-2} - 10^{-4}$
Becker (1996)	$10^{-3} - 10^{-4}$

Meyerhof (1995) suggests that a typical lifetime failure probability for a foundation is around 10^{-4} and so the numbers in Table 2.1, range on the high side of that suggested by Meyerhof. However, foundations are normally supported by more than a single pile, and multiple piles provide at least some degree of system redundancy which serves to reduce the system failure probability. If it is assumed that Meyerhof's 1995 estimate is for the entire foundation system, then the required failure probability for a single pile would be greater than the system failure probability of 10^{-4}. Although more research is required to determine the failure levels appropriate for redundant pile systems, the National Cooperative Highway Research Program (NCHRP) reports (Barker et al., 1991, and Paikowsky, 2004) are based on a lifetime failure probability of about 10^{-3} for an individual pile which suggests that NCHRP is considering pile redundancy. In this research, four maximum acceptable failure probabilities, $10^{-2}, 10^{-3}, 10^{-4}$ and 10^{-5}, will be considered. The failure

probabilities, $10^{-3}, 10^{-4}$, and 10^{-5}, might be appropriate for designs involving low (e.g. storage facilities), medium (typical structures), and high (e.g. hospitals and schools) failure consequence structures, respectively. The geotechnical resistance factors required to achieve these maximum acceptable failure probabilities will be recommended in Section 2.6.

2.2 The Random Soil Model

The soil cohesion, c, is assumed to be lognormally distributed with mean, μ_c, standard deviation, σ_c, and some spatial correlation structure (Fenton et al., 2008). The lognormal distribution is selected because it is commonly used to represent non-negative soil properties and has a simple relationship with the normal. A lognormally distributed random field can be obtained from a normally distributed random field, $G_{\ln c}(z)$, having zero mean, unit variance, and spatial correlation length, θ, through the transformation

$$c(z) = \exp\{\mu_{\ln c} + \sigma_{\ln c} G_{\ln c}(z)\} \tag{2.10}$$

where z is the spatial position at which c is desired. The mean and variance of $\ln c$ are obtained from the specified mean and variance of cohesion using the transformations

$$\sigma^2_{\ln c} = \ln\left(1 + v_c^2\right), \qquad \mu_{\ln c} = \ln(\mu_c) - \frac{1}{2}\sigma^2_{\ln c} \tag{2.11}$$

where v_c is the coefficient of variation of the cohesion, defined by $v_c = \sigma_c/\mu_c$.

The correlation coefficient between the log-cohesion at a point z_1 and a second point z_2, is specified by a correlation function, ρ. In this study, a simple exponentially decaying (Markovian) correlation function will be assumed, having the form

$$\rho(t) = \exp\left(-\frac{2|t|}{\theta}\right) \tag{2.12}$$

where $t = z_1 - z_2$ is the distance between the two points.

The spatial correlation length, θ, appearing in Eq. (2.12), is loosely defined as the separation distance within which two values of $\ln c$ are significantly correlated. Mathematically, θ is defined as the area under the correlation function, $\rho(t)$ (Vanmarcke,1984). The spatial correlation function, $\rho(t)$, has a corresponding variance reduction function, $\gamma(H)$, which specifies how the variance is reduced upon local averaging of $\ln c$ over some length H and is defined by,

$$\gamma(H) = \frac{1}{H^2}\int_0^H \int_0^H \rho(z_1 - z_2)\, dz_1\, dz_2 \tag{2.13}$$

It should be noted that the correlation function selected above acts between values of $\ln c$. This is because $\ln c$ is normally distributed, and a normally distributed random field is simply defined by its mean and covariance structure. In practice the correlation length θ can be estimated by evaluating spatial statistics of the log-cohesion data directly (see, e.g., Fenton 1999).

2.3 The Random Load Model

The load acting on a foundation is typically composed of dead loads, which are largely static, and live loads, which are largely dynamic. Dead loads are relatively well defined and can be computed by multiplying volumes by characteristic unit weights. The mean and variance of dead loads are reasonably well known. On the other hand, live loads are more difficult to characterize probabilistically. A typical definition of a live load is the extreme dynamic load (e.g., wind load, vehicle loads, bookshelves etc.) that a structure will experience during its design life. In other words, the distribution of live load really depends on the design life. Dead and live loads will be denoted as, F_D and F_L, respectively. Assuming that the total load, F is equal to the sum of the maximum lifetime live load, F_L, and the static dead load, F_D, i.e,

$$F = F_L + F_D \tag{2.14}$$

then mean and variance of F, assuming dead and live loads are independent, are given by,

$$\mu_F = \mu_L + \mu_D \tag{2.15a}$$

$$\sigma_F^2 = \sigma_L^2 + \sigma_D^2 \tag{2.15b}$$

The total load, $F = F_L + F_D$, is assumed to be lognormally distributed. This assumption was found to be reasonable by Fenton et al. (2008).

The total load distribution has parameters,

$$\mu_{\ln F} = \ln(\mu_F) - \tfrac{1}{2}\sigma_{\ln F}^2 \tag{2.16a}$$

$$\sigma_{\ln F}^2 = \ln\left(1 + \frac{\sigma_F^2}{\mu_F^2}\right) \tag{2.16b}$$

The design problem considered in this study involves a pile supporting loads having means and standard deviations shown in Table 2.2. The values in Table 2.2 used for mean loads to ensure that the designed pile length, H, doesn't exceed simulation depth, but results are scalable so the detailed means have little or no influence on final results.

Table 2.2 Load distribution parameters.

Parameters	μ_L	μ_D	σ_L	σ_D	μ_F	σ_F	$\mu_{\ln F}$	$\sigma_{\ln F}$
Values	20 kN	60 kN	6 kN	9 kN	80 kN	10.82 kN	4.4	0.14

Assuming bias factors k_D = 1.18 (Becker, 1996) and, k_L = 1.41 (Allen, 1975) and importance factor, I_i = 1.0, gives the characteristic live load, $\hat{F}_L$ = 1.41μ_L = 28.2 kN, dead load, $\hat{F}_D$ = 1.18μ_D = 70.8 kN, and characteristic total design load, $\alpha_L\hat{F}_L + \alpha_D\hat{F}_D$ = $1.5\hat{F}_L + 1.25\hat{F}_D$ = (1.5 × 28.2) + (1.25 × 70.8) = 130.8 kN.

2.4 Analytical Approach to Estimating the Probability of Failure

In order to estimate the probability of failure of a pile, the soil should first be modeled as a spatially varying random field. In general, cohesion will vary in all three dimensions, but there is little advantage in considering the 3^{rd} dimension since piles are essentially one-dimensional and only the 2^{nd} dimension is needed to consider distance between a sample and the pile location. Hence, this study considers a two-dimensional random field in which the pile is placed vertically at a certain position and soil samples, as in CPT or SPT sounding, are taken vertically at some, possibly different, position. The analytical approximation to the probability of pile failure in soils under total stress condition will be explained as follows.

When the soil properties are spatially variable, as they are in reality, then, Eq. (2.9) can be replaced by

$$R_u = pH\alpha\bar{c} \tag{2.17}$$

where $\bar{c}$ is the equivalent cohesion, defined as the uniform cohesion value which leads to the same ultimate strength as observed in the spatially varying soil over a pile of length, H. It is hypothesized here that $\bar{c}$ is the arithmetic average of the spatially variable cohesion over the pile length H,

$$\bar{c} = \frac{1}{H}\int_0^H c(z)\,dz \simeq \frac{1}{n}\sum_{i=1}^{n}\bar{c_i} \tag{2.18}$$

where $c(z)$ is interpreted as an average cohesion around the pile perimeter at depth z. If the pile is broken up into a series of n elements (as will be done in the simulation), the average is determined using the sum at the right of Eq. (2.18), where $\bar{c_i}$ is the local average of $c(z)$ over the i^{th} element, for $i = 1, ..., n$.

The required minimum design pile length, H, can be obtained by substituting Eq. (2.9) into

Eq. (2.5) (taking I_i = 1.0),

$$\varphi_{gu} p H \alpha \hat{c} = \alpha_L \hat{F}_L + \alpha_D \hat{F}_D \quad \rightarrow \quad H = \frac{\alpha_L \hat{F}_L + \alpha_D \hat{F}_D}{\varphi_{gu} p \alpha \hat{c}} \tag{2.19}$$

By further substituting Eq. (2.19) into Eq. (2.17), the ultimate resistance, R_u, can be estimated as,

$$R_u = \left(\frac{\alpha_L \hat{F}_L + \alpha_D \hat{F}_D}{\varphi_{gu}} \right) \left(\frac{\bar{c}}{\hat{c}} \right) \tag{2.20}$$

The reliability-based design goal in this study is to find the required length H such that the probability of the actual load, F, exceeding the actual resistance, R_u, is less than some maximum acceptable failure probability, p_m. The actual failure probability, p_f, is

$$p_f = \mathrm{P}\left[F > R_u\right] \tag{2.21}$$

and a successful design methodology will have $p_f \leq p_m$. Substituting Eq. (2.20) into Eq. (2.21) leads to

$$p_f = \mathrm{P}\left[F > \left(\frac{\alpha_L \hat{F}_L + \alpha_D \hat{F}_D}{\varphi_{gu}} \right) \left(\frac{\bar{c}}{\hat{c}} \right) \right] = \mathrm{P}\left[\frac{F \hat{c}}{\bar{c}} > \frac{\alpha_L \hat{F}_L + \alpha_D \hat{F}_D}{\varphi_{gu}} \right] \tag{2.22}$$

Letting

$$W = \frac{F \hat{c}}{\bar{c}} \tag{2.23a}$$

$$q = \alpha_L \hat{F}_L + \alpha_D \hat{F}_D \tag{2.23b}$$

means that

$$p_f = \mathrm{P}\left[W > \frac{q}{\varphi_{gu}} \right] \tag{2.24}$$

The computation of the probability in Eq. (2.24) involves the determination of the distribution of W. If the random load, F, and cohesion values, $\hat{c}$ and $\bar{c}$, are all assumed to be lognormally distributed, which is a reasonable assumption (Fenton and Griffiths, 2008, and Fenton et al., 2008), then the term, W will also be lognormally distributed and its parameters can be determined by considering the individual distributions of F, $\ln \hat{c}$, and $\ln \bar{c}$.

If W is lognormally distributed, then

$$\ln W = \ln F + \ln \hat{c} - \ln \bar{c} \tag{2.25}$$

is normally distributed and p_f can be found from

$$\begin{aligned} p_f &= \mathrm{P}\left[W > q/\varphi_{gu}\right] = \mathrm{P}\left[\ln W > \ln\left(q/\varphi_{gu}\right)\right] \\ &= 1 - \Phi\left(\frac{\ln\left(q/\varphi_{gu}\right) - \mu_{\ln W}}{\sigma_{\ln W}}\right) \end{aligned} \tag{2.26}$$

where Φ is the standard normal cumulative distribution function.

The failure probability p_f in Eq. (2.26) can be estimated once the mean and variance of $\ln W$ are determined. The mean and variance of $\ln W$ are

$$\mu_{\ln W} = \mu_{\ln F} + \mu_{\ln \hat{c}} - \mu_{\ln \bar{c}} \tag{2.27a}$$

$$\sigma^2_{\ln W} = \sigma^2_{\ln F} + \sigma^2_{\ln \hat{c}} + \sigma^2_{\ln \bar{c}} - 2\mathrm{Cov}\left[\ln \bar{c}, \ln \hat{c}\right] \tag{2.27b}$$

where the total load, F, and cohesion, c, are assumed to be independent. By applying first-order Taylor series approximations to the means, variances and covariance of $\ln \hat{c}$ and $\ln \bar{c}$, the components of Eq. (2.27) can be computed as follows ;

1) As discussed in section 2.3, the total load, F, is equal to the sum of the live load, F_L, and the static dead load, F_D, i.e. $F = F_L + F_D$, and the mean and variance of $\ln F$ can be evaluated using Eq's. (2.15) and (2.16).

2) With reference to Eq. (2.8),

$$\mu_{\ln \hat{c}} = \mathrm{E}\left[\ln \hat{c}\right] = \mathrm{E}\left[\ln\left(\frac{1}{m}\sum_{i=1}^{m} \hat{c}_i\right)\right] \simeq \ln(\mu_c) \tag{2.28a}$$

$$\sigma^2_{\ln \hat{c}} \simeq \frac{\sigma^2_{\ln c}}{m^2}\sum_{i=1}^{m}\sum_{j=1}^{m} \rho(z_i^o - z_j^o) \tag{2.28b}$$

In Eq. (2.28b), z_i^o is the spatial location of the center of the i'th soil sample ($i = 1, 2, \ldots, m$) and ρ is the correlation function defined by Eq. (2.12). Both equations make use of first-order Taylor series approximations (see Appendix A for more details). A further approximation occurs in the variance (Eq. (2.28b)) because of the fact that correlation coefficients between the local averages associated with observations are approximated by correlation coefficients between the local average centers. Assuming that $\ln \hat{c}$ actually represents a local average of $\ln c$ over the sample domain of size, D, then $\sigma^2_{\ln \hat{c}}$ is probably more accurately computed as

$$\sigma^2_{\ln \hat{c}} = \sigma^2_{\ln c}\gamma(D) \tag{2.29}$$

where $\gamma(D)$, is the variance reduction function that measures the reduction in variance due to local averaging over the sample domain D given by Eq. (2.13). In this research the

sample domain D, is assumed to be, $D = \Delta z \times m$, where m is the number of observations over sample domail D and Δz is the vertical dimention of a soil sample.

3) With reference to Eq. (2.18) and using many of the same arguments as in previous item, (see Appendix A for details)

$$\mu_{\ln \bar{c}} = \mathrm{E}\left[\ln\left(\frac{1}{H}\int_0^H c(z)\,dz\right)\right] \simeq \ln(\mu_c) \tag{2.30a}$$

$$\sigma^2_{\ln \bar{c}} \simeq \sigma^2_{\ln c}\gamma(H) \tag{2.30b}$$

where $\gamma(H)$ is defined by eq (2.13).

4) The covariance between the arithmetic average of the observed cohesion values over sample domain, $D = \Delta z \times m$, and the equivalent cohesion along the pile length, H, in Eq. (2.27) is obtained as follows (see Appendix A for details)

$$\begin{aligned}\mathrm{Cov}[\ln \bar{c}, \ln \hat{c}] &\simeq \frac{\sigma^2_{\ln c}}{mH}\sum_{i=1}^{m}\int_0^H \rho\left(\sqrt{r^2+(z-z_i^o)^2}\right)\,dz \\ &\simeq \sigma^2_{\ln c}\gamma_{HD}\end{aligned} \tag{2.31}$$

where γ_{HD} is the average correlation coefficient between the cohesion samples over domain D and the cohesion along the pile of length H, and ρ is the correlation function between $\ln c(z_i^o)$ and $\ln c(z)$. In detail, γ_{HD} is defined by,

$$\gamma_{HD} \simeq \frac{1}{mH}\sum_{i=1}^{m}\int_0^H \rho\left(\sqrt{r^2+(z-z_i^o)^2}\right)\,dz \tag{2.32}$$

where r is the horizontal distance between the pile centerline and the centerline of the soil sample column as shown in Figure 2.1. The approximation in the covariance arises both because the first-order Taylor series approximation and because of correlation coefficients between local averages associated with observations are approximated by correlation coefficients between the local average centers.

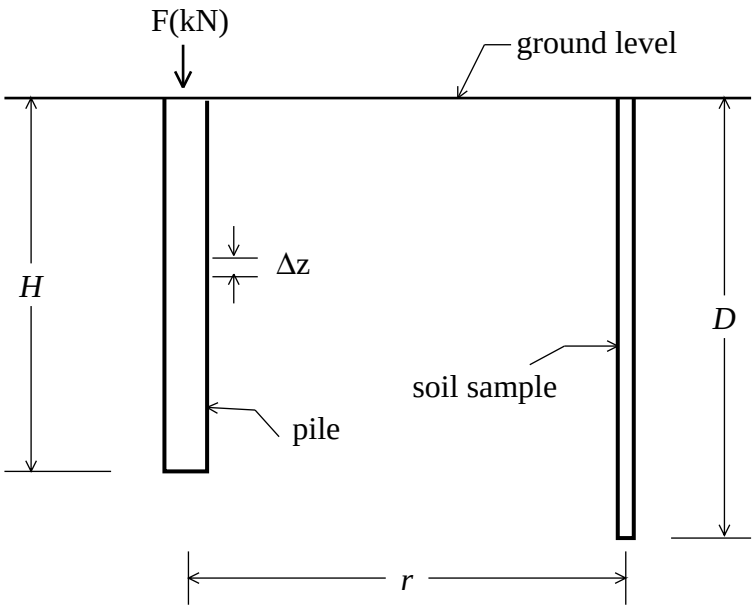

Figure 2.1 Relative locations of pile and soil sample.

Substituting Eq's (2.16), (2.28), (2.29), (2.30) and (2.31) into Eq. (2.27), leads to

$$\mu_{\ln W} = \mu_{\ln F} \tag{2.33a}$$

$$\sigma^2_{\ln W} \simeq \sigma^2_{\ln F} + \sigma^2_{\ln c}\left[\gamma(D) + \gamma(H) - 2\gamma_{HD}\right] \tag{2.33b}$$

which allows the probability of failure to be expressed as

$$p_f = 1 - \Phi\left(\frac{\ln\left(q/\varphi_{gu}\right) - \mu_{\ln W}}{\sigma_{\ln W}}\right) \tag{2.34}$$

The argument to Φ is the reliability index,

$$\beta = \frac{\ln q - \ln \varphi_{gu} - \mu_{\ln W}}{\sigma_{\ln W}} \tag{2.35}$$

If the reliability index is specified through knowledge of p_m, for example, then the geotechnical resistance factor is determined by

$$\varphi_{gu} = \exp\left(\ln q - \mu_{\ln W} - \beta\sigma_{\ln W}\right). \tag{2.36}$$

2.5 Simulation Results and Comparison with Predictions

In this section, probabilistic analyses of piles using Monte Carlo simulation are performed. The objective is to investigate the failure probability of a pile in soil under total stress condition with spatially varying cohesion field, c, via simulation in order to validate the theory developed in the previous section. Simulation essentially proceeds by carrying out a series of hypothetical designs on a series of simulated soil fields and checking to see what fraction of the designs fail.

In practice, the accuracy of the Monte Carlo method depends on how well the assumed probability distribution fits the real stochastic process. If the fit is reasonable, the accuracy increases with the number of simulation runs, i.e., better results will be obtained as the number of simulation realizations increases. In detail, the steps involved in the Monte Carlo simulation are as follows;

1) The cohesion, c, of a soil mass is simulated as a spatially variable random field using the Local Average Subdivision (LAS) method (Fenton and Vanmarcke, 1990). Cohesion is assumed to be lognormally distributed with mean 50 kPa and coefficient of variation, v_c, ranging from 0.1 to 0.5. The correlation length is varied from 0 to 50 m.

2) The simulated soil is sampled along a vertical line through the soil at some distance, r, from the pile. These virtually sampled soil properties are used to estimate the characteristic cohesion, $\hat{c}$, according to Eq. (2.8). Three sampling distances are considered: the first is at r = 0 m which means that the samples are taken at the pile location. In this case, uncertainty about the pile resistance only arises if the pile extends below the sampling depth. Typically, probabilities of failure when r = 0 m are very small. The other two sample distances considered are r = 4.5 m and r = 9.0 m, corresponding to reducing understanding of the soil conditions at the pile location. These rather arbitrary distances were based on preliminary random field simulations, which happened to involve fields 9 m in width. However, it is really the ratio, r/θ, which governs the failure probability.

3) The required design pile length, H, is calculated using Eq. (2.19).

4) Dead and live loads, F_D and F_L, are simulated as independent lognormally distributed random variables and then added to produce the actual total load on the pile, $F = F_L + F_D$. The means and standard deviations of the dead and live loads are assumed to be μ_D = 60kN, σ_D = 9kN and μ_L = 20kN, σ_L = 6kN, respectively.

5) The true ultimate pile resistance, R_u, is computed using Eq. (2.4).

6) The ultimate resistance, R_u, and total load F are compared. If $F > R_u$, then the pile, as designed, is assumed to have failed.

7) The entire process from step 1 to step 6 is repeated n_{sim} times (n_{sim} = 10000 in the present study). If n_f of these repetitions result in a pile failure, then an estimate of the probability of failure is $p_f = n_f/n_{sim}$.

8) Repeating steps 1 through 7 using various values of φ_{gu} in the design step allows plots of failure probability vs. geotechnical resistance factor to be produced for the various sampling distances, coefficient of variation of the cohesion, and correlation length.

The analytically estimated failure probabilities can be superimposed on the simulation-based failure probability plots, allowing a direct comparison of the methods. Figure 2.2 illustrates the agreement between failure probabilities estimated via simulation and those computed analytically using Eq. (2.34). Given all the approximations made in the theory, the agreement is considered to be excellent, allowing the geotechnical resistance factors to be computed analytically with reasonable confidence even at probability levels which the simulation cannot estimate – the simulation involved only 10000 realizations and so cannot properly resolve probabilities to less than about 10^{-4}.

It is immediately clear from Figure 2.2 that the probability of failure, p_f, increases with soil variability, v_c which is to be expected. Also, as expected, the probabilities of failure are smaller when the soil is sampled directly at the pile than when sampled some distance away from the pile centerline. This means that considerable construction savings can be achieved by improving the sampling scheme, especially when significant soil variability exists.

The failure probabilities are well predicted by the analytical technique when the sampling point is at the pile location (r = 0 m). There are some discrepancies for very small probabilities, but this maybe largely due to estimator error in the simulations. For example, if a simulation has 17 failures out of 10000, as in the highest point in Figure 2.2 a, the estimated probability of failure is p_f = 0.0017, which has standard error, $\sigma_{\hat{p_f}} = \sqrt{(0.0017)(0.9983)/10000} \simeq 0.0004$. and the 95% confidence interval on p_f is $0.0017 \pm 1.96(0.0004)$ = $[0.0009, 0.0025]$ which is quite wide. In fact, if only 5 failures are observed, then the 95% confidence interval on p_f is $[0.0001, 0.0009]$. In the other words, the simulation results cannot be trusted for p_f values less than about 0.001.

The good agreement between simulation and theory implies that the theory can be used to reliably estimate the pile failure probabilities. The theory will be used in the following section to provide recommendations regarding required geotechnical resistance factors for certain target probabilities of failure.

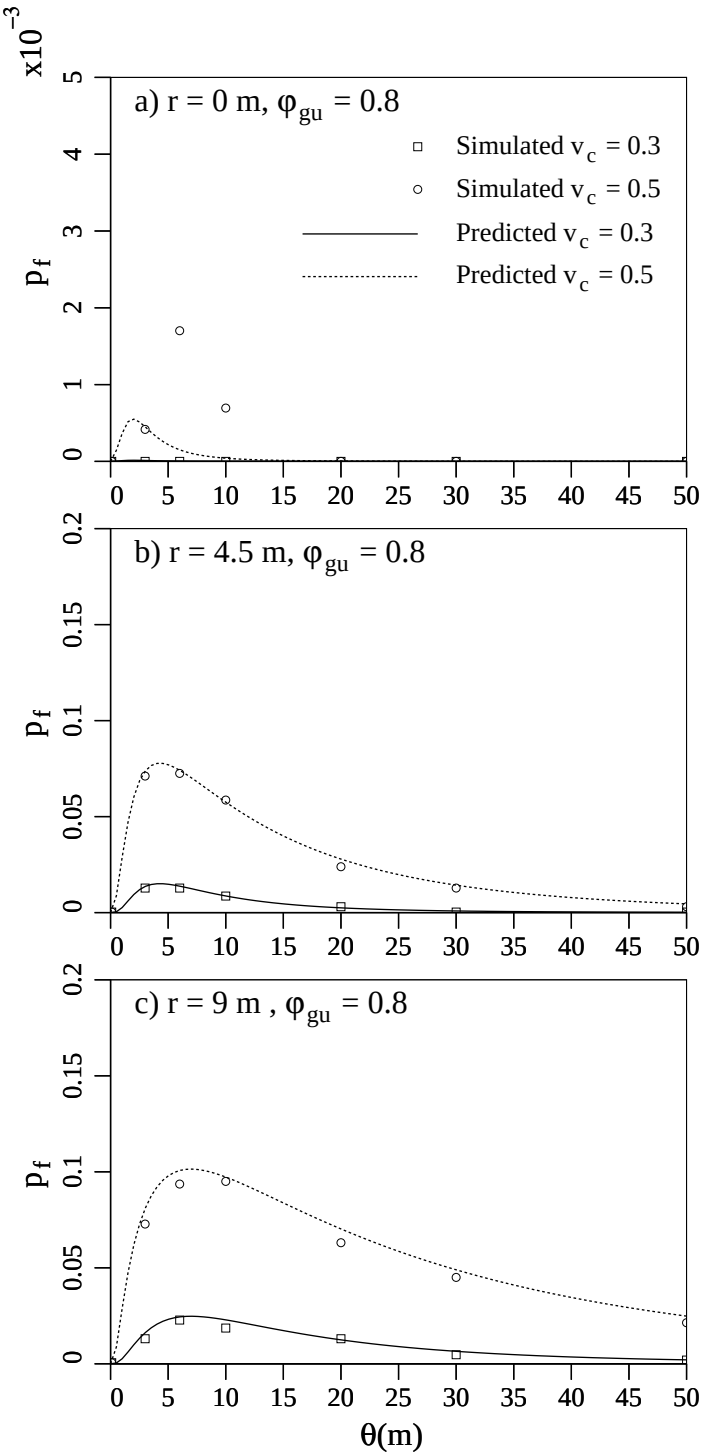

Figure 2.2 Comparison of failure probabilities estimated by simulation (10000 realizations) and analytical results for geotechnical resistance factor, φ_{gu} = 0.8, and three sampling locations.

2.6 Geotechnical Resistance Factors

In this section, the geotechnical resistance factors, φ_{gu}, required to achieve four maximum acceptable failure probability levels (10^{-2}, 10^{-3}, 10^{-4} and 10^{-5}) are theoretically investigated. The corresponding reliability indices of these four target probabilities are approximately 2.3, 3.1, 3.7, and 4.3, respectively.

Figures 2.3, 2.4, and 2.5 show the geotechnical resistance factors required for the cases where the soil is sampled at the pile location, at a distance of 4.5 m and at a distance of 9 m from the pile centerline, respectively.

Figure 2.3 corresponds to sampling at the pile location where the design conditions are so well understood that the geotechnical resistance factor exceeds 1.0 when $p_m \geq 10^{-3}$ (these cases are not shown).

The worse case geotechnical resistance factors occurs when the correlation length, θ is between about 1 and 10 m. This worst case is important, since the correlation length is very hard to estimate and will be unknown for most sites. In other words, in the absence of knowledge about the correlation length, the lowest geotechnical resistance factor in these plots, at the worst case correlation length, should be used.

To explain why a worst case exists, the nature of the correlation length must be considered. The correlation length, θ, measures the distance within which soil properties are significantly correlated. Low values of θ lead to soil properties which vary rapidly in space, while high values mean that the soil properties vary only slowly with position. A large correlation length, of say θ = 50 m, means that soil samples taken well within 50 m from the pile location (e.g. at 10 m) will be quite representative of the soil properties at the pile location. In other words, lower failure probabilities are expected when the soil is sampled well within the distance θ from the pile (see Appendix B for more details).

Interestingly, when θ is very small (say, 0.01 m), then the soil sample will consist of an large number of independent 'observations' whose average tends to be equal to the true mean. Since the pile also averages the soil properties, the pile 'sees' the same true mean value predicted by the soil sample. Therefore, the sample will accurately reflect the average conditions along the pile and in this case the failure probability is again low.

At intermediate correlation lengths, soil samples become imperfect estimators of conditions along the pile, and so the probability of failure increases, or conversely, the required geotechnical resistance factor decreases. Thus, the minimum required resistance factor will occur at some correlation length between 0.0 and infinity.

It is expected that the worst case correlation length will occur when θ is approximately equal to the distance from the pile to the sampling location. Notice in Figures 2.3, 2.4, and 2.5 that the worst case correlation length does show some increase as the distance to the sample location, r, increases.

As shown in Figure 2.5, the smallest geotechnical resistance factors correspond to the smallest acceptable failure probability shown, p_m = 10^{-5}, when the soil is sampled 9 m away from the pile centerline. When the cohesion coefficient of variation is relatively large, v_c = 0.5 the worst case values of φ_{gu} dip down to 0.15 in order to achieve p_m = 10^{-5}. In other words, there will be a significant construction cost penalty if a highly reliability pile is to be designed using a site investigation which is insufficient to reduce the residual variability to less than v_c = 0.5.

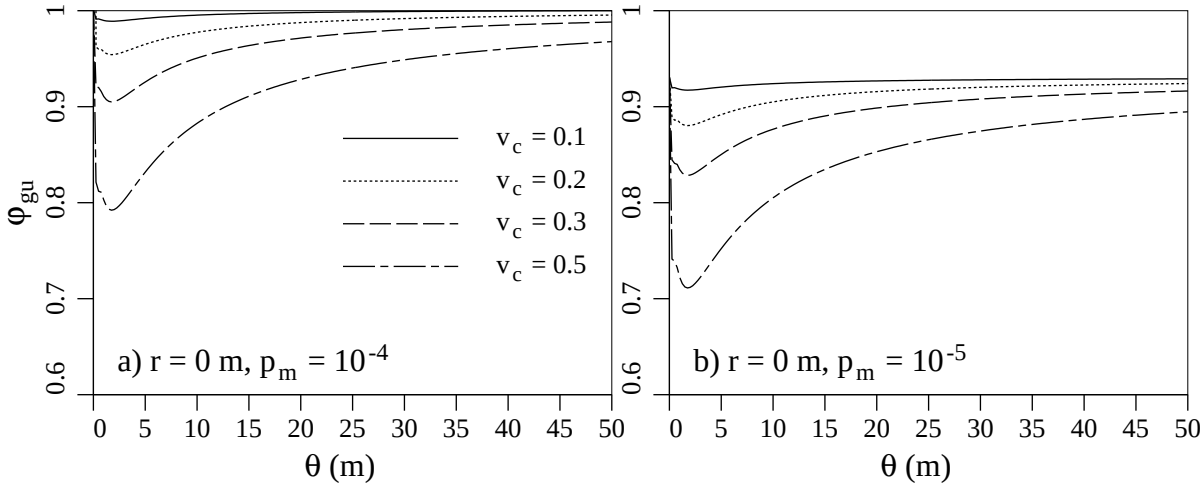

Figure 2.3 Geotechnical resistance factors when the soil has been sampled at the pile location (r = 0 m) (note the reduced vertical scale).

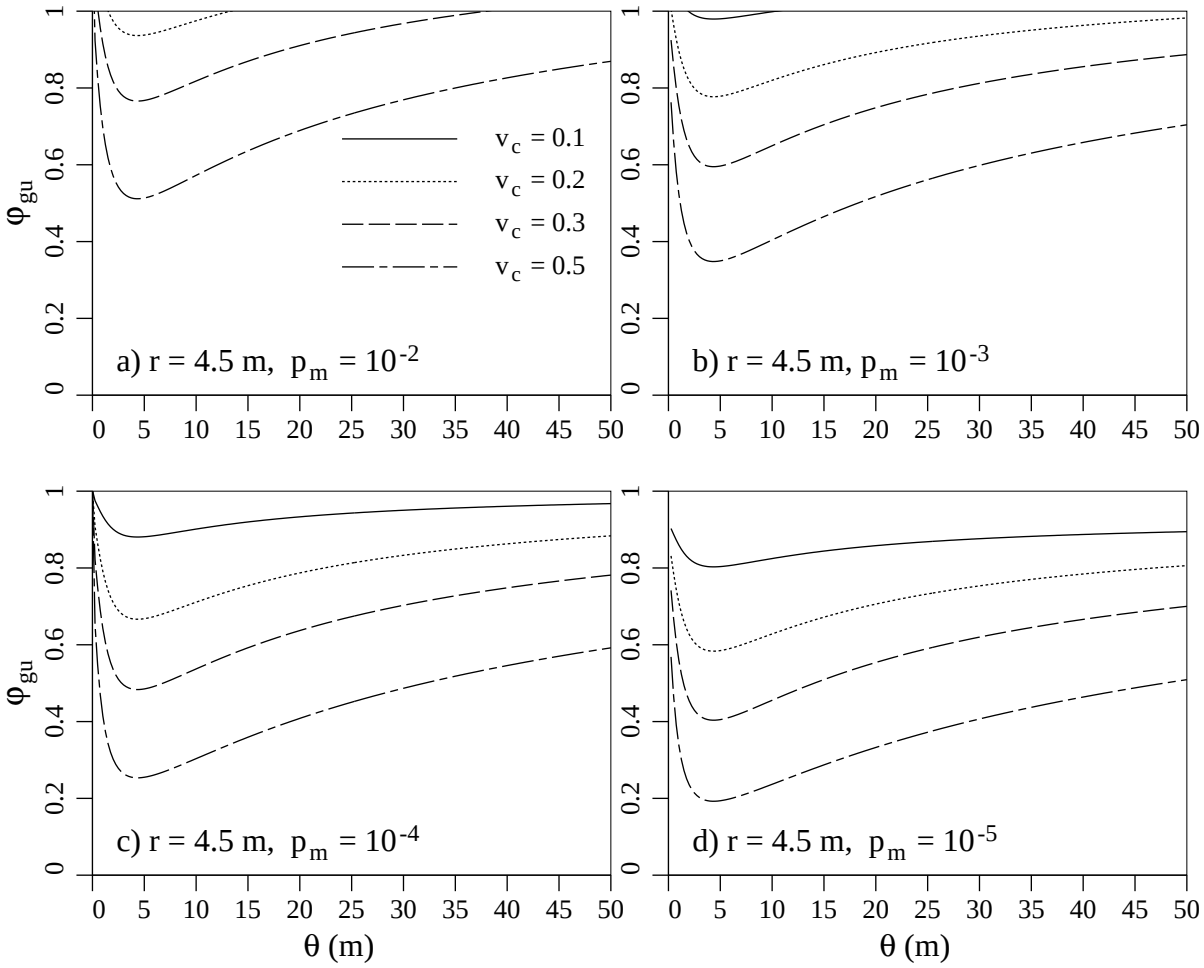

Figure 2.4 Geotechnical resistance factors when the soil has been sampled r = 4.5 m from the pile centerline.

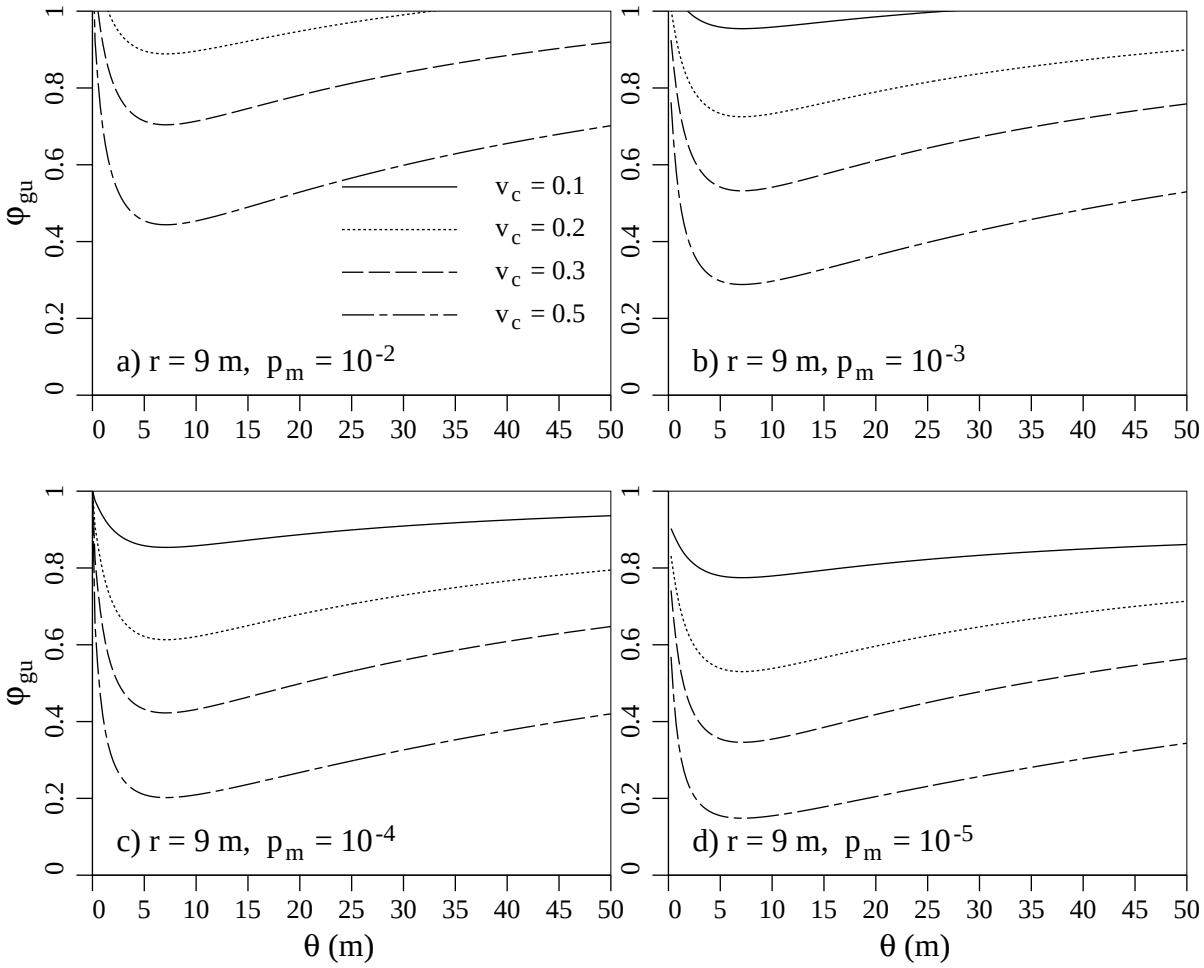

Figure 2.5 Geotechnical resistance factors when the soil has been sampled r = 9 m from the pile centerline

The worst case geotechnical resistance factors required to achieve the indicated maximum acceptable failure probabilities, as seen in Figures 2.3 through 2.5, are summarized in Table 2.3. Some of the geotechnical resistance factors recommended in this study for p_m = 10^{-2} are greater than 1.0, which may be because the load factors provide too much safety for the larger acceptable failure probabilities when the site is well understood.

Due to redundancy it is reasonable to use a lower reliability (larger p_m) for a single pile in pile groups. For example, if a single pile in a group has the smallest resistance and begins to fail, the load is transferred to other piles in the group with greater resistance and the overall foundation is less likely to fail. A reasonable value of maximum acceptable failure probability for single driven piles within a redundant group may be in the range of 10^{-2} and 10^{-3} (FHWA, 2005).

Table 2.3 Worst case geotechnical resistance factors for various coefficients of variation, v_c, distance to sampling location, r, and acceptable failure probabilities, p_m.

r (m)	v_c	Geotechnical Resistance Factor			
		p_m = 10^{-2}	p_m = 10^{-3}	p_m = 10^{-4}	p_m = 10^{-5}
0.0	0.1	1.20	1.08	0.99	0.92
0.0	0.2	1.17	1.05	0.95	0.88
0.0	0.3	1.13	1.00	0.91	0.83
0.0	0.5	1.04	0.90	0.79	0.71
4.5	0.1	1.15	0.98	0.88	0.80
4.5	0.2	0.94	0.78	0.66	0.58
4.5	0.3	0.78	0.60	0.49	0.41
4.5	0.5	0.51	0.35	0.25	0.20
9.0	0.1	1.09	0.95	0.85	0.77
9.0	0.2	0.89	0.73	0.61	0.53
9.0	0.3	0.70	0.53	0.42	0.36
9.0	0.5	0.43	0.29	0.20	0.15

Table 2.4 compares the resistance factors recommended in this study with those recommended by other sources. The resistance factors recommended in the current study (first three rows of Table 2.4), correspond to the case where v_c = 0.5 and r = 4.5 m for maximum acceptable failure probabilities, p_m = $10^{-3}, 10^{-4}$ and 10^{-5}.

To compare the recommended resistance factors, φ_{gu}, with values in other codes and the literature, the total load factor, $\hat{\alpha}_T$, and the ratio of the resistance factor to the total load

factor , $\varphi_{gu}/\hat{\alpha}_T$, which is the real measure of the overall "safety factor" used by each code, must be considered. According to Eq. (2.5), by increasing the value of the total load factor, $\hat{\alpha}_T$, the required resistance factor, φ_{gu}, increases. The dead load factor, α_D = 1.25, and live load factor, α_L = 1.5, are used in this study, as specified by the National Building Code of Canada (2005). The bias factors of k_D = 1.18 (Becker,1996), k_L = 1.41 (Allen, 1975) and the ratio of dead to live load μ_D/μ_L = 3.0 are chosen in this rsearch. Using these assumptions the characteristic dead to live load ratio, $\hat{R}_{D/L}$, and the total load factor, $\hat{\alpha}_T$, can be approximated by

$$\hat{R}_{D/L} = \frac{\hat{F}_D}{\hat{F}_D} = \frac{k_D\mu_D}{k_L\mu_L} = \frac{1.18(3\mu_L)}{1.41\mu_L} = \frac{1.18(3)}{1.41} = 2.5 \tag{2.37a}$$

$$\hat{\alpha}_T = \frac{\alpha_L\hat{F}_L + \alpha_D\hat{F}_D}{\hat{F}} = \frac{\alpha_L\hat{F}_L + \alpha_D\hat{F}_D}{\hat{F}_L + \hat{F}_D}$$

$$= \frac{\alpha_L + \alpha_D(\hat{F}_D/\hat{F}_L)}{1 + (\hat{F}_D/\hat{F}_L)} = \frac{1.5 + 1.25(2.5)}{1 + 2.5} = 1.32 \tag{2.37b}$$

The total load factors used in CFEM (2006), CHBDC (2006), and NBCC(2005) are all very close to the total load factor used in the current study and differ only because of a slight difference in the characteristic dead to live ratio, $\hat{R}_{D/L}$. The recommended ratios of the resistance factor to the total load factor, $\varphi_{gu}/\hat{\alpha}_T$, in CFEM(2006), CHBDC (2006), and NBCC (2005) are all very close to the recommended value in this study for r = 9 m and $p_m = 10^{-4}$.

As can be seen in Table 2.4, the total load factor used in Australian Standard, AS5100.3 (2004) is very close to the total load factor used in the current study. The recommended value for the ratio of the resistance factor to the total load factor, $\varphi_{gu}/\hat{\alpha}_T$, by Australian Standard, AS5100.3 (2004) is also very close to the recommended values in the current study for the maximum acceptable failure probability $p_m = 10^{-3}$ and both sample locations r = 4.5 m and r = 9 m.

The ratios of the resistance factor to the total load factor recommended by NCHRP 343 (Barker et al., 1991) and NCHRP 507 (Paikowsky, 2004) are based on a reliability index of 3.0 (p_m = 0.0013). The total load factor, $\hat{\alpha_T}$, considered in NCHRP 507 is close to the value used in this research and the recommended ratio of the resistance factor to the total load factor by NCHRP 507 is very close to the recommended value for r = 9 m and $p_m = 10^{-3}$. The recommended ratio of the resistance factor to the total load factor , $\varphi_{gu}/\hat{\alpha}_T$, by NCHRP343 tend to be in the range suggested in this research for maximum accaptable failure probabilies $p_m = 10^{-4}$ and 10^{-5}, despite its larger total load factor. Similarly,

recommended ratios of the resistance factor to the total load factor in ASSHTO (2002, 2004, and 2007) are very close to the range suggested in this research for p_m = 10^{-5}, which might be becasue of the larger total load factors used in AASHTO codes.

An explanation that the ratio of resistance factors to the total load factors proposed in the current study may be higher than the values from the codes in Table 2.4, is that the current study neglects measurement and model errors and so should be viewed as upper bounds to the resistance factors.

However, the code values correspond very well to those recommended in this research when samples are taken some distance away from the pile centerline, which may also be what the codes are assuming.

Table 2.4 Comparison of geotechnical resistance factors recommended in this study (first 6 lines) to those recommended by other sources, where $\hat{R}_{D/L}$ is the characteristic dead to live load ratio.

Source	**Load Factors**	$\hat{\alpha}_T$	φ_{gu}	$\varphi_{gu}/\hat{\alpha}_T$
r = 4.5 m, p_m = 10^{-3}	$\hat{R}_{D/L}$ = 2.5, α_L = 1.50, α_D = 1.25	1.32	0.60	0.45
r = 4.5 m, p_m = 10^{-4}	$\hat{R}_{D/L}$ = 2.5, α_L = 1.50, α_D = 1.25	1.32	0.49	0.37
r = 4.5 m, p_m = 10^{-5}	$\hat{R}_{D/L}$ = 2.5, α_L = 1.50, α_D = 1.25	1.32	0.41	0.31
r = 9.0 m, p_m = 10^{-3}	$\hat{R}_{D/L}$ = 2.5, α_L = 1.50, α_D = 1.25	1.32	0.53	0.40
r = 9.0 m, p_m = 10^{-4}	$\hat{R}_{D/L}$ = 2.5, α_L = 1.50, α_D = 1.25	1.32	0.42	0.32
r = 9.0 m, p_m = 10^{-5}	$\hat{R}_{D/L}$ = 2.5, α_L = 1.50, α_D = 1.25	1.32	0.36	0.27
CFEM (2006)	$\hat{R}_{D/L}$ = 3.0, α_L = 1.50, α_D = 1.25	1.31	0.40	0.31
NBCC (2005)	$\hat{R}_{D/L}$ = 3.0, α_L = 1.50, α_D = 1.25	1.31	0.40	0.31
CHBDC (2006)	$\hat{R}_{D/L}$ = 3.0, α_L = 1.70, α_D = 1.20	1.33	0.40	0.30
AS 5100.3 (2004)	$\hat{R}_{D/L}$ = 3.0, α_L = 1.80, α_D = 1.20	1.35	0.55	0.41
AASHTO (2004)	$\hat{R}_{D/L}$ = 3.7, α_L = 1.75, α_D = 1.25	1.36	0.39	0.29
NCHRP 507(2004)	$\hat{R}_{D/L}$ = 3.0, α_L = 1.70, α_D = 1.25	1.36	0.50	0.37
AASHTO (2007)	$\hat{R}_{D/L}$ = 3.0, α_L = 1.75, α_D = 1.25	1.38	0.40	0.29
AASHTO (2002)	$\hat{R}_{D/L}$ = 3.7, α_L = 2.17, α_D = 1.30	1.49	0.48	0.32
NCHRP 343 (1991)	$\hat{R}_{D/L}$ = 2.0, α_L = 2.17, α_D = 1.30	1.59	0.55	0.31

Chapter 3: Geotechnical Resistance Factors for Effective Stress Limit State Design of Deep Foundations

3.1 General

The soil supports the pile through a combination of end-bearing, and side friction and/or cohesion between the soil and pile. This chapter only examines effective stress resistance of piles (i.e. end-bearing is ignored). A mathematical theory is developed to analytically estimate the failure probability of deep foundations in soils under effective stress condition. The theoretical results are validated by simulation and then used to estimate failure probabilities and resistance factors required for design.

The ultimate geotechnical resistance of a pile R_u, due to effective stress resistance, δ, between the pile and its surrounding soil is approximated by,

$$R_u = \int_0^H p\tau(z)\,dz \tag{3.1}$$

where p is the effective perimeter length of the pile section, $\tau(z)$ is the average ultimate shear stress acting on the perimeter of the pile at depth z, and H is the embedded depth of the pile. The unit surface shear resistance in soils under effective stress condition can be represented by the equation,

$$\tau(z) = K(z)\sigma'_o(z)\tan\delta(z) \tag{3.2}$$

where $K(z)$ is the coefficient of lateral earth pressure at depth z, $\sigma'_o(z)$ is the effective vertical stress at depth z and $\delta(z)$ is the average interface friction angle between the soil and the pile perimeter at depth z. The effective vertical stress $\sigma'_o(z)$ and friction angle $\delta(z)$ can be written as,

$$\sigma'_o(z) = \gamma z \tag{3.3a}$$

$$\delta(z) = b\phi(z) \tag{3.3b}$$

where γ is the effective unit weight of soil, b is a reduction factor which from various investigations appears to be in the range of 0.5 to 0.8 (Das, 2000), and $\phi(z)$ is the average effective angle of internal friction of the soil around the pile perimeter at depth z.

The value of $K(z)$ is influenced by the friction angle, the method of pile installation, the compressibility and the degree of over consolidation as well as the material, size and shape of the pile. The value of $K(z)$ has been found to be approximately equal to the Rankine passive earth pressure coefficient, $K_p(z)$, at the top of the pile and may be less than the at-rest earth pressure coefficient, $K_o(z)$, at the pile tip (Das, 2000).

For coarse-grained soils, the coefficient of earth pressure at-rest can be estimated by the empirical relationship (Jaky, 1994)

$$K_o(z) = 1 - \sin\phi(z) \tag{3.4}$$

Based on presently available results, the following average values of $K(z)$ are recommended by Das (2000) for use in Eq. (3.2),

Table 3.1 Lateral earth pressure recommendations

Pile type	$K(z)$
Bored or jetted	$\simeq K_o(z) = 1 - \sin\phi(z)$
Low-displacement driven	$\simeq K_o(z) = 1 - \sin\phi(z)$ to $1.4K_o(z) = 1.4(1 - \sin\phi(z))$
High-displacement driven	$\simeq K_o(z) = 1 - \sin\phi(z)$ to $1.8K_o(z) = 1.8(1 - \sin\phi(z))$

In this research the earth pressure coefficient is assumed to be

$$K(z) = a(1 - \sin\phi(z)) \tag{3.5}$$

where a is in the range of $1 < a < 1.8$. According to Table 1, in this study three different values of a, namely $a = 1.0, 1.2$ and 1.4, are considered for bored, low-displacement and high-displacement driven piles, respectively (which are the midpoints of the ranges given in the Table 3.1).

Using the above information, the true ultimate effective stress resistance of a pile with length H and perimeter p, can be estimated to be,

$$R_u = \int_0^H p\gamma z a\,(1 - \sin\phi(z))\tan b\phi(z)\,dz \tag{3.6}$$

The Limit Sate Design (LSD) framework basically involves identifying possible failure modes (e.g. punching shear failure, and excessive settlement) and then ensuring that the factored geotechnical resistance at each limit state exceed the factored load. At the ultimate limit state, the design requirement is

$$\varphi_{gu}\hat{R}_u \geq \sum_i I_i\alpha_i\hat{F}_i \tag{3.7}$$

where φ_{gu} is the ultimate geotechnical resistance factor, $\hat{R}_u$ is the characteristic (design) ultimate geotechnical resistance, I_i is an importance factor corresponding to the i'th characteristic load effect, $\hat{F}_i$, and α_i is the i'th load factor.

The characteristic ultimate geotechnical resistance, $\hat{R}_u$, is determined using characteristic soil properties, in this case characteristic values of the soil's friction angle, ϕ. To obtain the characteristic soil properties, the soil is assumed to be sampled over a single column somewhere in the vicinity of the pile, for example by a CPT or SPT sounding near the pile. The sample is assumed to yield a sequence of m observed friction angle values, $\hat{\phi}_1, \hat{\phi}_2, \ldots, \hat{\phi}_m$. The characteristic value of the friction angle, $\hat{\phi}$, is defined in this research as an arithmetic average of the sampled observations, $\hat{\phi}_i$, which, can be computed as,

$$\hat{\phi} = \frac{1}{m} \sum_{i=1}^{m} \hat{\phi}_i \tag{3.8}$$

The characteristic ultimate geotechnical resistance, $\hat{R}_u$, is obtained by using the characteristic friction angle in Eq. (3.6),

$$\hat{R}_u = \frac{1}{2} pa\gamma H^2 (1 - \sin\hat{\phi}) \tan(b\hat{\phi}) \tag{3.9}$$

In order to determine the geotechnical resistance factor, φ_{gu}, required to achieve a certain acceptable reliability, the failure probability of the pile must be estimated. This probability will depend on the load distribution, the load and resistance factors selected, and the resistance distribution. The resistance and load distributions are discussed in Sections 3.2 and 2.3.

Section 3.3 develops the analytical framework and simulation algorithm for the failure probability estimate, and illustrates how the theoretical estimates agree with simulation.

The Load and Resistance Factor Design (LRFD) approach involves selecting a one or more maximum acceptable failure probability levels, p_m. The choice of p_m derives from a consideration of acceptable risk and directly influences the size of φ_{gu}. In this research, four maximum acceptable failure probabilities, $10^{-2}, 10^{-3}, 10^{-4}$ and 10^{-5}, will be considered, as discussed in chapter 2. Some of these failure probabilities, i.e $10^{-3}, 10^{-4}$, and 10^{-5}, might be appropriate for designs involving low (e.g. storage facilities), medium (typical structures), and high (e.g. hospitals and schools) failure consequence structures, respectively. The geotechnical resistance factors required to achieve these maximum acceptable failure probabilities will be recommended in Section 3.4.

3.2 The Random Soil Model

The friction angle, ϕ, is assumed to be bounded both above and below, ϕ_{max} = 0.7 radians and ϕ_{min} = 0.175 radians, so that neither normal nor lognormal distributions are appropriate. While a beta distribution is often used for bounded random variables, a beta distributed random field has a complex joint distribution and simulation is cumbersome and numerically difficult. To keep things simple, a bounded distribution is selected which resembles a beta distribution but which arises as a simple transformation of a standard normal random field, $G_\phi(z)$, according to

$$\phi(z) = \phi_{min} + \tfrac{1}{2}(\phi_{max} - \phi_{min}) \left\{ 1 + \tanh\left(\frac{sG_\phi(z)}{2\pi} \right) \right\} \tag{3.10}$$

where ϕ_{min} and ϕ_{max} are the minimum and maximum friction angles in radians, respectively, and s is a scale factor which governs the friction angle variability between its two bounds (see Fenton and Griffiths, 2008, for more details). Figure 3.2 shows how the distribution of ϕ changes as s changes, going from an almost uniform distribution at s = 5 to a very normal looking distribution for smaller s. Thus, varying s between about 0.1 and 5.0 leads to a wide range in the stochastic behaviour of ϕ. In all cases, the distribution is assumed to be symmetric so that the midpoint between ϕ_{min} and ϕ_{max} is the mean. Values of s greater than about 5 lead to a U-shaped distributions (higher at the boundaries), which are deemed to be unrealistic.

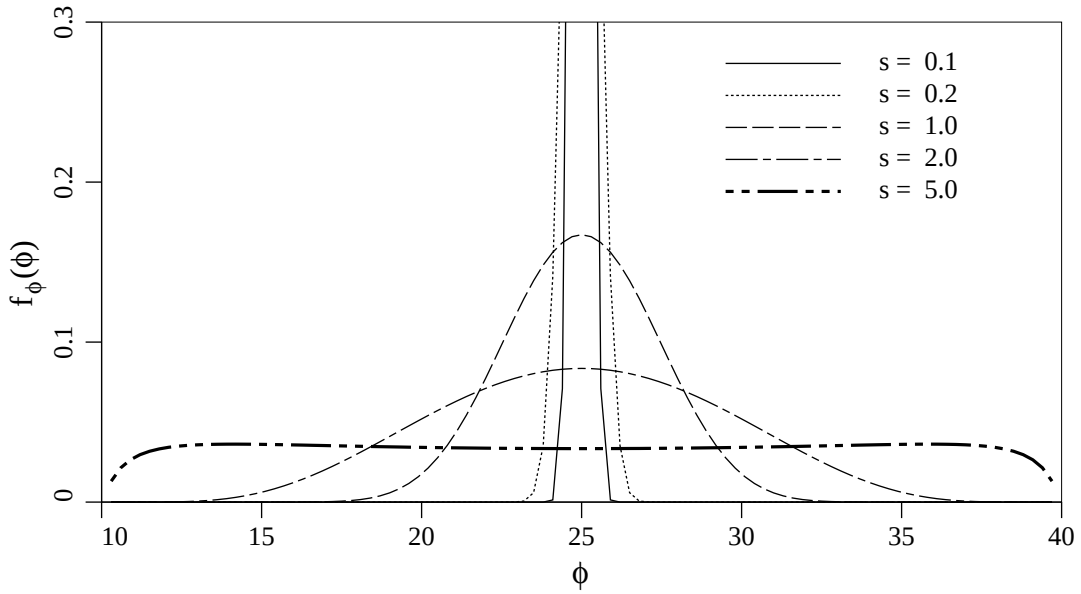

Figure 3.1 Bounded distribution of friction angle for ϕ_{min} = 10°(0.175 radians) and ϕ_{max} = 40°(0.70 radians)

The following relationship between s and the variance of ϕ derives from a third-order Taylor series approximation to tanh and a first-order approximation to the final expectation (Fenton and Griffiths, 2008),

$$\sigma_\phi \simeq \frac{0.46(\phi_{max} - \phi_{min})s}{\sqrt{4\pi^2 + s^2}} \tag{3.11}$$

where ϕ_{min} and ϕ_{max} are in radians. Equation (3.11) can be generalized to yield the covariance between $\phi(z_i)$ and $\phi(z_j)$, for any two spatial points z_i and z_j as follows,

$$\text{Cov}\left[\phi(z_i), \phi(z_j)\right] \simeq (0.46)^2(\phi_{max} - \phi_{min})^2 \frac{s^2\rho(z_i - z_j)}{4\pi^2 + s^2} \simeq \sigma_\phi^2 \rho(z_i - z_j) \tag{3.12}$$

where ρ is the correlation function between the friction angle at a point $G_\phi(z_i)$ and a second point $G_\phi(z_j)$. In this study, a simple exponentially decaying (Markovian) correlation function will be assumed, of the form

$$\rho(t) = \exp\left(-\frac{2|t|}{\theta}\right) \tag{3.13}$$

where $t = z_i - z_j$ is the distance between the two points. Note that the correlation function reflects the correlation between points in the underlying normally distributed random field, $G_\phi(z)$, and not directly between points in the friction field (although the correlation lengths in the different spaces are quite similar).

Two other results needed in the next section are as follows:

First, the variance reduction function, $\gamma(H)$, which specifies how the variance is reduced upon local averaging of ϕ over some depth H, is defined by,

$$\gamma(H) = \frac{1}{H^2}\int_0^H \int_0^H \rho(z_1 - z_2)\, dz_1\, dz_2 \tag{3.14}$$

Second, the relationship between the coefficient of variation of the friction angle , $v_\phi = \sigma_\phi/\mu_\phi$, and s can be obtained by using Eq. (3.11) (see Appendix C for details)

$$s \simeq \frac{2\pi v_\phi \mu_\phi}{\sqrt{(0.46)^2(\phi_{max} - \phi_{min})^2 - (v_\phi \mu_\phi)^2}} \tag{3.15}$$

By using Eq. (3.15) the friction angle coefficient of variations v_ϕ and their corresponding s values, for ϕ_{min} = 0.175 radians and ϕ_{max} = 0.70 radians, are given in Table 3.2.

Table 3.2 Coefficient of variations of friction angle and corresponding s values, for ϕ_{min} = 0.175 radians and ϕ_{max} = 0.70 radians.

v_ϕ	0.1	0.2	0.3	0.344
s	1.16	2.44	4.07	5

3.3 Analytical Estimation of Failure Probability

In order to estimate the probability of failure of a pile, the soil is first modeled as a spatially varying random field. This study considers a two-dimensional random field in which the pile is placed vertically at a certain position and soil samples as in a CPT or SPT sounding, are taken vertically at some, possibly different, position. The analytical approximation to estimate the failure probability of a pile in soils under effective stress condition can be explained as follows. When the soil properties are spatially variable, as they are in reality, then, Eq. (3.6) can be replaced by

$$R_u = \frac{1}{2} pa\gamma H^2 (1 - \sin\bar{\phi}) \tan(b\bar{\phi}) \tag{3.16}$$

where $\bar{\phi}$ is the equivalent friction angle of the soil, defined as the uniform (constant) soil parameter which leads to the same resistance as observed in the spatially varying soil over the entire pile length, H. It is assumed here that $\bar{\phi}$ is the arithmetic average of the spatially variable friction angle over the pile length H,

$$\bar{\phi} = \frac{1}{H} \int_0^H \phi(z)\, dz \simeq \frac{1}{n} \sum_{i=1}^{n} \bar{\phi}_i \tag{3.17}$$

where $\phi(z)$ is interpreted as an average friction angle of the soil around the perimeter of the pile at depth z. If the pile is broken up into a series of elements (as will be done in the simulation), $\bar{\phi}$ is determined using the sum at the right of Eq. (3.17), in which $\bar{\phi}_i$ is the local average of $\phi(z)$ over the i^{th} element, for $i = 1, ..., n$.

The required minimum design pile length, H, can be obtained by substituting Eq. (3.9) into Eq. (3.7) (taking $I_i = 1.0$),

$$\varphi_{gu} \left(\frac{1}{2} pa\gamma H^2 (1 - \sin\hat{\phi}) \tan(b\hat{\phi}) \right) = \alpha_L \hat{L}_L + \alpha_D \hat{L}_D \tag{3.18}$$

therefore

$$H = \sqrt{\frac{2\left(\alpha_L \hat{L}_L + \alpha_D \hat{L}_D\right)}{\varphi_{gu} pa\gamma (1 - \sin\hat{\phi}) \tan(b\hat{\phi})}} \tag{3.19}$$

By substituting Eq. (3.19) into Eq. (3.16), the ultimate geotechnical resistance, R_u, can be written as,

$$R_u = \left(\frac{\alpha_L \hat{L}_L + \alpha_D \hat{L}_D}{\varphi_{gu}} \right) \frac{(1 - \sin\bar{\phi}) \tan(b\bar{\phi})}{(1 - \sin\hat{\phi}) \tan(b\hat{\phi})} \tag{3.20}$$

The reliability-based design goal in this study is to find the required length H such that the probability that the actual load, F, exceeds the actual resistance, R_u, is less than some small acceptable failure probability, p_m. The actual failure probability, p_f, is

$$p_f = \mathrm{P}\left[F > R_u\right] \tag{3.21}$$

and a successful design methodology will have $p_f \leq p_m$. Substituting Eq. (3.20) into Eq. (3.21) leads to

$$\begin{aligned} p_f &= \mathrm{P}\left[F > \frac{\alpha_L \hat{L}_L + \alpha_D \hat{L}_D}{\varphi_{gu}} \left(\frac{(1-\sin\bar{\phi})\tan(b\bar{\phi})}{(1-\sin\hat{\phi})\tan(b\hat{\phi})}\right)\right] \\ &= \mathrm{P}\left[\frac{F(1-\sin\hat{\phi})\tan(b\hat{\phi})}{(1-\sin\phi)\tan(b\phi)} > \frac{\alpha_L \hat{L}_L + \alpha_D \hat{L}_D}{\varphi_{gu}}\right] \end{aligned} \tag{3.22}$$

Letting

$$\hat{X} = (1-\sin\hat{\phi})\tan(b\hat{\phi}) \tag{3.23a}$$

$$\bar{X} = (1-\sin\bar{\phi})\tan(b\bar{\phi}) \tag{3.23b}$$

$$q = \alpha_L \hat{F}_L + \alpha_D \hat{F}_D \tag{3.23c}$$

$$Y = \frac{F\hat{X}}{X} \tag{3.23d}$$

means that,

$$p_f = \mathrm{P}\left[Y > q/\varphi_{gu}\right] \tag{3.24}$$

The computation of the probability in Eq. (3.24) involves the determination of the distribution of Y. Assuming that Y is lognormally distributed (an assumption that is supported to some extent by the central limit theorem) then

$$\ln Y = \ln F + \ln\hat{X} - \ln\bar{X} \tag{3.25}$$

is normally distributed and p_f can be found from

$$\begin{aligned} p_f &= \mathrm{P}\left[Y > q/\varphi_{gu}\right] = \mathrm{P}\left[\ln Y > \ln\left(q/\varphi_{gu}\right)\right] \\ &= 1 - \Phi\left(\frac{\ln\left(q/\varphi_{gu}\right) - \mu_{\ln Y}}{\sigma_{\ln Y}}\right) \end{aligned} \tag{3.26}$$

where Φ is the standard normal cumulative distribution function.

The failure probability p_f in Eq. (3.26) can be estimated once the mean and variance of $\ln Y$ are determined. These are

$$\mu_{\ln Y} = \mu_{\ln F} + \mu_{\ln \hat{X}} - \mu_{\ln \bar{X}} \tag{3.27a}$$

$$\sigma^2_{\ln Y} = \sigma^2_{\ln F} + \sigma^2_{\ln \hat{X}} + \sigma^2_{\ln \bar{X}} - 2\text{Cov}\left[\ln \bar{X}, \ln \hat{X}\right] \tag{3.27b}$$

where the total load, F, and friction angle, ϕ, are assumed to be independent. By applying third-order Taylor series approximations to the means, variances and covariance of $\ln \hat{X}$ and $\ln \bar{X}$, the components of Eq. (3.27) can be computed as follows ;

1) Assuming that the total load F is equal to the sum of the maximum live load, F_L, acting over the lifetime of the structure and the static dead load, F_D, i.e. $F = F_L + F_D$, both of which are random, then

$$\mu_{\ln F} = \ln(\mu_F) - \tfrac{1}{2}\sigma^2_{\ln F} \tag{3.28a}$$

$$\sigma^2_{\ln F} = \ln\left(1 + \frac{\sigma^2_F}{\mu^2_F}\right) \tag{3.28b}$$

where $\mu_F = \mu_L + \mu_D$ is the sum of the mean live and dead loads, and σ^2_F is the variance of the total load defined by

$$\sigma^2_F = \sigma^2_L + \sigma^2_D \tag{3.29}$$

assuming dead and live loads to be independent.

2) With reference to Eq. (3.8) and the fact that the friction angle is assumed to be stationary,

$$\mu_{\hat{\phi}} = \text{E}\left[\frac{1}{m}\sum_{i=1}^{m}\hat{\phi}_i\right] = \frac{1}{m}\sum_{i=1}^{m}\mu_\phi = \mu_\phi \tag{3.30}$$

The mean and variance of $\ln \hat{X}$, can be obtained by using Eq. (3.30) and a third-order Taylor series approximation to the expectation of Eq. (3.23a) as follows (see Appendix E for details)

$$\mu_{\ln \hat{X}} \simeq \ln\left((1 - \sin\mu_\phi)\tan(b\mu_\phi)\right) + \frac{\sigma^2_{\hat{\phi}} d_2}{2} \tag{3.31a}$$

$$\sigma^2_{\ln \hat{X}} \simeq d_1^2\sigma^2_{\hat{\phi}} + \left(\frac{d_2^2}{2} + d_1 d_3\right)\sigma^4_{\hat{\phi}} + \frac{5d_3^2\sigma^6_{\hat{\phi}}}{12} \tag{3.31b}$$

where d_1, d_2 and d_3 are given in Eq. (C.2). The variance of $\hat{\phi}$ can be obtained from,

$$\sigma^2_{\hat{\phi}} \simeq \frac{\sigma^2_\phi}{m^2}\sum_{i=1}^{m}\sum_{j=1}^{m}\rho(z_i^o - z_j^o) \tag{3.32}$$

where σ_ϕ is given by Eq. (3.11), z_i^o is the spatial location of the center of the i'th soil sample ($i = 1, 2, \ldots, m$) and ρ is the correlation function defined by Eq. (3.13). The approximation in eq (3.32) arises because correlation coefficients between the local averages associated with observations are approximated by correlation coefficients between the local average centers. Assuming that $\hat{\phi}$ actually represents a local average of ϕ over a sample length of size, $D = \Delta z \times m$, where D is the depth over which the samples are taken, m is the number of observations over sample depth D and Δz is the vertical dimension of the soil sample then, $\sigma^2_{\hat{\phi}}$ is probably more accurately computed as

$$\sigma^2_{\hat{\phi}} = \sigma^2_\phi \gamma(D) \tag{3.33}$$

where $\gamma(D)$, is the variance reduction function that measures the reduction in variance due to local averaging over the sample length D, as given by Eq. (3.14). All angles are measured in radians, including those used in Eq's (3.11) and (3.12).

3) With reference to Eq. (3.17),

$$\mu_{\bar{\phi}} = \mathrm{E}\left[\left(\frac{1}{H}\int_0^H \phi(z)\,dz\right)\right] = \frac{1}{H}\int_0^H \mu_\phi\,dz = \mu_\phi \tag{3.34}$$

By applying Eq's (3.34) and (3.23b), the mean and variance of $\ln \bar{X}$ can be obtained in the same fashion as for $\ln \hat{X}$ (in fact, they only differ due to differing local averaging in the variance calculation).

$$\mu_{\ln \bar{X}} \simeq \ln\left((1 - \sin\mu_\phi)\tan(b\mu_\phi)\right) + \frac{\sigma^2_{\bar{\phi}} d_2}{2} \tag{3.35a}$$

$$\sigma^2_{\ln \bar{X}} \simeq d_1^2 \sigma^2_{\bar{\phi}} + \left(\frac{d_2^2}{2} + d_1 d_3\right)\sigma^4_{\bar{\phi}} + \frac{5 d_3^2 \sigma^6_{\bar{\phi}}}{12} \tag{3.35b}$$

$$\sigma^2_{\bar{\phi}} \simeq \sigma^2_\phi \gamma(H) \tag{3.35c}$$

where d_1, d_2, d_3 and $\gamma(H)$ are defined by eq's (C.2) and (3.14), respectively.

4) The covariance between $\ln \hat{X}$ over sample depth, $D = \Delta z \times m$, and $\ln \bar{X}$ along the pile length, H, in Eq. (3.27) is approximated by

$$\begin{aligned}\mathrm{Cov}\left[\ln \bar{X}, \ln \hat{X}\right] \simeq\ & d_1^2 \sigma^2_\phi \gamma_{HD} + \sigma^2_\phi \gamma_{HD}\left(\frac{d_1 d_3}{2}(\sigma^2_{\hat{\phi}} + \sigma^2_{\bar{\phi}}) + \frac{d_3^2}{4}\sigma^2_{\hat{\phi}}\sigma^2_{\bar{\phi}}\right) \\ & + \frac{d_2^2}{2}\left(\sigma^2_\phi \gamma_{HD}\right)^2 + \frac{d_3^2}{6}\left(\sigma^2_\phi \gamma_{HD}\right)^3\end{aligned} \tag{3.36}$$

where γ_{HD} is the average correlation coefficient between the sample length D and pile length H. In detail, γ_{HD} is defined by,

$$\gamma_{HD} \simeq \frac{1}{mH}\sum_{i=1}^{m}\int_0^H \rho\left(\sqrt{r^2 + (z - z_i^o)^2}\right)\,dz \tag{3.37}$$

where r is the horizontal distance between the pile centerline and the centerline of the soil sample column and ρ is the correlation coefficient between $\phi(z_i^o)$ and $\phi(z)$, as illustrated in Figure 3.3.

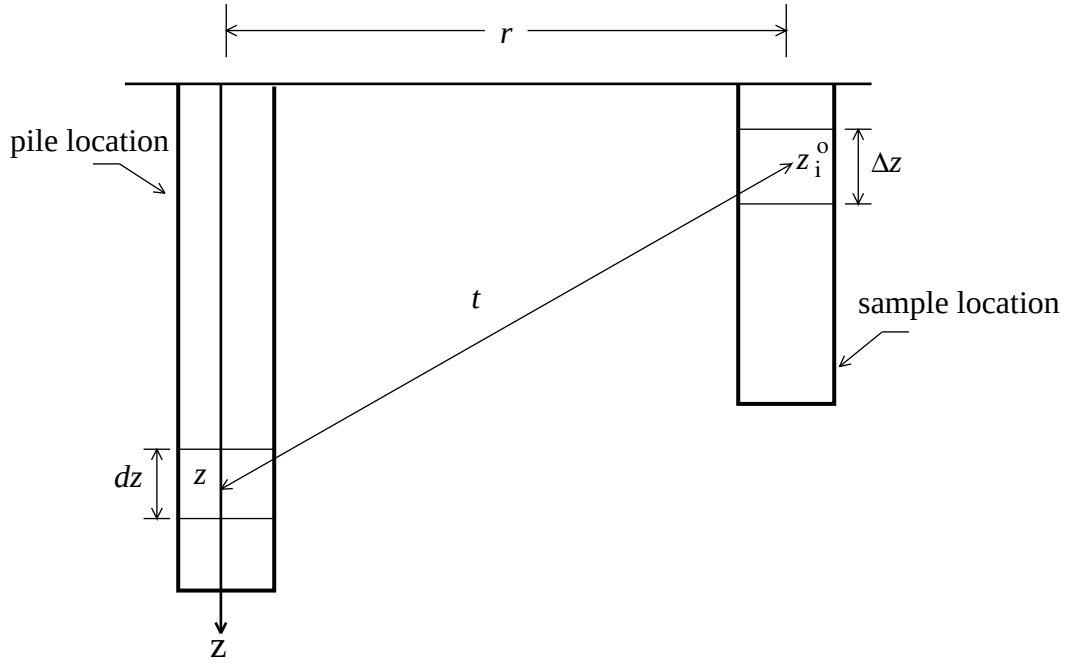

Figure 3.2 Correlation between local averages is approximated by the correlation function, $\rho(t)$, between centers.

The approximation in the covariance (Eq. (3.36)) arises both because of the use of a third-order Taylor series approximation and because correlation coefficients between local averages associated with observations are approximated by correlation coefficients between the local average centers.

Substituting Eq's (3.28), (3.31), (3.35) and (3.36) into Eq. (3.27), leads to

$$\mu_{\ln Y} \simeq \mu_{\ln F} + \frac{d_2}{2}(\sigma_{\hat{\phi}}^2 - \sigma_{\bar{\phi}}^2) \tag{3.38a}$$

$$\sigma_{\ln Y}^2 \simeq \sigma_{\ln F}^2 + d_1^2(\sigma_{\bar{\phi}}^2 + \sigma_{\hat{\phi}}^2) + \left(\frac{d_2^2}{2} + d_1 d_3\right)(\sigma_{\bar{\phi}}^4 + \sigma_{\hat{\phi}}^4)$$
$$+ \frac{5d_3^2}{12}(\sigma_{\bar{\phi}}^6 + \sigma_{\hat{\phi}}^6) - 2\mathrm{Cov}\left[\ln \bar{X}, \ln \hat{X}\right] \tag{3.38b}$$

which allows the probability of failure to be expressed as

$$p_f = 1 - \Phi\left(\frac{\ln\left(q/\varphi_{gu}\right) - \mu_{\ln Y}}{\sigma_{\ln Y}}\right) \tag{3.39}$$

where Φ is the standard normal cumulative distribution function. The argument to Φ is the reliability index,

$$\beta = \frac{\ln q - \ln \varphi_{gu} - \mu_{\ln Y}}{\sigma_{\ln Y}} \tag{3.40}$$

If the reliability index is specified through knowledge of p_m, for example, then the geotechnical resistance factor is determined by

$$\varphi_{gu} = \exp\left(\ln q - \mu_{\ln Y} - \beta\sigma_{\ln Y}\right). \tag{3.41}$$

3.4 Comparison of Analytical Estimation of Failure Probability with Simulation

To test the proposed analytical results, a series of n_{sim} = 10000 realizations of a pile are simulated for each of a range of soil variability parameters and sampling distances. The resulting Monte Carlo simulation-based failure probability estimates are then compared to the analytical results presented in section 3.3.

In detail the Monte Carlo simulation proceeds as follows;

1) The friction angle, ϕ, of a soil mass is simulated as a spatially variable random field using the Local Average Subdivision (LAS) method (Fenton and Vanmarcke, 1990). The number of soil cells in X and Y directions are assumed to be 128 $\times$ 128 and each cell size dimentions are taken to be 0.1 $\times$ 0.1. The correlation length is varied from 0 to 50 m, and two coefficients of variation of friction angle, v_ϕ, are considered: v_ϕ = 0.2 (s = 2.44) and v_ϕ = 0.3 (s = 4.07). The friction angle is assumed to range from ϕ_{min} = 0.175 radians (10°) and ϕ_{max} = 0.70 radians (40°).

2) The simulated soil is sampled along a vertical line through the soil at some distance, r, from the pile. These virtually sampled soil properties are used to estimate the characteristic friction angle, $\hat{\phi}$, according to Eq. (3.8). Three sampling distances are considered: the first is at r = 0 m which means that the samples are taken at the pile location. In this case, uncertainty about the pile resistance only arises if the pile extends below the sampling depth. Typically, probabilities of failure when r = 0 m are very small. The other two sample distances considered are r = 4.5 m and r = 9.0 m, corresponding to reduced understanding of the soil conditions at the pile location (see

Figure 3.4). These rather arbitrary distances were based on preliminary random field simulations, which happened to involve fields 9 m in width. However, it is really the ratio, r/θ, which governs the failure probability. No attempt is made here to include the effects of measurement error nor of errors in mapping actual observations, e.g. CPT values, to engineering properties such as friction angle. Thus the predicted failure probability (either from theory or simulation) will be somewhat unconservative (failure probability increases as measurement error increases). However both the analytical technique and the simulation treat measurement errors in the same way, allowing a consistent comparison between the two.

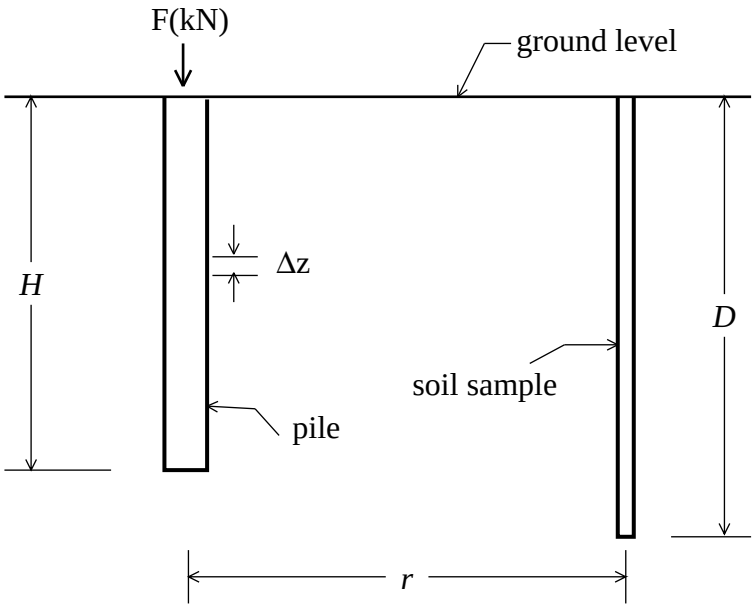

Figure 3.3 Relative locations of pile and soil sample.

3) The required design pile length, H, is calculated using Eq. (3.19).

4) Dead and live loads, F_D and F_L, are simulated as independent lognormally distributed random variables and then added to produce the actual total load on the pile, $F = F_L + F_D$. The means and standard deviations of the dead and live loads are assumed to be μ_D = 60kN, σ_D = 9kN and μ_L = 20kN, σ_L = 6kN, respectively.

5) The true ultimate pile resistance, R_u, is computed using Eq. (3.6).

6) The ultimate resistance, R_u, and total load F are compared. If $F > R_u$, then the pile, as designed, is assumed to have failed.

7) The entire process from step 1 to step 6 is repeated n_{sim} times (n_{sim} = 10000 in the present study). If n_f of these repetitions result in a pile failure, then an estimate of the probability of failure is $p_f \simeq n_f/n_{sim}$.

8) Repeating steps 1 through 7 using various values of φ_{gu} in the design step allows plots of failure probability vs. geotechnical resistance factor to be produced for the various sampling distances, coefficients of variation of the friction angle, and correlation length.

The comparison between the probabilistic analyses of piles using Monte Carlo simulation based on 10000 realizations with those computed analytically by Eq. (3.39) for the values of the pile interface friction angle coefficient, b = 0.8 and coefficient of earth pressure a = 1.2, are illustrated in Figure 3.5 (see Appendix F for more figures).

It can be seen from Figure 3.5 that the agreement between theory and simulations, is good and theory can be used to produce the required geotechnical resistance factors to achieve the maximum acceptable failure probabilities $10^{-2}, 10^{-3}, 10^{-4}$ and 10^{-5}.

It is immediately clear in Figure 3.5 that the probability of failure, p_f, increases with soil variability, v_ϕ which is to be expected. Also, as expected, the probabilities of failure are smaller when the soil is sampled directly at the pile than when sampled some distance away from the pile centerline. This means that considerable construction savings can be achieved by improving the sampling scheme, especially when significant soil variability exists.

As seen in Appendix F (Figures F.1, F.2 and F.3) , when the soil is sampled at r = 4.5 m and r = 9 m, the probability of failure slightly increases with pile interface friction angle coefficient, b, and earth pressure coefficient, a. According to Eq. (3.19), The design pile length, H, depends on the values of b and a, and decreases with increasing values of b and a. By decreasing the H, covariance functions $\gamma(H)$ and γ_{HD} increase (Eq's. (3.37) and (3.14)). Also, first, second and third order derivatives, d_1, d_2 and d_3 increase by b. This implies that $\sigma_{\ln Y}$, also increases with b and a, which means increasing probability of failure in Eq. (3.39).

When the samples are taken at the pile location (r = 0 m), $\gamma(H) \simeq \gamma_{HD}$ (Eq. (3.37)). By increasing the values of a and b, both $\gamma(H)$ and γ_{HD} increase but $\gamma(H) \simeq \gamma_{HD}$. This implies that $\sigma^2_{\ln \bar{X}} \simeq \text{Cov}\left[\ln \hat{X}, \ln \bar{X}\right]$ (Eq's (3.35) and (3.36)) which means that by increasing a and b the variance of $\ln Y$ and therefore failure probability p_f, decreases.

The failure probabilities are well predicted by the analytical technique when the sampling point is at the pile location (r = 0 m). There are some discrepancies for very small probabilities, but this maybe largely due to estimator error in the simulations. In fact, for those simulations having 1 failures out of 10000, the estimated probability of failure is

$p_f = 10^{-4}$, which has standard error, $\sigma_{\hat{p_f}} = \sqrt{(10^{-4})(0.9999)/10000} \simeq 10^{-4}$. This means that the simulation cannot be used to validate small probabilities, i.e. probabilities less than about 10^{-4}, so the location of the points with failure probability less than 10^{-4} is highly uncertain. The potential for large estimator error is seen in both Figure 3.5 (a) where most failure probability estimates are zero, except for those "worst" cases where 1 in 10000 realizations failed.

Overall, however, the agreement between simulation and theory is good, implying that the theory can be used to reliably estimate the pile failure probabilities. The analytical results will be used in the following section to provide recommendations regarding required geotechnical resistance factors for certain target probabilities of failure.

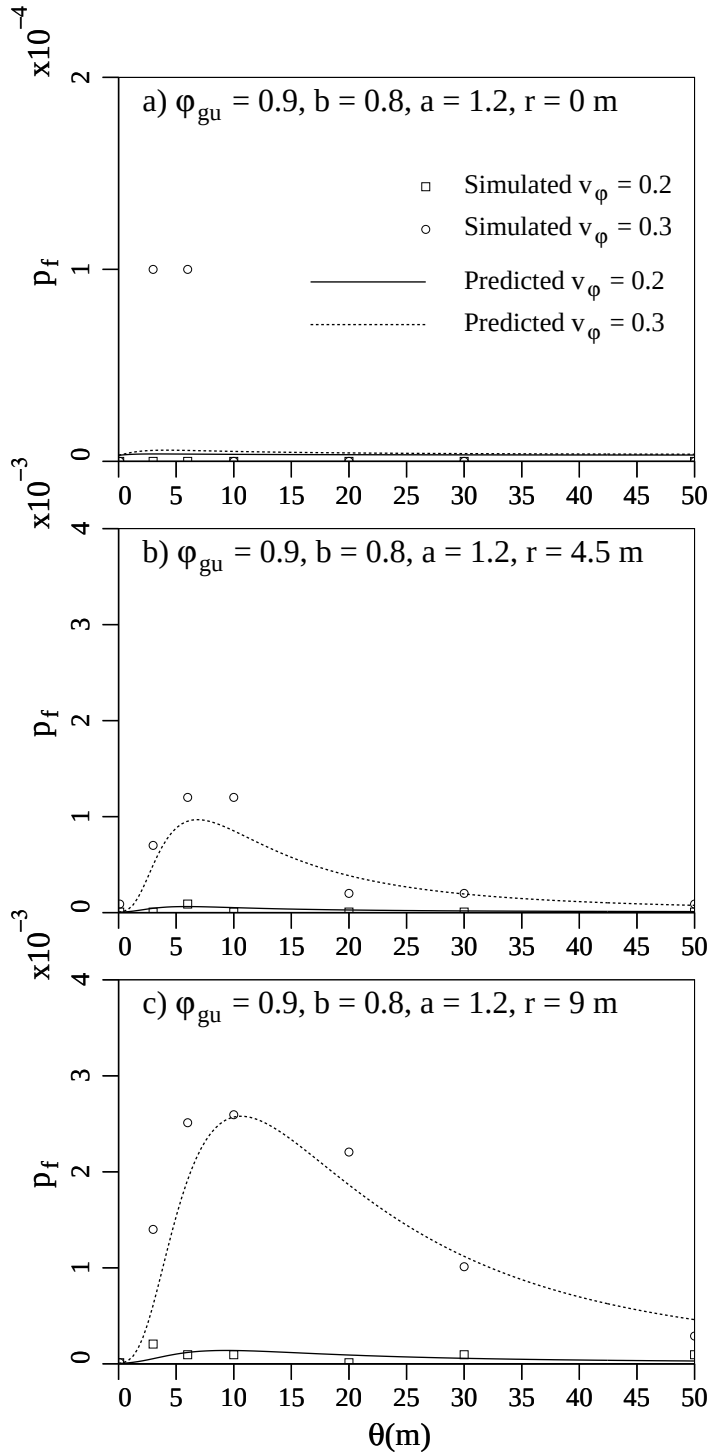

Figure 3.4 Comparison of failure probabilities estimated by simulation (10000 realizations) and analytical results for geotechnical resistance factor, φ_{gu} = 0.9, b = 0.8, a = 1.2 and three sampling locations.

3.5 Geotechnical Resistance Factors

In this section, the geotechnical resistance factor, φ_{gu}, required to achieve four maximum acceptable failure probability levels (10^{-2}, 10^{-3}, 10^{-4} and 10^{-5}) will be investigated. The corresponding reliability indices of these four target probabilities are approximately 2.3, 3.1, 3.7, and 4.3, respectively.

Figures 3.7 through 3.9 show the geotechnical resistance factors required for the cases where the soil is sampled at the pile location, at a distance of r = 4.5 m and at a distance of r = 9 m from the pile centerline for the pile interface friction angle coefficient, b = 0.8 and earth pressure coefficient a = 1.2. Four coefficient of variations, v_ϕ = 0.1 (s = 1.16), v_ϕ = 0.2 (s = 2.44), v_ϕ = 0.3 (s = 4.07) and v_ϕ = 0.344 (s = 5) are considered for the three sampling locations.

In the cases where the samples are taken at the pile location and the design conditions are well understood, the geotechnical resistance factor exceeds 1.0 when $p_m \geq 10^{-3}$. In the cases where the samples are taken 4.5 m and 9 m from pile centerline, the geotechnical resistance factor exceeds 1.0 when $p_m \geq 10^{-2}$. The cases where $\varphi_{gu} > 1.0$ are not shown.

The worse case geotechnical resistance factors occurs when the correlation length, θ is between about 1 and 10 m. This worst case is important, since the correlation length is very hard to estimate and will be unknown for most sites, as was discussed in Chapter 2.

As seen in Figure 3.9, the smallest geotechnical resistance factors correspond to the smallest acceptable failure probability considered, p_m = 10^{-5}, when the soil is sampled 9 m away from the pile centerline, as expected. When the friction angle coefficient of variation, v_ϕ, are relatively large (v_ϕ = 0.344) the worst case values of φ_{gu} dip down to 0.57 in order to achieve p_m = 10^{-5}. In other words, there will be a significant construction cost penalty if a highly reliability pile is to be designed using a site investigation which is insufficient to reduce the residual variability to less than v_ϕ = 0.344.

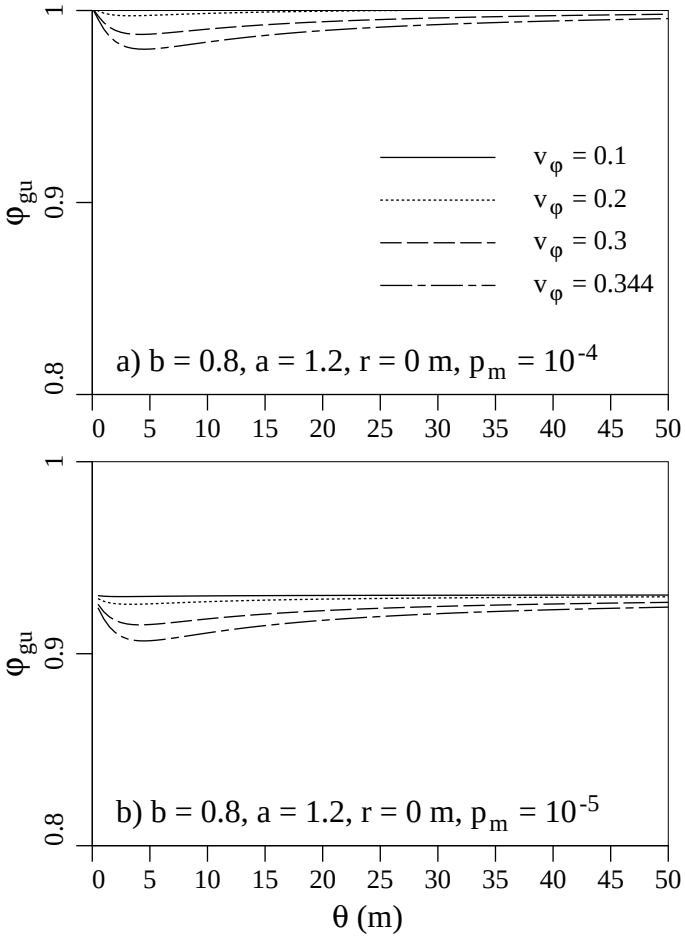

Figure 3.5 Geotechnical resistance factors when the soil has been sampled at the pile location (r = 0 m) (note the reduced vertical scale).

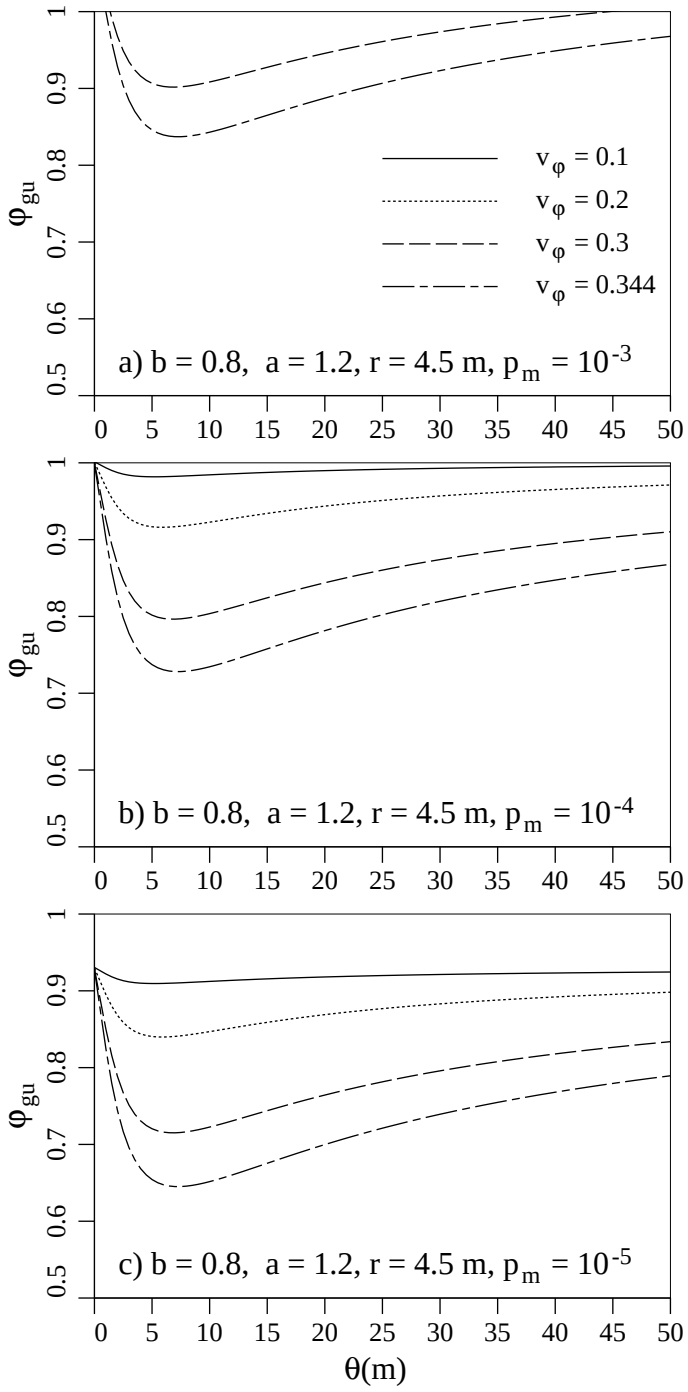

Figure 3.6 Geotechnical resistance factors when the soil has been sampled r = 4.5 m from the pile centerline.

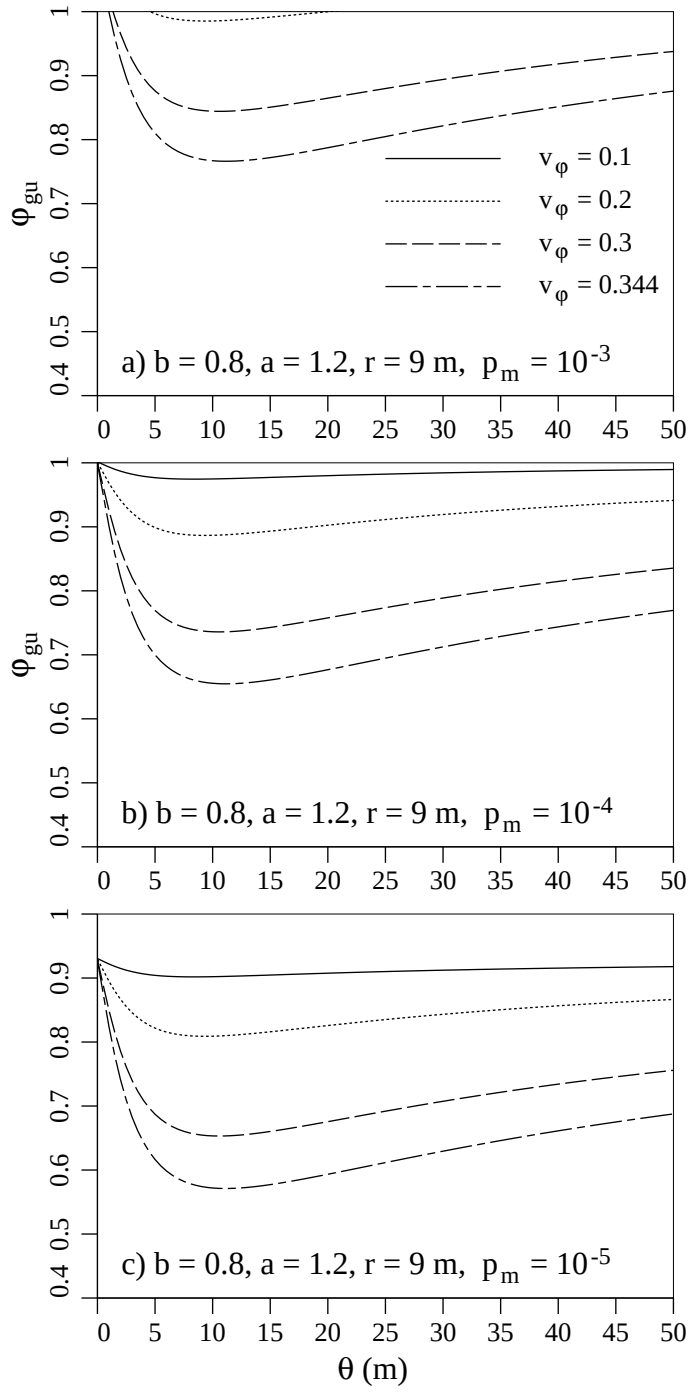

Figure 3.7 Geotechnical resistance factors when the soil has been sampled r = 9 m from the pile centerline

The worst case geotechnical resistance factors required to achieve the indicated maximum acceptable failure probabilities, as seen in Figure 3.7 through 3.9, is summarized in Table

3.3. Some of the geotechnical resistance factors recommended in this study for p_m = 10^{-2} and p_m = 10^{-3} are greater than 1.0, which may be because the load factors provide too much safety for the larger acceptable failure probabilities when the site is well understood. A reasonable value of maximum acceptable failure probability for single driven piles within a redundant group may be in the range of 10^{-2} to 10^{-3} (FHWA, 2005).

Table 3.3 Worst case geotechnical resistance factors for pile interface friction angle coefficient, b = 0.8, earth pressure coefficient a = 1.2, various coefficients of variation, v_ϕ, distance to sampling location, r, and acceptable failure probabilities, p_m.

r (m)	v_ϕ	Geotechnical Resistance Factor			
		p_m = 10^{-2}	p_m = 10^{-3}	p_m = 10^{-4}	p_m = 10^{-5}
0.0	0.1	1.21	1.09	1.00	0.93
0.0	0.2	1.20	1.08	0.99	0.93
0.0	0.3	1.19	1.06	0.99	0.92
0.0	0.344	1.17	1.04	0.98	0.91
4.5	0.1	1.19	1.08	0.98	0.91
4.5	0.2	1.15	1.02	0.92	0.84
4.5	0.3	1.06	0.90	0.80	0.71
4.5	0.344	1.00	0.85	0.72	0.64
9.0	0.1	1.19	1.07	0.98	0.90
9.0	0.2	1.13	0.99	0.89	0.81
9.0	0.3	1.02	0.85	0.74	0.65
9.0	0.344	0.93	0.77	0.65	0.57

Table 3.4 compares the geotechnical resistance factors recommended in this study with those recommended by other sources. The geotechnical resistance factors recommended in the current study occupy the first six rows of Table 3.4 and correspond to the cases where v_ϕ = 0.344 and samples are taken 4.5 m and 9 m from the pile centerline for maximum acceptable failure probabilities, p_m = $10^{-3}, 10^{-4}$ and 10^{-5}.

To compare the recommended geotechnical resistance factors, φ_{gu}, with values in other codes and the literature, the total load factor, $\hat{\alpha}_T$, and the ratio of the geotechnical resistance factor to the total load factor , $\varphi_{gu}/\hat{\alpha}_T$, which is the real measure of the overall "safety factor" used by each code, must be considered. According to Eq. (3.7), by increasing the value of the total load factor, $\hat{\alpha}_T$, the required geotechnical resistance factor, φ_{gu}, increases. The dead load factor, α_D = 1.25, and live load factor, α_L = 1.5, are used in this study, as

specified by the National Building Code of Canada (2005). The total load factors $\hat{\alpha}_T$ given in Table 3.4, are computed by using Eq. (2.37).

It can be seen from Table 3.4 that the ratio of the geotechnical resistance factor to the total load factor, $\varphi_{gu}/\hat{\alpha}_T$, recommended in this research when the soil is sampled 9 m from the pile centerline for p_m = 10^{-4}, 0.49, is close to those given by AASHTO (2004). The recommended $\varphi_{gu}/\hat{\alpha}_T$ ratio given by AASHTO (2004) is reasonably close the recommended ratios in this research when r = 4.5 m and p_m = 10^{-4} and also when r = 9 m and p_m = 10^{-3}.

The reason that the geotechnical resistance factors proposed in the current study are generally higher than the values from the other codes in Table 3.4 might be because measurement and model errors have been included in the other codes when estimating the geotechnical resistance factors. For example, CPT tests were used for the estimation of the geotechnical resistance factors suggested by the Australian Standard Bridge Design Code (2004), which presumably include measurement errors as part of the overall estimation process.

Table 3.4 Comparison of geotechnical resistance factors recommended in this study (first six lines) to those recommended by other sources for pile interface friction angle coefficient, b = 0.8, earth pressure coefficient a = 1.2 and characteristic dead to live load ratio $\hat{R}_{D/L}$.

Source	**Load Factors**	$\hat{\alpha}_T$	φ_{gu}	$\varphi_{gu}/\hat{\alpha}_T$
r = 4.5 m, p_m = 10^{-3}	$\hat{R}_{D/L}$ = 2.5, α_L = 1.50, α_D = 1.25	1.32	0.85	0.64
r = 4.5 m, p_m = 10^{-4}	$\hat{R}_{D/L}$ = 2.5, α_L = 1.50, α_D = 1.25	1.32	0.72	0.55
r = 4.5 m, p_m = 10^{-5}	$\hat{R}_{D/L}$ = 2.5, α_L = 1.50, α_D = 1.25	1.32	0.64	0.48
r = 9.0 m, p_m = 10^{-3}	$\hat{R}_{D/L}$ = 2.5, α_L = 1.50, α_D = 1.25	1.32	0.77	0.58
r = 9.0 m, p_m = 10^{-4}	$\hat{R}_{D/L}$ = 2.5, α_L = 1.50, α_D = 1.25	1.32	0.65	0.49
r = 9.0 m, p_m = 10^{-5}	$\hat{R}_{D/L}$ = 2.5, α_L = 1.50, α_D = 1.25	1.32	0.57	0.43
CFEM (2006)	$\hat{R}_{D/L}$ = 3.0, α_L = 1.50, α_D = 1.25	1.31	0.40	0.31
NBCC (2005)	$\hat{R}_{D/L}$ = 3.0, α_L = 1.50, α_D = 1.25	1.31	0.40	0.31
CHBDC (2006)	$\hat{R}_{D/L}$ = 3.0, α_L = 1.70, α_D = 1.20	1.33	0.40	0.30
AS5100.3 (2004)	$\hat{R}_{D/L}$ = 3.0, α_L = 1.80, α_D = 1.20	1.35	0.55	0.41
AASHTO (2004)	$\hat{R}_{D/L}$ = 3.7, α_L = 1.75, α_D = 1.25	1.36	0.70	0.50
NCHRP507 (2004)	$\hat{R}_{D/L}$ = 3.0, α_L = 1.70, α_D = 1.25	1.36	0.50	0.37
AASHTO (2007)	$\hat{R}_{D/L}$ = 3.0, α_L = 1.75, α_D = 1.25	1.38	0.40	0.29
AASHTO (2002)	$\hat{R}_{D/L}$ = 3.7, α_L = 2.17, α_D = 1.30	1.49	0.48	0.32
NCHRP343 (1991)	$\hat{R}_{D/L}$ = 2.0, α_L = 2.17, α_D = 1.30	1.59	0.55	0.35

Chapter 4: Conclusion

4.1 Summary and Conclusions

This study proposes reliability-based design provisions for the Load and Resistance Factor Design (LRFD) of ultimate limit state design of deep foundations under axial compression loading in soils under effective stress and total stress conditions. The load factors are as used in the National Building Code of Canada (NRC, 2005). A mathematical theory was developed to analytically estimate the probability of pile failure. The analytical model assumes a statistically random soil with lognormally distributed cohesion, c, for soils under total stress condition and tanh distributed friction angle, ϕ, for soils under effective stress condition. The effect of the soil's spatial variability and site underestanding on the geotechnical resistance factor has been investigated via simulation and theory, by considering various soil statistics and sampling locations. The simulation involved 10000 realizations for each set of parameters and the results of the Monte Carlo simulation were compared to the proposed theory. Optimal geotechnical resistance factors were recommended for the design of deep foundations for four target probability of failures ($10^{-2}, 10^{-3}, 10^{-4}$ and 10^{-5}).

The suggested design procedure using the proposal Load and Resistance Factor Design(LRFD) method is summarized as follows:

1) decide on a maximum acceptable failure probability, p_m for the pile. The choice of p_m depends on the severity of failure consequences;
2) sample the soil and estimate the characteristic soil property using Eq's (2.8) or (3.8). The characteristic ultimate resistance is calculated using Eq's (2.9) or (3.9);
3) determine load factors from structural design codes as described in section 2.3;
4) select an upper bound geotechnical resistance factor for the maximum acceptable failure probability, p_m, and sampling location from Table 2.3. The actual geotechnical resistance factor used in design maybe reduced somewhat, depending on the magnitude of model and measurement errors;

5) estimate the required pile length given load factors, α_L and α_D, geotechnical resistance factor, φ_{gu} and the effective pile perimeter, p, using LRFD as described in Eq's (2.19) and (3.19).

No attempt is made here to include the effects of measurement error nor of errors in mapping actual observations, e.g. CPT values, to engineering properties such as friction angle. Thus the predicted failure probability (either from theory or simulation) will be somewhat unconservative (failure probability increases as measurement error increases). However both the analytical technique and the simulation treat measurement errors in the same way, allowing a consistent comparison between two. Also, this can be accomodated to some extent by using a σ_c^2 or v_ϕ value larger than the actual value.

The recommended geotechnical resistance factors for ultimate limit state design of deep foundations should be considered to be upper bounds because the measurement and model errors are not considered in this study. The statistics of measurement errors are very difficult to determine, since the true values need to be known. Similarly, model errors, which relate both the errors associated with translating measured values (e.g. CPT measurements to friction angle values) and the errors associated with predicting effective stress and total stress resistance by equations, such as Eq's (2.2) and (3.2), to the actual effective stress and total stress resistance are extremely difficult to measure simply because the true effective stress - total stress resistance along with the true soil properties, are rarely, if ever, known. When confidence in the measured soil properties or in the model used is low, the results presented here can still be employed by assuming that the soil samples were taken further away from the the pile centerline than they actually were (e.g. if low-quality soil samples are taken at the pile location, r = 0, the geotechnical resistance factor corresponding to a larger value of r, say r = 4.5 m should be used), or by using a larger variance.

The evaluation of geotechnical resistance factors for pile design involves the soil field's uncertainty level (e.g. coefficient of variations of cohesion, v_c and friction angle, v_ϕ), the pile interface friction angle coefficients, b, (soils under effective stress condition) correlation level (e.g. correlation length, θ) and sampling locations. Since coefficients of variation, v_c and v_ϕ, the pile interface friction angle coefficient, b, and correlation length, θ, are usually unknown for a given site, various values for v_c, v_ϕ and b are considered in this study for deep foundation limit state design, along with a worse case value of θ, i.e. the intermediate value of θ corresponding to the higher probabilities of failure.

Three sampling schemes have been considered in this study. Better estimates of conditions at the pile can be obtained when samples are taken at the pile location (r = 0 m). Specifically, lower probability of failures and larger geotechnical resistance factor values are obtained

by sampling at the pile location.

Both the theory and the simulation demonstrates that a worst case correlation length exists. The good agreement between the geotechnical resistance factors based on this worst case, shown in Tables 2.4 and 3.4, and current literature and LRFD code recommendations, suggests that the theory is in reasonable agreement with past experience.

The overall agreement between the analytically derived geotechnical resistance factors proposed in this study and those currently used in other codes, as shown in Tables 2.4 and 3.4, is encouraging. The current study now provides a rigorous basis for the determination of upper bound geotechnical resistance factors in pile design in soils under effective and total stress conditions and the theory provides a framework to extend code provisions beyond calibration with the past.

4.2 Future Work

Additional areas in need of additional research are as follows;

1) This research concentrates on reliability-based design of a single pile. Similar research is also needed on the reliability-based design of pile groups taking redundancy into account.

2) In this research interpretation and model errors are not included. Further study should be carried out to consider these errors and also include the assesment of load tests on full scale productive piles.

3) There are two soil parameters considered random in this research, c and ϕ. They were studied separately, additional study are required to the more general case of $c - \phi$. The unit weight of soil γ, also needed to be considered as random field for future work.

References

AASHTO (2002). Standard Specifications for Highways Bridges. American Association of State Highway and Transportation Officials, Seventeenth Edition Washington, DC.

AASHTO (2004). LRFD Bridge Design Specifications. American Association of State Highway and Transportation Officials, Third Edition Washington, DC.

AASHTO (2007). LRFD Bridge Design Specifications, American Association of State Highway and Transportation Officials, Washington, DC.

Allen, D.E. (1975). Limit States Design – A probabilistic study. *Canadian Journal of Civil Engineering*, 36 (2): 36–49.

Australian Standard (2004). Bridge Design, Part 3: Foundations and Soil-Supporting Structures, AS 5100.3–2004, Sydney, Australia.

Barker, R., Duncan, J., Rojiani, K., Ooi, P., Tan, C., and Kim, S. (1991). NCHRP Report 343: Manuals for the design of bridge foundations. TRB, National Research Council, Washington, DC.

Becker D.E. (1996 a) Eighteenth Canadian Geotechnical Colloquium: Limit States Design For Foundations. Part 1. An overview of the foundation design process, *Canadian Geotechnical Journal*, 33(6), 956-983.

Becker D.E. (1996 b) Eighteenth Canadian Geotechnical Colloquium: Limit States Design For Foundations. Part 2. Development for National Building Codes of Canada, *Canadian Geotechnical Journal*, 33(6), 984-1007.

CHBDC – Canadian Standards Association (2006) Canadian Highway Bridge Design Code (CHBDC), A National Standard of Canada, CAN/CSA Standard S6-06, CSA International, Rexdale, Ontario.

Canadian Geotechnical Society (2006). Canadian Foundation Engineering Manual, 4th Ed., BiTech publications, Vancouver, BC.

Cherubini, C. (2000). Reliability evaluation of shallow foundation bearing capacity on c', ϕ' soils. Canadian Geotechnical Journal, 37: 264–269.

Das, B.M. (2000) Fundamentals of Geotechnical Engineering, Brooks/Cole, Pacific Grove, CA.

Fenton, G.A. and Vanmarcke, E.H. (1990) Simulation of random fields via Local Average Subdivision, *ASCE Journal of Engineering Mechanics*, 116(8), 1733-1749.

Fenton, G.A. (1999) Estimation for stochastic soil models, *ASCE Journal of Geotechnical and Geoenvironmental Engineering*, 125(6), 470-485.

Fenton, G.A., and Griffiths, D.V. (2003) Bearing capacity prediction of spatially random $c - \phi$ soils, *Canadian Geotechnical Journal*, 40(1), 54-65.

Fenton, G.A. and Griffiths, D.V. (2007). Reliability-based deep foundation design. In Probabilistic Applications in Geotechnical Engineering, Geotechnical Special Publication No. 170, Pub. ASCE, pp. 1-12.

Fenton, G.A. and Griffiths, D.V. (2008). Risk Assessment in Geotechnical Engineering. John Wiley & Sons, New York.

Fenton, G.A., Griffiths, D.V., and Zhang, X.Y. (2008). Load and resistance factor design of shallow foundations against bearing failure. Canadian Geotechnical Journal, 45(11): 1556-1571.

FHWA (2001) Load and Resistance Factor Design (LRFD) for Highway Bridge Substructures, Washington, D.C.

FHWA (2005). Development of Geotechnical Resistance Factors and Downdrag Load Facors for LRFD Foundation Strength Limit State Design, Report No. FHWA-NHI-05-052, U.S. Department of Transportations.

Hamilton, J., and Murff, J. (1992). Selection of LRFD resistance factors for pile foundation design. American Society of Civil Engineers Structures Congress, April 1315, San Antonio, Texas, Proceedings Structures Congress 92, ASCE.

Hansen, B. (1953). Earth Pressure Calculation. Danish Technical Press, Copenhagen, Denmark.

Hansen, B. (1956). Limit Design and Safety Factors in Soil Mechanics. Bulletin No. 1, Danish Geotechnical Institute, Copenhagen, Denmark.

Hansen, B. (1966). Code of Practice for Foundation Engineering. Bulletin No. 22, Danish Geotechnical Institute, Copenhagen, Denmark.

Jaky, J. (1944). The coefficient of earth pressure at rest. Journal of the Society of Hungarian Architects and Engineers, Vol. 7, 355-358.

Kulhawy, F., and Phoon, K. (1996). Engineering judgment in the evolution from deterministic to reliability-based foundation design. Proceedings of the 1996 Conference

on Uncertainty in the Geologic Environment, UNCERTAINTY96. Part 1 (of 2), July 31Aug. 31, Madison, WI, ASCE, NY, pp. 2948.

MacGregor, J.G. (1976) Safety and limit states design for reinforced concrete, *Canadian Journal of Civil Engineering*, 3, 484-513.

Meyerhof G.G. (1970) Safety factors in soil mechanics, *Canadian Geotechnical Journal*, 7, 349-355.

Meyerhof G.G. (1993) Development of geotechnical limit state design, In *proceedings of the International Symposium on Limit State Design in Geotechnical Engineering*, Copenhagen, May 26-28, sponsored by the Danish Geotechnical Society, 1, 1-12.

Meyerhof G.G. (1995) Development of geotechnical limit state design, *Canadian Geotechnical Journal*, 32, 128-136.

National Research Council (NRC) (1995). Probabilistic Methods in Geotechnical Engineering. National Academies Press, Washington, DC, pp. 96.

National Research Council (NRC) (2005). National Building Code of Canada. National Research Council of Canada, Ottawa.

National Research Council (NRC) (2006). User's Guide – NBC 2005 Structural Commentaries (Part 4 of Division B), 2nd ed. National Research Council of Canada, Ottawa.

NCHRP 507 (2004) *Load and Resistance Factor Design (LRFD) for Deep Foundations*, Transportation Research Board, NRC, Washington, D.C.

ONeill, M. (1995). LRFD Factors for deep foundations through direct experimentation. In Proceedings of US/Taiwan Geotechnical Engineering Collaboration Workshop. Sponsored by the National Science Foundation (USA) and the National Science Council (Taiwan, ROC), A.B. Huang, Y.S. Fang, P.W. Mayne, and S.G. Paikowsky eds., Taipei, January 911, pp. 100114.

Simpson, B., Pappin, J.W., and Croft, D.D. (1981) An approach to limit state calculations in geotechnics, *Ground Engineering*, 14(6), 21-28.

Paikowsky, S.G . (2004). Load and Resistance Factor Design (LRFD) for Deep Foundations. NCHRP Report 507, TRB, National Research Council, Washington, DC.

Tang, W. (1993). Recent developments in geotechnical reliability. Proceedings of the Conference on Probabilistic Methods in Geotechnical Engineering Li, K., and Lo, S-C. eds., Canberra, Aus-tralia, February 1012, Balkema, Rotterdam, The Netherlands, pp. 328.

Vanmarcke, E.H. (1984). Random Fields: Analysis and Synthesis, The MIT Press, Cambridge, Massachusetts.

Appendix A

Estimation of Means, Variances and Covariance of $\ln \hat{c}$ and $\ln \bar{c}$

If Y is an arbitrary function of several variables, $Y = g(X_1, X_2, ..., X_n)$, then the corresponding first order Taylor's series of Y expansion is

$$Y = g(\mu_{X_1}, \mu_{X_2}, ..., \mu_{X_n}) + \sum_{i=1}^{n} (X_i - \mu_{X_i}) \frac{dg}{dX_i}\Big|_{\mu} \tag{A.1}$$

Assuming that $\hat{c}$ and $\bar{c}$ represent the local averages of c over the sample length of size, $D = \Delta z \times m$ and pile length $H = \Delta z \times n$, respectively, the first-order Taylor series approximations of $\ln \hat{c}$ and $\ln \bar{c}$ can be written as

$$\ln \hat{c} \simeq \ln \mu_c + \sum_{i=1}^{m} (\hat{c}_i - \mu_c) \left(\frac{d \ln \hat{c}}{d\hat{c}_i}\Big|_{\mu_c} \right) \tag{A.2a}$$

$$\ln \bar{c} \simeq \ln \mu_c + \sum_{i=1}^{m} (\bar{c}_i - \mu_c) \left(\frac{d \ln \bar{c}}{d\bar{c}_i}\Big|_{\mu_c} \right) \tag{A.2b}$$

Since $\mu_{\ln \hat{c}} = \mu_{\ln \hat{c}} = \mu_c$, then

$$\ln \bar{c} - \mu_{\ln \hat{c}} \simeq \sum_{j=1}^{n} (\bar{c}_j - \mu_c) \left(\frac{d \ln \bar{c}}{d\bar{c}_j}\Big|_{\mu_c} \right) \tag{A.3a}$$

$$\ln \hat{c} - \mu_{\ln \hat{c}} \simeq \sum_{i=1}^{m} (\hat{c}_i - \mu_c) \left(\frac{d \ln \hat{c}}{d\hat{c}_i}\Big|_{\mu_c} \right) \tag{A.3b}$$

By applying Eq's (A.2) and (A.3), the variance and covariance of $\ln \hat{c}$ and $\ln \bar{c}$, using first-order Taylor series approximation, can be determined as follows;

$$\begin{aligned}
\sigma^2_{\ln \hat{c}} &= \mathrm{Var}[\ln \hat{c}] = \mathrm{E}\left[(\ln \hat{c} - \mu_{\ln \hat{c}})^2 \right] \\
&\simeq \mathrm{E}\left[\left(\sum_{i=1}^{m} (\hat{c}_i - \mu_c) \left(\frac{d \ln \hat{c}}{d\hat{c}_i}\Big|_{\mu_c} \right) \right)^2 \right] \\
&\simeq \sum_{i=1}^{m} \sum_{j=1}^{m} \left(\frac{d \ln \hat{c}}{d\hat{c}_i}\Big|_{\mu_c} \right) \left(\frac{d \ln \hat{c}}{d\hat{c}_j}\Big|_{\mu_c} \right) \mathrm{E}\left[(\hat{c}_i - \mu_c)(\hat{c}_j - \mu_c) \right] \\
&\simeq \sum_{i=1}^{m} \sum_{j=1}^{m} \left(\frac{d \ln \hat{c}}{d\hat{c}_i}\Big|_{\mu_c} \right) \left(\frac{d \ln \hat{c}}{d\hat{c}_j}\Big|_{\mu_c} \right) \mathrm{Cov}\left[\hat{c}_i, \hat{c}_j \right] \\
&\simeq \left(\frac{1}{m\hat{c}}\Big|_{\mu_c} \right)^2 \sum_{i=1}^{m} \sum_{j=1}^{m} \mathrm{Cov}\left[\hat{c}_i, \hat{c}_j \right]
\end{aligned}$$

$$\begin{aligned}
&\simeq \left(\frac{1}{\mu_c}\right)^2 \left(\frac{1}{m^2}\sum_{i=1}^{m}\sum_{j=1}^{m} \mathrm{Cov}\left[\hat{c}_i, \hat{c}_j\right]\right) \\
&\simeq \left(\frac{\sigma_c}{\mu_c}\right)^2 \left(\frac{1}{m^2}\sum_{i=1}^{m}\sum_{j=1}^{m} \rho(z_i^o - z_j^o)\right) \\
&\simeq \frac{v_c^2}{m^2}\sum_{i=1}^{m}\sum_{j=1}^{m} \rho(z_i^o - z_j^o) \qquad (A.4)
\end{aligned}$$

In the same fashion $\sigma^2_{\ln \bar{c}}$, can be obtained by

$$\begin{aligned}
\sigma^2_{\ln \bar{c}} = \mathrm{Var}\left[\ln \bar{c}\right] &\simeq \frac{v_c^2}{n^2}\sum_{i=1}^{n}\sum_{j=1}^{n} \rho(z_i - z_j) \\
&\simeq \frac{v_c^2}{H^2}\int_0^H \int_0^H \rho(z_1 - z_2)\, dz_1\, dz_2 \qquad (A.5)
\end{aligned}$$

The covariance of $\ln \hat{c}$ and $\ln \bar{c}$, by applying Eq. (A.3) is

$$\begin{aligned}
\mathrm{Cov}\left[\ln \bar{c}, \ln \hat{c}\right] &= \mathrm{E}\left[(\ln \bar{c} - \mu_{\ln \hat{c}})(\ln \hat{c} - \mu_{\ln \hat{c}})\right] \\
&\simeq \mathrm{E}\left[\left(\sum_{i=1}^{m}(\hat{c}_i - \mu_c)\left(\frac{d\ln \hat{c}}{d\bar{c}_i}\Big|_{\mu_c}\right)\right)\left(\sum_{j=1}^{n}(\bar{c}_j - \mu_c)\left(\frac{d\ln \bar{c}}{d\bar{c}_j}\Big|_{\mu_c}\right)\right)\right] \\
&\simeq \sum_{i=1}^{m}\sum_{j=1}^{n}\left(\frac{d\ln \bar{c}}{d\bar{c}_j}\Big|_{\mu_c}\right)\left(\frac{d\ln \hat{c}}{d\hat{c}_i}\Big|_{\mu_c}\right)\mathrm{E}\left[(\hat{c}_i - \mu_c)\left(\bar{c}_j - \mu_c\right)\right] \\
&\simeq \sum_{i=1}^{m}\sum_{j=1}^{n}\left(\frac{d\ln \bar{c}}{d\bar{c}_j}\Big|_{\mu_c}\right)\left(\frac{d\ln \hat{c}}{d\hat{c}_i}\Big|_{\mu_c}\right)\mathrm{Cov}\left[\hat{c}_i, \bar{c}_j\right] \\
&\simeq \left(\frac{1}{n\bar{c}}\Big|_{\mu_c}\right)\left(\frac{1}{m\hat{c}}\Big|_{\mu_c}\right)\sum_{i=1}^{m}\sum_{j=1}^{n}\mathrm{Cov}\left[\hat{c}_i, \bar{c}_j\right] \\
&\simeq \left(\frac{1}{\mu_c}\right)^2\left(\frac{1}{mn}\right)\sum_{i=1}^{m}\sum_{j=1}^{n}\mathrm{Cov}\left[\hat{c}_i, \bar{c}_j\right] \\
&\simeq \left(\frac{\sigma_c}{\mu_c}\right)^2\left(\frac{1}{mn}\right)\sum_{i=1}^{m}\sum_{j=1}^{n}\rho\left(\sqrt{r^2 + (z_j - z_i^o)^2}\right) \\
&\simeq \frac{v_c^2}{mn}\sum_{i=1}^{m}\sum_{j=1}^{n}\rho\left(\sqrt{r^2 + (z_j - z_i^o)^2}\right) \\
&\simeq \frac{v_c^2}{mH}\sum_{j=1}^{n}\int_0^H \rho\left(\sqrt{r^2 + (z - z_i^o)^2}\right)\, dz \qquad (A.6)
\end{aligned}$$

The Taylor series expression of the variance of $\ln c$ can be expressed in the form

$$\sigma^2_{\ln c} = \ln(1 + v_c^2) \simeq v_c^2 + \frac{v_c^4}{2} + O(v_c^6) \qquad (A.6)$$

Substituting Eq. (A.6) in Eq's. (A.4), (A.5) and (A.6) provides

$$\sigma^2_{\ln \hat{c}} \simeq \frac{\sigma^2_{\ln c}}{m^2} \sum_{i=1}^{m} \sum_{j=1}^{m} \rho(z_i^o - z_j^o) \qquad (A.6a)$$

$$\sigma^2_{\ln \bar{c}} \simeq \frac{\sigma^2_{\ln c}}{H^2} \int_0^H \int_0^H \rho(z_1 - z_2)\, dz_1\, dz_2 \qquad (A.6b)$$

$$\mathrm{Cov}\,[\ln \bar{c}, \ln \hat{c}] \simeq \frac{\sigma^2_{\ln c}}{mH} \sum_{i=1}^{m} \int_0^H \rho\left(\sqrt{r^2 + (z - z_i^o)^2}\right)\, dz \qquad (A.6c)$$

Appendix B

Probability of Failure for $\theta \to 0$ and $\theta \to \infty$

The analysis of accuracy of the theory developed by estimation of the failure probability of deep foundations for zero and infinity scale of fluctuations is as follows;

The variance reduction functions $\gamma(H)$, $\gamma(D)$ and γ_{HD}, using first-order Taylor series approximation, can be estimated as

$$\gamma(H) = \frac{1}{H^2}\int_0^H \int_0^H \rho(z_1 - z_2)\, dz_1\, dz_2 \simeq \frac{\theta}{H} \tag{B.1a}$$

$$\gamma(D) = \frac{1}{m^2}\sum_{i=1}^{m}\sum_{j=1}^{m} \rho(z_i^o - z_j^o) \simeq \frac{\theta}{D} \tag{B.1b}$$

$$\gamma_{HD} = \frac{1}{mH}\sum_{i=1}^{m}\int_0^H \rho(z, z_i^o)\, dz \simeq \frac{\theta}{|H - D|} \tag{B.1c}$$

when the scale of fluctuation $\theta \to 0$, the variance reduction of any local average goes to zero. The variance and covariance terms also become zero. In the other words, as $\theta \to 0$,

$$\sigma^2_{\ln \hat{c}} \to 0 \tag{B.2a}$$

$$\sigma^2_{\ln \bar{c}} \to 0 \tag{B.2b}$$

$$\mathrm{Cov}\left[\ln \hat{c}, \ln \bar{c}\right] \to 0 \tag{B.2c}$$

In this case, Eq. (2.28) turns out to be

$$\mu_{\ln W} = \mu_{\ln F} \tag{B.3a}$$

$$\sigma_{\ln W} = \sigma_{\ln F} \tag{B.3b}$$

and the failure probability of Eq. (2.28) for zero correlation length becomes

$$p_f = 1 - \Phi\left(\frac{\ln q - \ln \varphi_{gu} - \mu_{\ln F}}{\sigma_{\ln F}}\right) \tag{B.4}$$

This implies that for zero correlation length the probability of failure of deep foundations only depends on the load and resistance factors and the load distribution. This is obviously true because of the fact that if there is no effective variability in the averaged soil properties, the failure of the pile involves only load variability.

When the scale of fluctuation $\theta \to \infty$, all soil points in the field become perfectly correlated. The field becomes a uniform field. The analysis becomes dependent on a single random variable. This means all correlation coefficient terms and variance reduction functions are one, and since $\hat{c} = \overline{c} = c$.

$$\sigma_{\ln \hat{c}} = \sigma_{\ln \overline{c}} = \sigma_{\ln c} \tag{$B.5a$}$$

$$\mathrm{Cov}\left[\ln \hat{c}, \ln \overline{c}\right] = \sigma^2_{\ln c} \tag{$B.5b$}$$

and

$$\mu_{\ln W} = \mu_{\ln F} \tag{$B.6a$}$$

$$\sigma_{\ln W} = \sigma_{\ln F} \tag{$B.6b$}$$

$$p_f = 1 - \Phi\left(\frac{\ln q - \ln \varphi_{gu} - \mu_{\ln F}}{\sigma_{\ln F}}\right) \tag{$B.6c$}$$

This means that the same probability of failure can be estimated for zero and infinity correlation length, involving only load and resistance factors.

Appendix C

Relationship between s and the Friction angle's Coefficient of Variation

The following relationship between s and the friction angle's coefficient of variation can be obtained from

$$v_\phi = \frac{\sigma_\phi}{\mu_\phi} \simeq \frac{2(0.46)\,(\phi_{max} - \phi_{min})\,s}{\sqrt{4\pi^2 + s^2}\,(\phi_{max} + \phi_{min})} \tag{C.1}$$

$$\rightarrow \quad v_\phi^2 \simeq \frac{4(0.46)^2\,(\phi_{max} - \phi_{min})^2\,s^2}{(4\pi^2 + s^2)\,(\phi_{max} + \phi_{min})^2}$$

Therefore

$$\begin{aligned} s^2 &\simeq \frac{4\pi^2 v_\phi^2 (\phi_{max} + \phi_{min})^2}{4(0.46)^2(\phi_{max} - \phi_{min})^2 - v_\phi^2(\phi_{max} + \phi_{min})^2} \\ &\simeq \frac{16\pi^2 v_\phi^2 \mu_\phi^2}{4(0.46)^2(\phi_{max} - \phi_{min})^2 - 4v_\phi^2\mu_\phi^2} \end{aligned} \tag{C.2}$$

and

$$s \simeq \frac{2\pi v_\phi \mu_\phi}{\sqrt{(0.46)^2(\phi_{max} - \phi_{min})^2 - v_\phi^2\mu_\phi^2}} \tag{C.3}$$

Appendix D

The Multivariate Gaussian Distribution

The joint characteristic function of n random variables $X_1, X_2, ..., X_{2M}$ is defined as,

$$\Psi_{12...2M} = \mathrm{E}\left[(X_1 - \mu_{X_1})(X_2 - \mu_{X_2})...(X_{2M} - \mu_{X_{2M}})\right] \qquad (D.1)$$

All central moments of odd orders are zero (Vanmarcke, 1984), the central moments of even orders can be evaluated using the following procedure. Assume we have $2M$ random variables $X_1, X_2, ..., X_{2M}$ jointly distributed and bounded. According to the transformation,

$$X_i = \phi_{min} + \tfrac{1}{2}(\phi_{max} - \phi_{min})\left\{1 + \tanh\left(\frac{sG_i}{2\pi}\right)\right\}, \quad (i = 1, 2, ..., 2M) \qquad (D.2)$$

since G_i is standard normal (having zero mean and unit variance) then,

$$\mu_{X_i} = \mathrm{E}[X_i] = (\phi_{min} + \phi_{max})/2, \quad (i = 1, 2, ..., 2M) \qquad (D.3)$$

and this provides,

$$X_i - \mu_{X_i} = \frac{1}{2}(\phi_{max} - \phi_{min})\left\{\tanh\left(\frac{sG_i}{2\pi}\right)\right\}, \quad (i = 1, 2, ..., 2M) \qquad (D.4)$$

From a third-order Taylor series approximation to tanh and a first-order approximation to the expectation, and applying Eq. (D.4) the moment of order n, can be expressed as follows,

$$\begin{aligned}
\Psi_{12...2M} &= \mathrm{E}\left[(X_1 - \mu_{X_1})(X_2 - \mu_{X_2})...(X_{2M} - \mu_{X_{2M}})\right] \\
&= (0.5)^{2M}(\phi_{max} - \phi_{min})^{2M}\mathrm{E}\left[\prod_{i=1}^{2M}\tanh\left(\frac{sG_i}{2\pi}\right)\right] \\
&\simeq (0.5)^{2M}(\phi_{max} - \phi_{min})^{2M}\mathrm{E}\left[\frac{\prod_{i=1}^{2M}\left[\frac{sG_i}{2\pi}\right]}{1 + (1/2)\left\{\sum_{i=1}^{2M}\left[\frac{sG_i}{2\pi}\right]^2\right\}}\right] \\
&\simeq (0.5)^{2M}(\phi_{max} - \phi_{min})^{2M} \times \frac{\prod_{i=1}^{2M}\mathrm{E}\left[\frac{sG_i}{2\pi}\right]}{1 + (1/2)\left\{\sum_{i=1}^{2M}\mathrm{E}\left[\left(\frac{sG_i}{2\pi}\right)^2\right]\right\}} \\
&\simeq (0.46)^{2M}(\phi_{max} - \phi_{min})^{2M} \times \frac{\left(\frac{s}{2\pi}\right)^{2M}\mathrm{E}[G_1G_2...G_{2M}]}{1 + M\left(\frac{s}{2\pi}\right)^2} \qquad (D.5)
\end{aligned}$$

where the moment of order $2M$ of $G_1, G_2, ..., G_{2M}$ ($2M$ random variables which are jointly normally distributed having zero mean and unit variance) can be expressed as a sum of products of covariances (Vanmarcke, 1984),

$$\mathrm{E}\left[G_1 G_2 ... G_{2M}\right] = \sum \mathrm{E}\left[G_{k_1} G_{k_2}\right] \mathrm{E}\left[G_{k_1} G_{k_2}\right] ... \mathrm{E}\left[G_{k_{2M-1}} G_{k_{2M}}\right] \qquad (D.6)$$

where the summation is over all possible arrangements of the indexes $1, 2, ..., 2M$ into exactly M pairs. The number of such arrangements is $1.3.5...(2M-1)$. Applying Eq. (D.6) leads immediately to the following results for the second, forth and sixth order joint central moments of G_i's:

$$\mathrm{E}\left[G_j G_j\right] = B_{ij} \qquad (D.7a)$$

$$\mathrm{E}\left[G_i G_j G_k G_h\right] = B_{ij}B_{jh} + B_{ik}B_{jh} + B_{ih}B_{jk} \qquad (D.7b)$$

$$\begin{aligned}\mathrm{E}\left[G_i G_j G_k G_h G_l G_s\right] = {} & B_{ij}B_{kh}B_{ls} + B_{ij}B_{kl}B_{hs} + B_{ij}B_{ks}B_{hl} \\ & + B_{ik}B_{jh}B_{ls} + B_{ik}B_{jl}B_{hs} + B_{ik}B_{js}B_{hl} \\ & + B_{ih}B_{jk}B_{ls} + B_{ih}B_{jl}B_{ks} + B_{ih}B_{js}B_{kl} \\ & + B_{il}B_{jk}B_{hs} + B_{il}B_{jh}B_{ks} + B_{il}B_{js}B_{kh} \\ & + B_{is}B_{jk}B_{hl} + B_{is}B_{jh}B_{kl} + B_{is}B_{js}B_{kh}\end{aligned} \qquad (D.7c)$$

where $B_{kl} = \mathrm{Cov}\left[G_k, G_l\right] = \rho_{kl}$. Letting,

$$\Psi^X_{ij} = \mathrm{E}\left[(X_i - \mu_{X_i})(X_j - \mu_{X_j})\right] \qquad (D.8a)$$

$$\Psi^X_{ijkh} = \mathrm{E}\left[(X_i - \mu_{X_i})(X_j - \mu_{X_j})(X_k - \mu_{X_k})(X_h - \mu_{X_h})\right] \qquad (D.8b)$$

$$\Psi^X_{ijkhls} = \mathrm{E}\left[(X_i - \mu_{X_i})(X_j - \mu_{X_j})(X_k - \mu_{X_k})(X_h - \mu_{X_h})(X_l - \mu_{X_l})(X_s - \mu_{X_s})\right] \qquad (D.8c)$$

and

$$\sigma^2_X \simeq (0.46)^2(\phi_{max} - \phi_{min})^2 \frac{\left(\frac{s}{2\pi}\right)^2}{1 + \left(\frac{s}{2\pi}\right)^2} \qquad (D.9a)$$

$$\sigma^4_X \simeq (0.46)^4(\phi_{max} - \phi_{min})^4 \frac{\left(\frac{s}{2\pi}\right)^4}{1 + 2\left(\frac{s}{2\pi}\right)^2} \qquad (D.9b)$$

$$\sigma^6_X \simeq (0.46)^6(\phi_{max} - \phi_{min})^6 \frac{\left(\frac{s}{2\pi}\right)^6}{1 + 3\left(\frac{s}{2\pi}\right)^2} \qquad (D.9c)$$

the second, forth and sixth order joint central moments of $X_1, X_2, ..., X_{2M}$, by using Eq's (D.5) through (D.9) can be written as,

$$\Psi^X_{ij} \simeq \sigma^2_X \rho_{ij} \qquad (D.10a)$$

$$\Psi^X_{ijkh} \simeq \sigma^4_X \mathrm{E}\left[G_i G_j G_k G_h\right] \qquad (D.10b)$$

$$\Psi^X_{ijkhls} \simeq \sigma^6_X \mathrm{E}\left[G_i G_j G_k G_h G_l G_s\right] \qquad (D.10c)$$

Appendix E

Estimation of Means, Variances and Covariance of $\ln \hat{X}$ and $\ln \overline{X}$

E.1 Third Order Taylor Series Approximation

If Y is an arbitrary function of several variables, $Y = g(X_1, X_2, ..., X_n)$, then the corresponding Taylor's series expansion is

$$\begin{aligned} Y = {} & g(\mu_{X_1}, \mu_{X_2}, ..., \mu_{X_n}) + \sum_{i=1}^{n}(X_i - \mu_{X_i})\frac{dg}{dX_i}\Big|_{\mu} \\ & + \frac{1}{2}\sum_{i=1}^{n}\sum_{j=1}^{n}(X_i - \mu_{X_i})(X_j - \mu_{X_j})\frac{d^2g}{dX_i dX_j}\Big|_{\mu} \\ & + \frac{1}{6}\sum_{i=1}^{n}\sum_{j=1}^{n}\sum_{k=1}^{n}(X_i - \mu_{X_i})(X_j - \mu_{X_j})(X_k - \mu_{X_i})\frac{d^3g}{dX_i dX_j dX_k}\Big|_{\mu} + ... \end{aligned} \tag{E.1}$$

Assuming that $\hat{\phi}$ and $\bar{\phi}$ represent the local averages of ϕ over the sample length of size, $D = \Delta z \times m$ and pile length $H = \Delta z \times n$, respectively, and letting,

$$d_1 = \frac{d\ln\hat{X}}{d\hat{\phi}}\Big|_{\mu_\phi} = \frac{d\ln\bar{X}}{d\phi}\Big|_{\mu_\phi} \tag{E.2a}$$

$$d_2 = \frac{d^2\ln\hat{X}}{d\hat{\phi}^2}\Big|_{\mu_\phi} = \frac{d^2\ln\bar{X}}{d\phi^2}\Big|_{\mu_\phi} \tag{E.2b}$$

$$d_3 = \frac{d^3\ln\hat{X}}{d\hat{\phi}^3}\Big|_{\mu_\phi} = \frac{d^3\ln\bar{X}}{d\phi^3}\Big|_{\mu_\phi} \tag{E.2c}$$

means that,

$$\frac{d\ln\hat{X}}{d\hat{\phi}_i}\Big|_{\mu_\phi} = \frac{d_1}{m}, \qquad \frac{d\ln\bar{X}}{d\phi_i}\Big|_{\mu_\phi} = \frac{d_1}{n} \tag{E.3a}$$

$$\frac{d^2\ln\hat{X}}{d\hat{\phi}_i d\hat{\phi}_j}\Big|_{\mu_\phi} = \frac{d_2}{m^2}, \qquad \frac{d^2\ln\bar{X}}{d\phi_i d\phi_j}\Big|_{\mu_\phi} = \frac{d_2}{n^2} \tag{E.3b}$$

$$\frac{d^3\ln\hat{X}}{d\hat{\phi}_i d\hat{\phi}_j d\hat{\phi}_k}\Big|_{\mu_\phi} = \frac{d_3}{m^3}, \quad \frac{d^3\ln\bar{X}}{d\phi_i d\phi_j d\phi_k}\Big|_{\mu_\phi} = \frac{d_3}{n^3} \tag{E.3c}$$

where,

$$d_1 = \frac{\cos(\phi)}{(\sin(\phi) - 1)} + \frac{2b}{\sin(2b\phi)} \tag{E.4a}$$

$$d_2 = \frac{1}{(\sin(\phi) - 1)} - \frac{4b^2\cos(2b\phi)}{\sin^2(2b\phi)} \tag{E.4b}$$

$$d_3 = \frac{-\cos(\phi)}{(1-\sin(\phi))^2} + \frac{8b^3}{\sin(2b\phi)} + \frac{2\cos^2(2b\phi)}{\sin^3(2b\phi)} \tag{E.4c}$$

By using the information in Eq's (E.1) through (E.4), the third-order Taylor series approximations of $\ln \hat{X}$ and $\ln \bar{X}$ are

$$\begin{aligned}
\ln \hat{X} \simeq \ln \hat{X}\Big|_{\mu_\phi} &+ \frac{d_1}{m}\sum_{i=1}^{m}(\hat{\phi}_i - \mu_\phi) \\
&+ \frac{d_2}{2m^2}\sum_{i=1}^{m}\sum_{j=1}^{m}(\hat{\phi}_i - \mu_\phi)(\hat{\phi}_j - \mu_\phi) \\
&+ \frac{d_3}{6m^3}\sum_{i=1}^{m}\sum_{j=1}^{m}\sum_{k=1}^{m}(\hat{\phi}_i - \mu_\phi)(\hat{\phi}_j - \mu_\phi)(\hat{\phi}_k - \mu_\phi)
\end{aligned} \tag{E.5a}$$

$$\begin{aligned}
\ln \bar{X} \simeq \ln \bar{X}\Big|_{\mu_\phi} &+ \frac{d_1}{n}\sum_{i=1}^{n}(\bar{\phi}_i - \mu_\phi) \\
&+ \frac{d_2}{2n^2}\sum_{i=1}^{n}\sum_{j=1}^{n}(\bar{\phi}_i - \mu_\phi)(\bar{\phi}_j - \mu_\phi) \\
&+ \frac{d_3}{6n^3}\sum_{i=1}^{n}\sum_{j=1}^{n}\sum_{k=1}^{n}(\bar{\phi}_i - \mu_\phi)(\bar{\phi}_j - \mu_\phi)(\bar{\phi}_k - \mu_\phi)
\end{aligned} \tag{E.5b}$$

E.2 Means of $\ln \hat{X}$ and $\ln \bar{X}$

The means of third-order Taylor series approximations of $\ln \hat{X}$ and $\ln \bar{X}$ then, can be written as

$$\begin{aligned}
\mu_{\ln \hat{X}} = \mathrm{E}\left[\ln \hat{X}\right] \simeq \ln \hat{X}\Big|_{\mu_\phi} &+ \frac{d_1}{m}\sum_{i=1}^{m}\mathrm{E}\left[(\hat{\phi}_i - \mu_\phi)\right] \\
&+ \frac{d_2}{2m^2}\sum_{i=1}^{m}\sum_{j=1}^{m}\mathrm{E}\left[(\hat{\phi}_i - \mu_\phi)(\hat{\phi}_j - \mu_\phi)\right] \\
&+ \frac{d_3}{6m^3}\sum_{i=1}^{m}\sum_{j=1}^{m}\sum_{k=1}^{m}\mathrm{E}\left[(\hat{\phi}_i - \mu_\phi)(\hat{\phi}_j - \mu_\phi)(\hat{\phi}_k - \mu_\phi)\right]
\end{aligned} \tag{E.6a}$$

$$\begin{aligned}
\mu_{\ln \bar{X}} = \mathrm{E}\left[\ln \bar{X}\right] \simeq \ln \bar{X}\Big|_{\mu_\phi} &+ \frac{d_1}{n}\sum_{i=1}^{n}\mathrm{E}\left[(\bar{\phi}_i - \mu_\phi)\right] \\
&+ \frac{d_2}{2n^2}\sum_{i=1}^{n}\sum_{j=1}^{n}\mathrm{E}\left[(\bar{\phi}_i - \mu_\phi)(\bar{\phi}_j - \mu_\phi)\right]
\end{aligned}$$

$$+\frac{d_3}{6n^3}\sum_{i=1}^{n}\sum_{j=1}^{n}\sum_{k=1}^{n}\mathrm{E}\left[(\bar{\phi}_i-\mu_\phi)(\bar{\phi}_j-\mu_\phi)(\bar{\phi}_k-\mu_\phi)\right] \qquad (E.6b)$$

By using Eq's (D.8) through (D.10), the means of $\ln\hat{X}$ and $\ln\bar{X}$, can be describe by

$$\begin{aligned}
\mu_{\ln\hat{X}} = \mathrm{E}\left[\ln\hat{X}\right] &\simeq \ln\hat{X}\Big|_{\mu_\phi} + \frac{d_2}{2}\left(\frac{1}{m^2}\sum_{i=1}^{m}\sum_{j=1}^{m}\Psi_{ij}^{\hat{\phi}}\right)\\
&\simeq \ln\hat{X}\Big|_{\mu_\phi} + \frac{d_2}{2}\left(\frac{\sigma_\phi^2}{m^2}\sum_{i=1}^{m}\sum_{j=1}^{m}\rho_G(z_i^o-z_j^o)\right)\\
&\simeq \ln\hat{X}\Big|_{\mu_\phi} + \frac{d_2}{2}(\sigma_\phi^2\gamma(D))\\
&\simeq \ln\left((1-\sin\mu_\phi)\tan(b\mu_\phi)\right) + \frac{d_2\sigma_{\hat{\phi}}^2}{2} \qquad (E.7a)\\
\mu_{\ln\bar{X}} = \mathrm{E}\left[\ln\bar{X}\right] &\simeq \ln\bar{X}\Big|_{\mu_\phi} + \frac{d_2}{2}\left(\frac{1}{n^2}\sum_{i=1}^{n}\sum_{j=1}^{n}\Psi_{ij}^{\bar{\phi}}\right)\\
&\simeq \ln\bar{X}\Big|_{\mu_\phi} + \frac{d_2}{2}\left(\frac{\sigma_\phi^2}{n^2}\sum_{i=1}^{n}\sum_{j=1}^{n}\rho_G(z_i-z_j)\right)\\
&\simeq \ln\bar{X}\Big|_{\mu_\phi} + \frac{d_2}{2}(\sigma_\phi^2\gamma(H))\\
&\simeq \ln\left((1-\sin\mu_\phi)\tan(b\mu_\phi)\right) + \frac{d_2\sigma_{\bar{\phi}}^2}{2} \qquad (E.7b)
\end{aligned}$$

E.3 Variances and covariance of $\ln\hat{X}$ and $\ln\bar{X}$

In order to estimate the third-order Taylor series approximations of variances and covariance of $\ln\hat{X}$ and $\ln\bar{X}$, the expressions , $\ln\hat{X}-\mu_{\ln\hat{X}}$ and $\ln\bar{X}-\mu_{\ln\bar{X}}$, by using Eq. (E.7), can be obtained by

$$\begin{aligned}
\ln\hat{X}-\mu_{\ln\hat{X}} &\simeq \frac{d_1}{m}\sum_{i=1}^{m}(\hat{\phi}_i-\mu_\phi) + \frac{d_2}{2m^2}\sum_{i=1}^{m}\sum_{j=1}^{m}(\hat{\phi}_i-\mu_\phi)(\hat{\phi}_j-\mu_\phi)\\
&\quad + \frac{d_3}{6m^3}\sum_{i=1}^{m}\sum_{j=1}^{m}\sum_{k=1}^{m}(\hat{\phi}_i-\mu_\phi)(\hat{\phi}_j-\mu_\phi)(\hat{\phi}_k-\mu_\phi) - \frac{d_2\sigma_{\hat{\phi}}^2}{2} \qquad (E.8a)\\
\ln\bar{X}-\mu_{\ln\bar{X}} &\simeq \frac{d_1}{n}\sum_{i=1}^{n}(\bar{\phi}_i-\mu_\phi) + \frac{d_2}{2n^2}\sum_{i=1}^{n}\sum_{j=1}^{n}(\bar{\phi}_i-\mu_\phi)(\bar{\phi}_j-\mu_\phi)
\end{aligned}$$

$$+\frac{d_3}{6n^3}\sum_{i=1}^{n}\sum_{j=1}^{n}\sum_{k=1}^{n}(\bar{\phi}_i-\mu_\phi)(\bar{\phi}_j-\mu_\phi)(\bar{\phi}_k-\mu_\phi)-\frac{d_2\sigma_{\bar{\phi}}^2}{2} \qquad (E.8b)$$

By applying Eq's (D.8) and (E.8), variance of $\ln\hat{X}$ can be written as

$$\begin{aligned}\mathrm{Var}\left[\ln\hat{X}\right] &= \mathrm{E}\left[(\ln\hat{X}-\mu_{\ln\hat{X}})^2\right]\simeq\\ &d_1^2\left(\frac{1}{m^2}\sum_{i=1}^{m}\sum_{j=1}^{m}\Psi_{ij}^{\hat{\phi}}\right)+\frac{d_2^2}{4}\left(\frac{1}{m^4}\sum_{i=1}^{m}\sum_{j=1}^{m}\sum_{k=1}^{m}\sum_{h=1}^{m}\Psi_{ijkh}^{\hat{\phi}}\right)\\ &+\frac{d_3^2}{36}\left(\frac{1}{m^6}\sum_{i=1}^{m}\sum_{j=1}^{m}\sum_{k=1}^{m}\sum_{h=1}^{m}\sum_{l=1}^{m}\sum_{s=1}^{m}\Psi_{ijkhls}^{\hat{\phi}}\right)+\frac{d_2^2\sigma_{\hat{\phi}}^4}{4}\\ &+\frac{d_1d_3}{3}\left(\frac{1}{m^4}\sum_{i=1}^{m}\sum_{j=1}^{m}\sum_{k=1}^{m}\sum_{h=1}^{m}\Psi_{ijkh}^{\hat{\phi}}\right)-\frac{d_2^2\sigma_{\hat{\phi}}^2}{2}\left(\frac{1}{m^2}\sum_{i=1}^{m}\sum_{j=1}^{m}\Psi_{ij}^{\hat{\phi}}\right) \qquad (E.9)\end{aligned}$$

and applying Eq's (D.5) through (D.10) into Eq. (E.9) leads to,

$$\begin{aligned}&\mathrm{Var}\left[\ln\hat{X}\right]\simeq\\ &d_1^2\left(\frac{\sigma_\phi^2}{m^2}\sum_{i=1}^{m}\sum_{j=1}^{m}\rho_G(z_i^o-z_j^o)\right)\\ &+\frac{3d_2^2}{4}\left[\left(\frac{\sigma_\phi^2}{m^2}\sum_{i=1}^{m}\sum_{j=1}^{m}\rho_G(z_i^o-z_j^o)\right)\left(\frac{\sigma_\phi^2}{m^2}\sum_{k=1}^{m}\sum_{h=1}^{m}\rho_G(z_k^o-z_h^o)\right)\right]\\ &+\frac{15d_3^2}{36}\left[\left(\frac{\sigma_\phi^2}{m^2}\sum_{i=1}^{m}\sum_{j=1}^{m}\rho_G(z_i^o-z_j^o)\right)\left(\frac{\sigma_\phi^2}{m^2}\sum_{k=1}^{m}\sum_{h=1}^{m}\rho_G(z_k^o-z_h^o)\right)\left(\frac{\sigma_\phi^2}{m^2}\sum_{l=1}^{m}\sum_{s=1}^{m}\rho_G(z_l^o-z_s^o)\right)\right]\\ &+\frac{d_2^2\sigma_{\hat{\phi}}^4}{4}+d_1d_3\left[\left(\frac{\sigma_\phi^2}{m^2}\sum_{i=1}^{m}\sum_{j=1}^{m}\rho_G(z_i^o-z_j^o)\right)\left(\frac{\sigma_\phi^2}{m^2}\sum_{k=1}^{m}\sum_{h=1}^{m}\rho_G(z_k^o-z_h^o)\right)\right]\\ &-\frac{d_2^2\sigma_{\hat{\phi}}^2}{2}\left(\frac{\sigma_\phi^2}{m^2}\sum_{i=1}^{m}\sum_{j=1}^{m}\rho_G(z_i^o-z_j^o)\right)\\ &\simeq d_1^2\sigma_{\hat{\phi}}^2+\sigma_{\hat{\phi}}^4\left(\frac{d_2^2}{2}+d_1d_3\right)+\frac{5d_3^2\sigma_{\hat{\phi}}^6}{12} \qquad (E.10)\end{aligned}$$

In the fashion, the third-order Taylor series approximation of variance of $\ln\bar{X}$ can be estimated to be

$$\sigma_{\ln\bar{X}}^2=\mathrm{Var}\left[\ln\bar{X}\right]\simeq d_1^2\sigma_{\bar{\phi}}^2+\sigma_{\bar{\phi}}^4\left(\frac{d_2^2}{2}+d_1d_3\right)+\frac{5d_3^2\sigma_{\bar{\phi}}^6}{12} \qquad (E.11)$$

The covariance of $\ln \hat{X}$ and $\ln \bar{X}$, by using Eq. (E.8) is

$$\begin{aligned}\mathrm{Cov}\left[\ln \hat{X}, \ln \bar{X}\right] = \mathrm{E}\left[(\ln \hat{X} - \mu_{\ln \hat{X}})(\ln \bar{X} - \mu_{\ln \bar{X}})\right] \simeq \\ d_1^2 \left(\frac{1}{mn}\sum_{i=1}^{m}\sum_{j=1}^{m}\Omega_{ij}^{\phi}\right) - \frac{d_2^2\sigma_{\bar{\phi}}^2}{4}\left(\frac{1}{m^2}\sum_{i=1}^{m}\sum_{j=1}^{m}\Psi_{ij}^{\hat{\phi}}\right) \\ - \frac{d_2^2\sigma_{\hat{\phi}}^2}{4}\left(\frac{1}{n^2}\sum_{i=1}^{n}\sum_{j=1}^{n}\Psi_{ij}^{\bar{\phi}}\right) + \frac{d_2^2\sigma_{\hat{\phi}}^2\sigma_{\bar{\phi}}^2}{4} \\ + \frac{d_1 d_3}{6}\left(\frac{1}{mn^3}\sum_{i=1}^{m}\sum_{j=1}^{n}\sum_{k=1}^{n}\sum_{h=1}^{n}\Omega_{ijkh}^{\bar{\phi}}\right) \\ + \frac{d_2^2}{4}\left(\frac{1}{n^2m^2}\sum_{i=1}^{m}\sum_{j=1}^{m}\sum_{k=1}^{n}\sum_{h=1}^{n}\Omega_{ijkh}^{\phi}\right) \\ + \frac{d_1 d_3}{6}\left(\frac{1}{m^3n}\sum_{i=1}^{m}\sum_{j=1}^{m}\sum_{k=1}^{m}\sum_{h=1}^{n}\Omega_{ijkh}^{\hat{\phi}}\right) \\ + \frac{d_3^2}{36}\left(\frac{1}{m^3n^3}\sum_{i=1}^{m}\sum_{j=1}^{m}\sum_{k=1}^{m}\sum_{h=1}^{n}\sum_{l=1}^{n}\sum_{s=1}^{n}\Omega_{ijkhls}^{\phi}\right) \qquad (E.12)\end{aligned}$$

where $\Psi_{ij}^{\hat{\phi}}$ and $\Psi_{ij}^{\bar{\phi}}$ are according to Eq. (D.9) and,

$$\Omega_{ij}^{\phi} = \mathrm{E}\left[(\hat{\phi}_i - \mu_\phi)(\bar{\phi}_j - \mu_\phi)\right] \qquad (E.13a)$$

$$\Omega_{ijkh}^{\hat{\phi}} = \mathrm{E}\left[(\hat{\phi}_i - \mu_\phi)(\hat{\phi}_j - \mu_\phi)(\hat{\phi}_k - \mu_\phi)(\bar{\phi}_h - \mu_\phi)\right] \qquad (E.13b)$$

$$\Omega_{ijkh}^{\bar{\phi}} = \mathrm{E}\left[(\hat{\phi}_i - \mu_\phi)(\bar{\phi}_j - \mu_\phi)(\bar{\phi}_k - \mu_\phi)(\bar{\phi}_h - \mu_\phi)\right] \qquad (E.13c)$$

$$\Omega_{ijkh}^{\phi} = \mathrm{E}\left[(\hat{\phi}_i - \mu_\phi)(\hat{\phi}_j - \mu_\phi)(\bar{\phi}_k - \mu_\phi)(\bar{\phi}_h - \mu_\phi)\right] \qquad (E.13d)$$

$$\Omega_{ijkh}^{\phi} = \mathrm{E}\left[(\hat{\phi}_i - \mu_\phi)(\hat{\phi}_j - \mu_\phi)(\hat{\phi}_k - \mu_\phi)(\bar{\phi}_k - \mu_\phi)(\bar{\phi}_l - \mu_\phi)(\bar{\phi}_s - \mu_\phi)\right] \qquad (E.13e)$$

by making a use of Eq. (D.10), the covariance of $\ln \hat{X}$ and $\ln \bar{X}$, can be written as

$$
\begin{aligned}
\mathrm{Cov}\left[\ln \hat{X}, \ln \bar{X}\right] \simeq \\
& d_1^2 \left(\frac{\sigma_\phi^2}{mn^2} \sum_{i=1}^{m} \sum_{j=1}^{n} \rho_G(z_i^o, z_j) \right) - \frac{d_2^2 \sigma_{\bar{\phi}}^2}{4} \left(\frac{\sigma_\phi^2}{m^2} \sum_{i=1}^{m} \sum_{j=1}^{m} \rho_G(z_i^o - z_j^o) \right) \\
& - \frac{d_2^2 \sigma_{\hat{\phi}}^2}{4} \left(\frac{\sigma_\phi^2}{n^2} \sum_{i=1}^{n} \sum_{j=1}^{n} \rho_G(z_i - z_j) \right) + \frac{d_2^2 \sigma_{\hat{\phi}}^2 \sigma_{\bar{\phi}}^2}{4} \\
& + \frac{d_1 d_3}{2} \left[\left(\frac{\sigma_\phi^2}{mn} \sum_{i=1}^{m} \sum_{j=1}^{n} \rho_G(z_i^o, z_j) \right) \left(\frac{\sigma_\phi^2}{n^2} \sum_{k=1}^{n} \sum_{h=1}^{n} \rho_G(z_k - z_h) \right) \right] \\
& + \frac{d_2^2}{4} \left[\left(\frac{\sigma_\phi^2}{m^2} \sum_{i=1}^{m} \sum_{j=1}^{m} \rho_G(z_i^o - z_j^o) \right) \left(\frac{\sigma_\phi^2}{n^2} \sum_{k=1}^{n} \sum_{h=1}^{n} \rho_G(z_k - z_h) \right) \right] \\
& + \frac{d_2^2}{2} \left[\left(\frac{\sigma_\phi^2}{mn} \sum_{i=1}^{m} \sum_{k=1}^{n} \rho_G(z_i^o, z_k) \right) \left(\frac{\sigma_\phi^2}{mn} \sum_{j=1}^{m} \sum_{h=1}^{n} \rho_G(z_j^o, z_h) \right) \right] \\
& + \frac{d_1 d_3}{2} \left[\left(\frac{\sigma_\phi^2}{m^2} \sum_{i=1}^{m} \sum_{j=1}^{m} \rho_G(z_i^o - z_j^o) \right) \left(\frac{\sigma_\phi^2}{mn} \sum_{k=1}^{m} \sum_{h=1}^{n} \rho_G(z_k^o, z_h) \right) \right] \\
& + \frac{d_3^2}{4} \left[\left(\frac{\sigma_\phi^2}{m^2} \sum_{i=1}^{m} \sum_{j=1}^{m} \rho_G(z_i^o - z_j^o) \right) \left(\frac{\sigma_\phi^2}{mn} \sum_{k=1}^{m} \sum_{h=1}^{n} \rho_G(z_k^o, z_h) \right) \left(\frac{\sigma_\phi^2}{n^2} \sum_{l=1}^{n} \sum_{s=1}^{n} \rho_G(z_l - z_s) \right) \right] \\
& + \frac{d_3^2}{6} \left[\left(\frac{\sigma_\phi^2}{mn} \sum_{i=1}^{m} \sum_{h=1}^{n} \rho_G(z_i^o, z_h) \right) \left(\frac{\sigma_\phi^2}{mn} \sum_{j=1}^{m} \sum_{l=1}^{n} \rho_G(z_j^o, z_l) \right) \left(\frac{\sigma_\phi^2}{mn} \sum_{k=1}^{m} \sum_{s=1}^{n} \rho_G(z_k^o, z_s) \right) \right] \\
& \simeq \\
& d_1^2 \sigma_\phi^2 \gamma_{HD} - \frac{d_2^2 \sigma_{\hat{\phi}}^2 \sigma_{\bar{\phi}}^2}{4} - \frac{d_2^2 \sigma_{\hat{\phi}}^2 \sigma_{\bar{\phi}}^2}{4} + \frac{d_2^2 \sigma_{\hat{\phi}}^2 \sigma_{\bar{\phi}}^2}{4} + \frac{d_1 d_3}{2} \sigma_{\hat{\phi}}^2 \sigma_{\bar{\phi}}^2 \gamma_{HD} \\
& + \frac{d_2^2 \sigma_{\hat{\phi}}^2 \sigma_{\bar{\phi}}^2}{4} + \frac{d_2^2}{2} \left(\sigma_\phi^2 \gamma_{HD} \right)^2 + \frac{d_1 d_3}{2} \sigma_{\hat{\phi}}^2 \sigma_\phi^2 \gamma_{HD} + \frac{d_3^2}{4} \sigma_{\hat{\phi}}^2 \sigma_{\bar{\phi}}^2 \sigma_\phi^2 \gamma_{HD} + \frac{d_3^2}{6} \left(\sigma_\phi^2 \gamma_{HD} \right)^3
\end{aligned}
\tag{E.14}
$$

$$
\begin{aligned}
\mathrm{Cov}\left[\ln \hat{X}, \ln \bar{X}\right] \simeq d_1^2 \sigma_\phi^2 \gamma_{HD} + \sigma_\phi^2 \gamma_{HD} \left(\frac{d_1 d_3}{2} (\sigma_{\hat{\phi}}^2 + \sigma_{\bar{\phi}}^2) + \frac{d_3^2}{4} \sigma_{\hat{\phi}}^2 \sigma_{\bar{\phi}}^2 \right) \\
+ \frac{d_2^2}{2} \left(\sigma_\phi^2 \gamma_{HD} \right)^2 + \frac{d_3^2}{6} \left(\sigma_\phi^2 \gamma_{HD} \right)^3
\end{aligned}
\tag{E.15}
$$

Appendix F

Failure Probability and Resistance Factors Figures and Tables

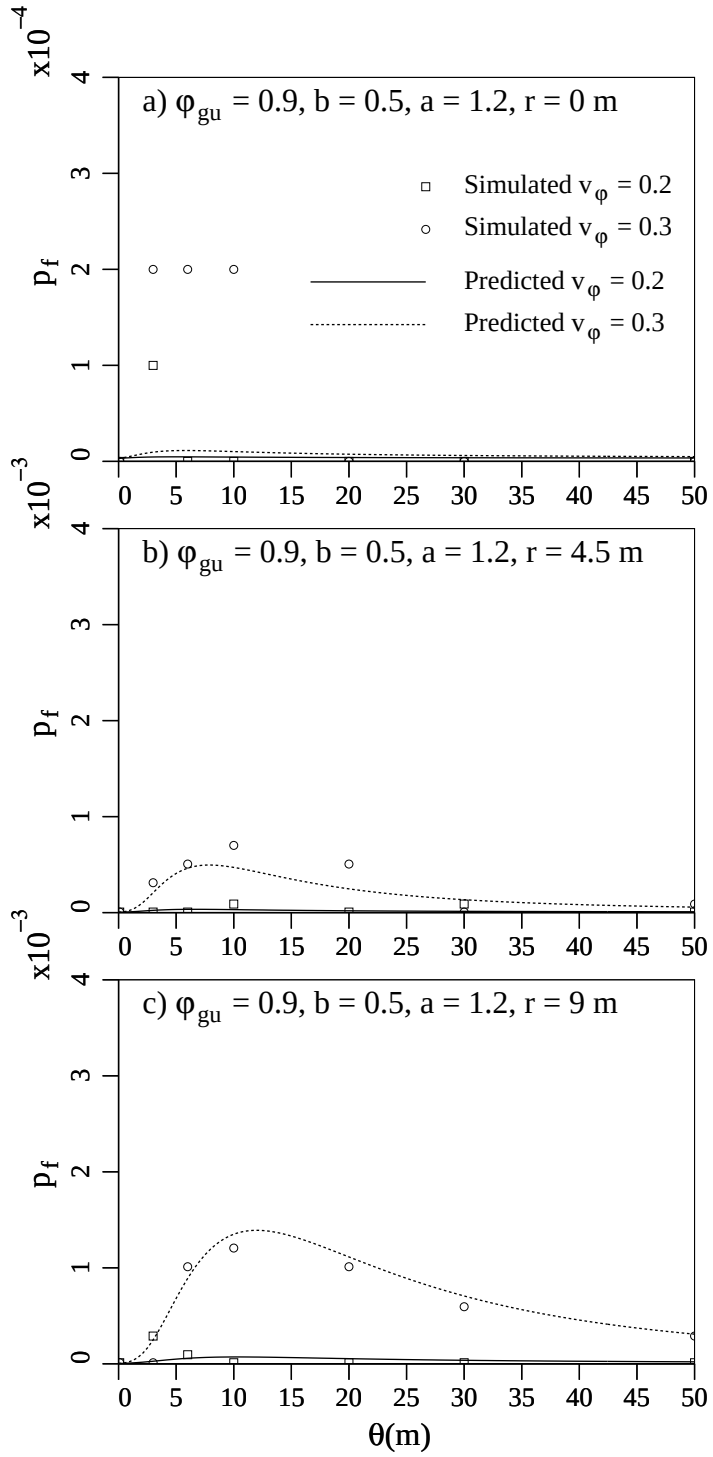

Figure F.1 Comparison of failure probabilities estimated by simulation (10000 realizations) and analytical results for resistance factor, φ_{gu} = 0.9, b = 0.5, a = 1.2 and three sampling locations.

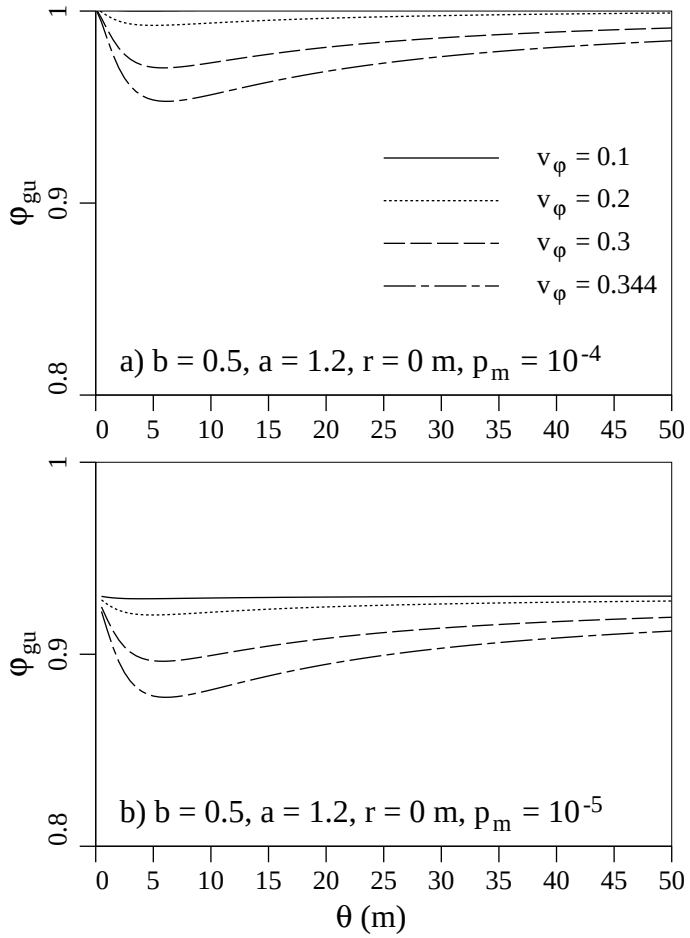

Figure F.2 Resistance factors when the soil has been sampled at the pile location (r = 0 m), for b = 0.5 and a = 1.2 (note the reduced vertical scale).

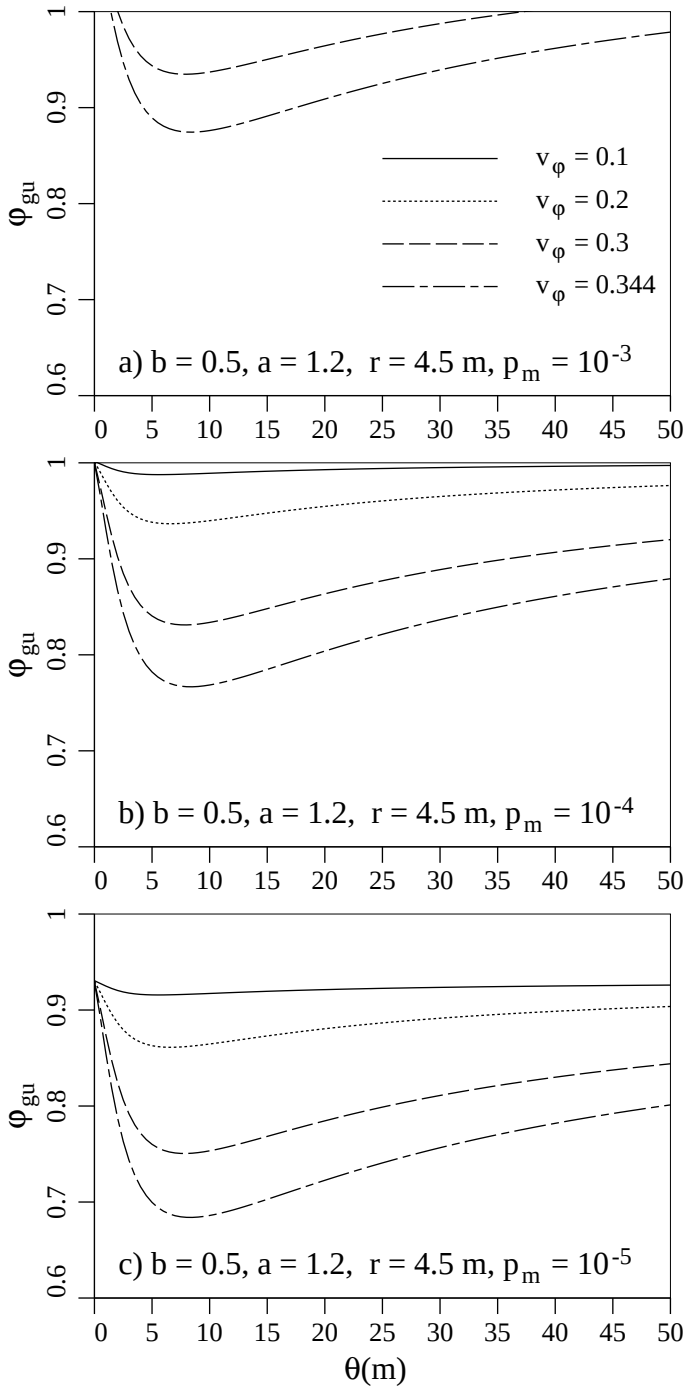

Figure F.3 Resistance factors when the soil has been sampled r = 4.5 m from the pile centerline , for b = 0.5 and a = 1.2.

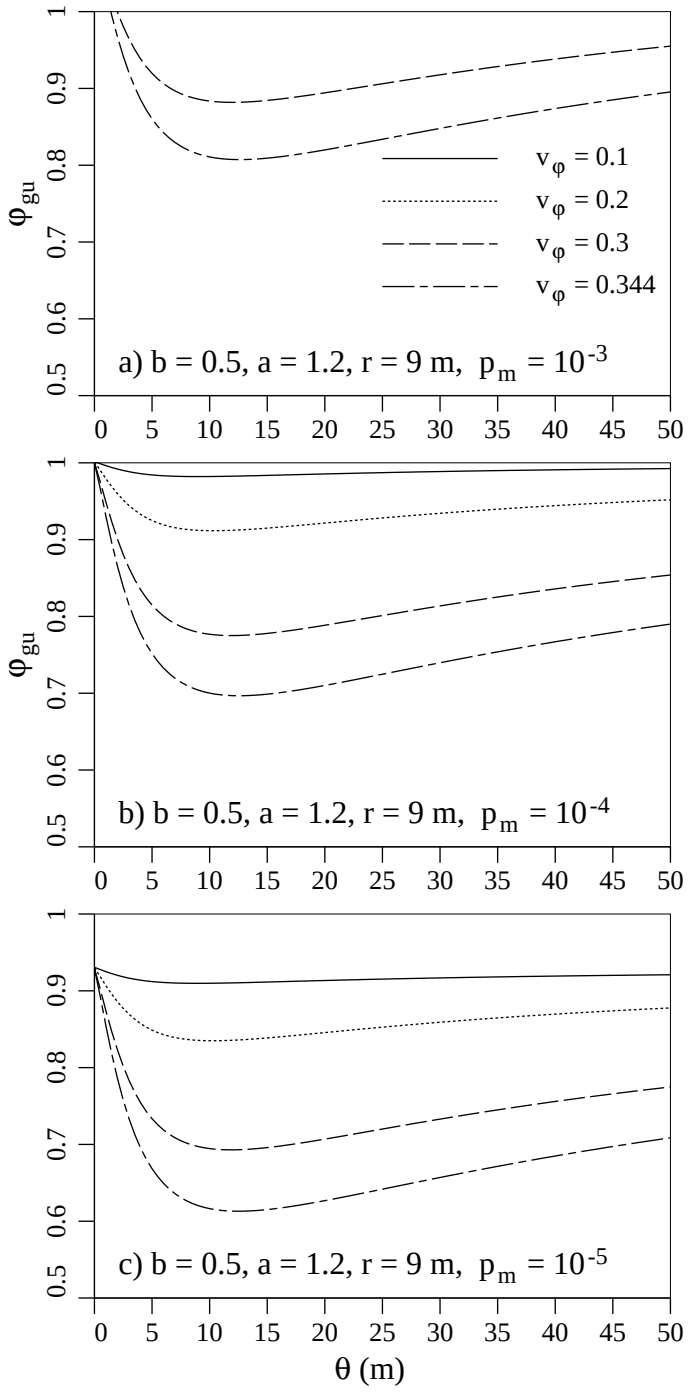

Figure F.4 Resistance factors when the soil has been sampled r = 9 m from the pile centerline , for b = 0.5 and a = 1.2.

Table F.1 Worst case resistance factors for pile interface friction angle coefficient, b = 0.5, earth pressure coefficient a = 1.2, various coefficients of variation, v_ϕ, distance to sampling location, r, and acceptable failure probabilities, p_m.

r (m)	v_ϕ	Resistance Factor			
		$p_m = 10^{-2}$	$p_m = 10^{-3}$	$p_m = 10^{-4}$	$p_m = 10^{-5}$
0.0	0.1	1.20	1.09	1.00	0.93
0.0	0.2	1.19	1.07	0.99	0.92
0.0	0.3	1.17	1.04	0.97	0.90
0.0	0.344	1.15	1.02	0.95	0.88
4.5	0.1	1.20	1.07	0.99	0.92
4.5	0.2	1.16	1.03	0.94	0.86
4.5	0.3	1.09	0.93	0.83	0.75
4.5	0.344	1.04	0.87	0.77	0.68
9.0	0.1	1.19	1.07	0.98	0.91
9.0	0.2	1.14	1.01	0.91	0.84
9.0	0.3	1.03	0.88	0.78	0.69
9.0	0.344	0.97	0.81	0.70	0.61

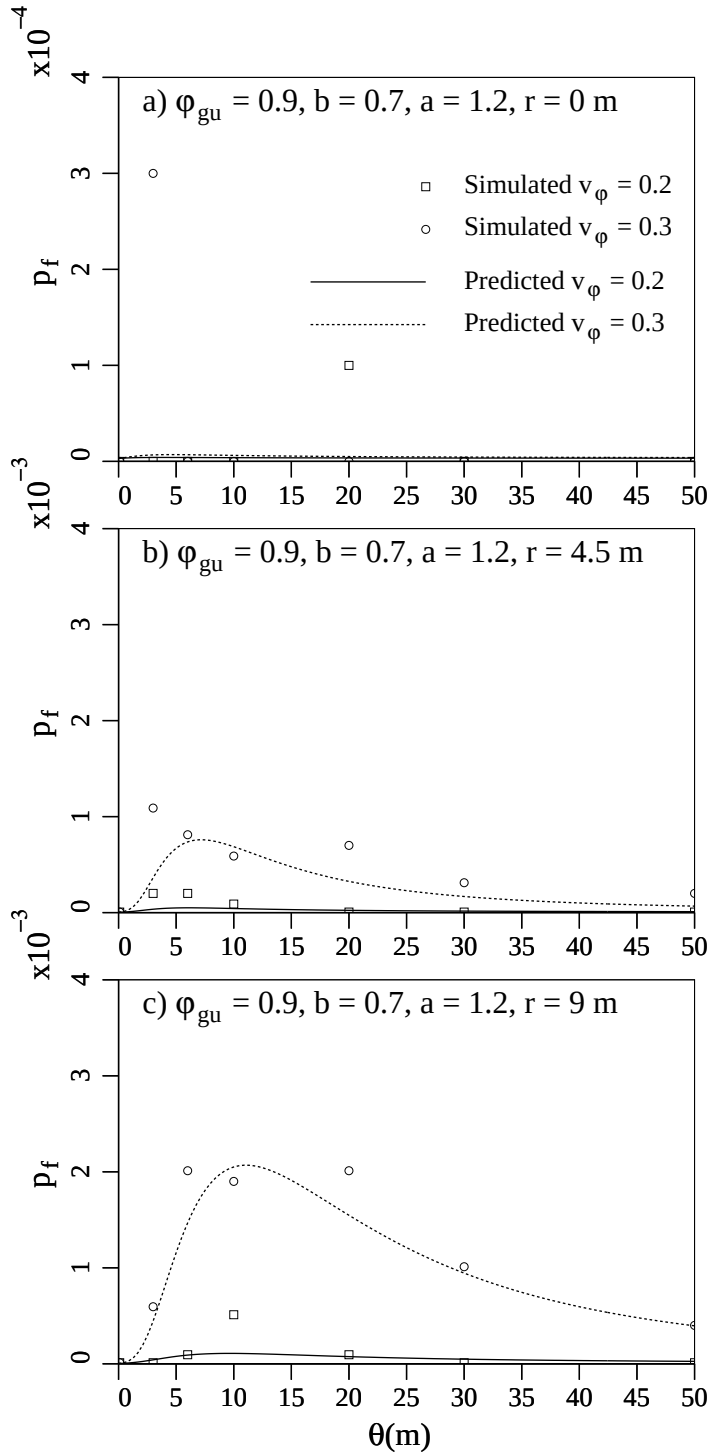

Figure F.5 Comparison of failure probabilities estimated by simulation (10000 realizations) and analytical results for resistance factor, φ_{gu} = 0.9, b = 0.7, a = 1.2 and three sampling locations.

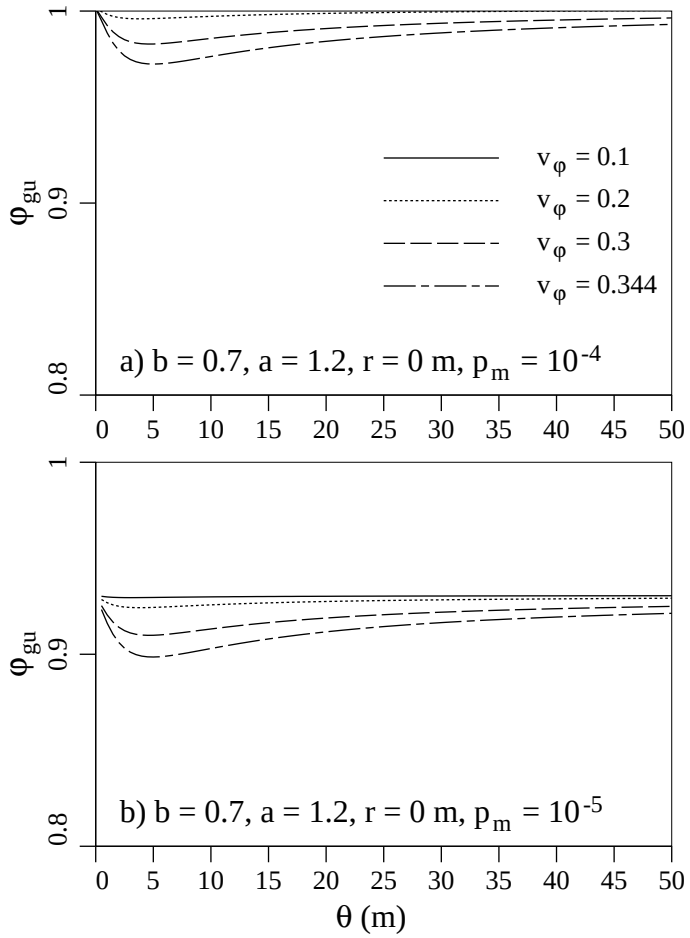

Figure F.6 Resistance factor when the soil has been sampled at the pile location (r = 0 m), for b = 0.7 and a = 1.2 (note the reduced vertical scale).

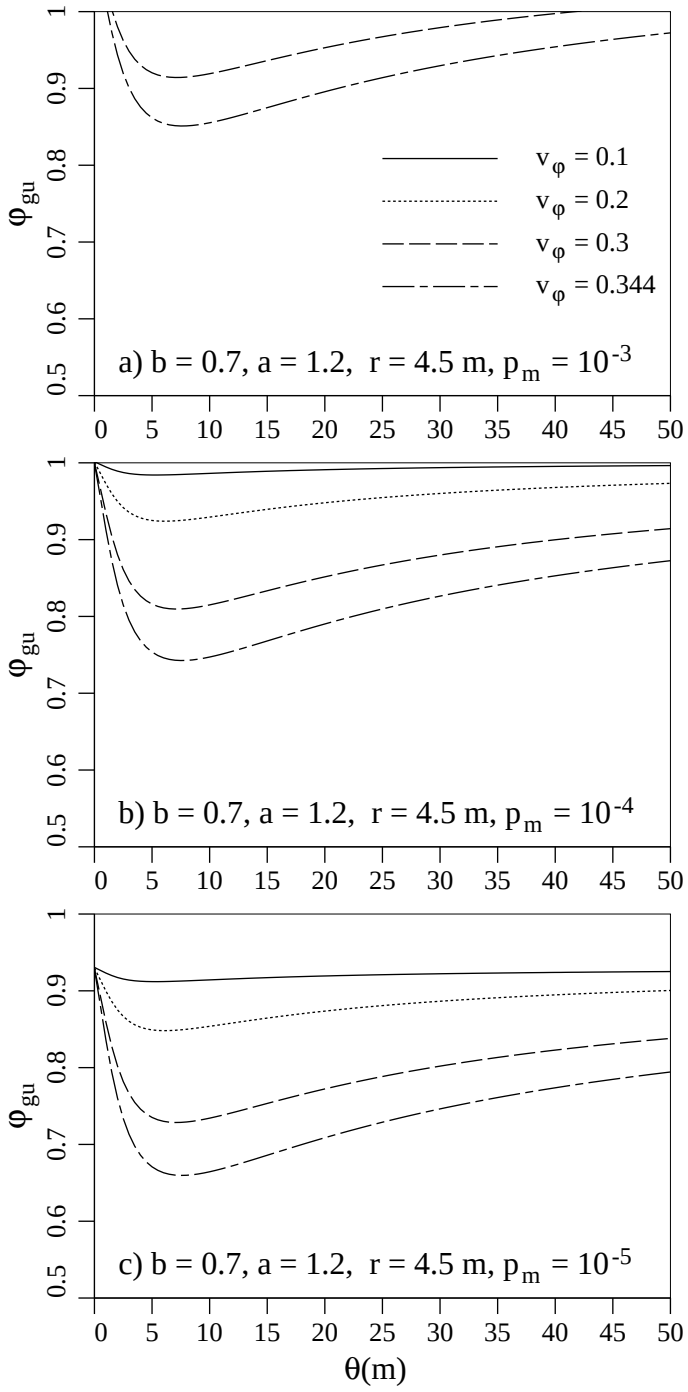

Figure F.7 Resistance factors when the soil has been sampled r = 4.5 m from the pile centerline , for b = 0.7 and a = 1.2.

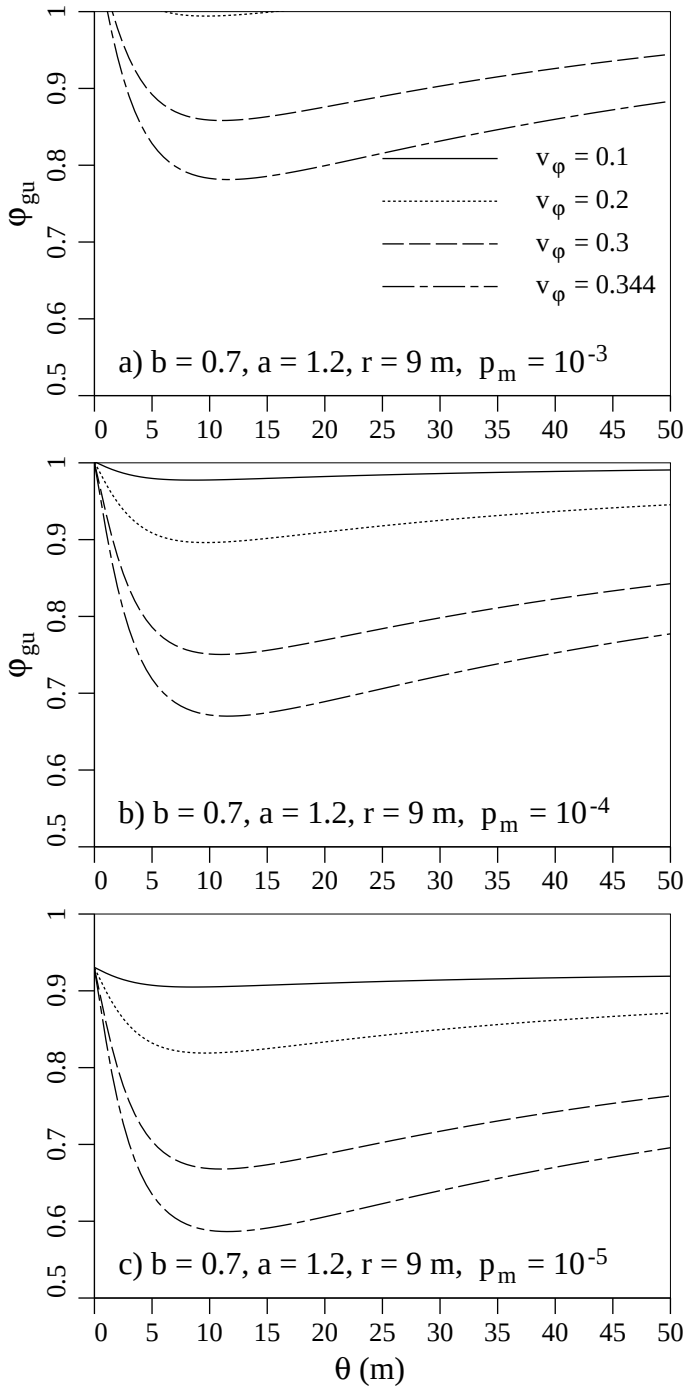

Figure F.8 Resistance factors when the soil has been sampled r = 9 m from the pile centerline , for b = 0.7 and a = 1.2.

Table F.2 Worst case resistance factors for pile interface friction angle coefficient, b = 0.7, earth pressure coefficient a = 1.2, various coefficients of variation, v_ϕ, distance to sampling location, r, and acceptable failure probabilities, p_m.

r (m)	v_ϕ	Resistance Factor			
		$p_m = 10^{-2}$	$p_m = 10^{-3}$	$p_m = 10^{-4}$	$p_m = 10^{-5}$
0.0	0.1	1.21	1.09	1.00	0.93
0.0	0.2	1.20	1.08	0.99	0.92
0.0	0.3	1.19	1.06	0.98	0.91
0.0	0.344	1.17	1.04	0.97	0.90
4.5	0.1	1.19	1.08	0.98	0.92
4.5	0.2	1.15	1.02	0.93	0.86
4.5	0.3	1.06	0.92	0.81	0.74
4.5	0.344	1.00	0.86	0.74	0.67
9.0	0.1	1.19	1.07	0.98	0.91
9.0	0.2	1.13	1.00	0.90	0.82
9.0	0.3	1.02	0.86	0.75	0.67
9.0	0.344	0.94	0.78	0.67	0.59